Shifting baselines in a wavering ocean: Insights from Neolithic fishbone remains

Atlantic bluefin tuna population structure, demographic history, and the genetic effects of human exploitation

Emma Falkeid Eriksen

UNIVERSITETET I OSLO

Master Thesis (60 credits)

Ecology and Evolution

Centre for Ecological and Evolutionary Synthesis

Department of Biosciences

Faculty of Mathematics and Natural Sciences

UNIVERSITY OF OSLO

May 2022

Shifting baselines in a wavering ocean: Insights from Neolithic fishbone remains

Atlantic bluefin tuna population structure, demographic history, and the genetic effects of human exploitation

Emma Falkeid Eriksen

Shifting baselines in a wavering ocean: Insights from Neolithic fishbone remains
Emma Falkeid Eriksen
https://www.duo.uio.no/
Print: Reprosentralen, Universitetet i Oslo

Acknowledgments

Throughout my project I have received a great deal of support and assistance from a range of people at the Institute of Bioscience at the University of Oslo (UiO), as well as collaborators from other institutes, family, and friends.

First of all, I want to thank my wonderful supervisors Dr. Bastiaan Star and Lane Atmore for their patience and enthusiasm. Your encouragement and feedback have been invaluable in driving my project forward, and you have provided me with the tools and confidence I have needed along the way. Lane, you are an inspiration and have been a brilliant mentor to me. Bastiaan, you have envisioned the project and generously shared your ideas and creativity while keeping me grounded and moving forward. I could not wish for better supervisors.

I would also like to thank the people of the Archaeogenomics group, UiO, for keeping their doors open and welcoming me into the group. A special thanks to Oliver, Giada, Lulú and Angelica who have been a huge part of the laboratory processing of my samples, has trained me in the laboratory methods and answered my many questions on Slack.

My collaborators Svein Vatsvåg Nielsen and Per Åke Persson at the Cultural History Museum, UiO, provided the ancient specimens for this project, and have been a great assistance in application processes and metadata collection. Their open communication and interest in my project have been valuable and motivating.

I also want to express my appreciation for the social and academic environment at the Centre for Ecological and Evolutionary Synthesis (CEES), UiO. The regular coffee-breaks and lunches have given me the opportunity to discuss my project and gather inspiration from others research.

Finally, I want to thank my closest friends and family. Preben and Kristine, you are always there to comfort and encourage me, and you sparkle up my life with your stories and excellent humor. Marius, you have been my rock and provided constant support with our discussions and walks. Bernhard and Therese, the apples of my eyes and the most awesome siblings anyone could wish for. Pappa, for always believing in me and Mamma for being my guiding star.

So many more people deserve to be mentioned, but you know who you are and I really appreciate you being there for me.


© Arild Aldehölm, IMR

Abstract

Atlantic bluefin tuna is a commercially important marine apex predator distributed across the Atlantic Ocean from the Gulf of Mexico to the Mediterranean and the Norwegian Sea. In recent history, Atlantic bluefin tuna has experienced severe overfishing, resulting in population collapse and a listing on the IUCN red list. Humans are known to have harvested Atlantic bluefin for millennia – trap fisheries around the Mediterranean have been documented by historical sources for the past 2600 years, and archaeological findings along the Skagerrak coast indicate Atlantic bluefin exploitation in Scandinavian Mesolithic and Neolithic periods. However, the impact of human exploitation on tuna evolution and ecology remains poorly understood.

Recent excavations at Jortveit, in southern Norway, have produced an abundance of tuna bones dated to the Early and Middle Neolithic period (3900-2350 BCE). Producing more tuna bones than any other known location in Scandinavia, the Jortveit excavations provide a unique opportunity for a population-scale study of ancient tuna and allow for comparative analyses between ancient and modern populations. Ancient DNA provides non-extrapolated information about past genetic variation and population structure, making it possible to directly compare the genetic effects of human exploitation. By successfully retrieving mitochondrial genomes of Atlantic bluefin tuna from the Jortveit site and comparing to modern conspecifics from across the Atlantic Ocean, I provide the oldest population-scale baseline comparison of Atlantic bluefin tuna.

In this thesis I analyze 39 ancient specimens with exceptional ancient DNA preservation, for which sequencing libraries were obtained of all specimens, yielding about 24% endogenous DNA on average. I compare these data with 77 modern tuna specimens from all major spawning regions and the Norwegian coast foraging area. My results indicate that –despite heavy exploitation– no loss of mitogenomic diversity has occurred over the past ~4600 years and provides evidence that hybridization of Atlantic and Pacific bluefin had already taken place in the Neolithic period. Through genetic investigations of Atlantic bluefin specimens from before the period of heavy anthropogenic exploitation, I provide a more solid basis for conservation and management decisions in the future.

“Great fish do not swim in shallow waters”

- Matshona Dhliwayo

Table of contents

1. Introduction

The Atlantic bluefin tuna (*Thunnus thynnus thynnus*, Linneaus 1758) is a highly migratory predator in the order of Scombriform fishes. With a body size of up to 3.3 meters and 725 kg, it is among the largest of all bony fishes (J. Cort et al., 2013). Due to their high metabolic rate and ability to thermoregulate muscle temperature, the Atlantic bluefin thrive in waters as cold as 3°C and can be found throughout the North Atlantic Ocean and the Mediterranean Sea (Block, 2001; Carey & Lawson, 1973; Stevens et al., 2000). In Norway, Atlantic bluefin has been observed all the way up to Laksefjord in Finnmark (Nøttestad et al., 2020).

Atlantic bluefin tuna has been an important trade product for at least 2600 years (Oppianus, 177 BCE; Plinius, 65 CE; Aristotelis, 1635; Di Natale, 2012). Tuna harvests are known from the Byzantine era (Puncher, Onar, et al., 2015), the Hanseatic fish trade in the middle ages (Küchelmann, 2020), as well as modern seine and longline fishing (B. Collette et al., 2011; SCRS, 2019). This extensive history of exploitation makes it difficult to quantify the long-term human impacts on Atlantic tuna, as exploitation may lead to low or gradually decreasing population size over time, even before scientific observations. Such gradual losses over time have been called the shifting baseline syndrome (Pauly, 1995) and this concept can be applied to genetic changes over time as well (Pinnegar & Engelhard, 2008). It is therefore imperative to know the history of human harvest of bluefin tuna to help manage the stocks sustainably today. Directly quantifying possible genetic impacts of human exploitation, such as gradually reduced genetic diversity, is impossible to do without knowledge about the original diversity of haplotypes that existed before human impact. Nonetheless, ancient DNA approaches can aid in obtaining such genetic estimates by directly comparing the genomes of specimens dated before major exploitation. In the next section I present an historical overview, a timeline, of human exploitation of the Atlantic bluefin tuna to establish the background for my population genetic investigations.

1.1 History and management of Atlantic bluefin tuna

The Atlantic bluefin is currently managed as two separate stocks, the larger spawning in the Mediterranean and a smaller stock spawning in the Gulf of Mexico (ICCAT, 2021). Whether these stocks are in fact separate biological populations has long been debated (Galuardi et al., 2010; Alvarado Bremer et al., 2005; Ely et al., 2002) and trans-Atlantic migration of adult fish is well documented (Arregui et al., 2018; Wilson et al., 2015; Rooker et al., 2014; Galuardi et al., 2010; Rooker et al., 2006; Block et al., 2005; Block, 2001; Lutcavage et al., 1999).

However, electronic tagging and otolith isotope studies suggest strong natal homing behavior (e.g. Block et al., 2005; Boustany et al., 2008; Brophy et al., 2016), and recent studies using genome-wide SNPs support genetically distinct, reproductively separated populations (Andrews et al., 2021; Rodríguez-Ezpeleta et al., 2019; Puncher et al., 2018; Albaina et al., 2013) despite population mixing during the rest of the year. Shared foraging grounds and migration patterns are still important to consider when assessing the management of Atlantic bluefin over time, especially for fisheries targeting large adult fish outside of spawning season and spawning areas. Throughout the thesis I will refer to the management units as eastern and western *stocks*, while reserving the term *population* for discussions of biological evidence for population structure.

Atlantic bluefin tuna exploitation has likely occurred in the Mediterranean and North seas since the Stone Age (Di Natale, 2012, 2014; Puncher, Cariani, et al., 2015; Ravier & Fromentin, 2001). In Grotta del Genovese (Sicily, Italy), cave paintings of bluefin tuna may be as old as 9000 BCE (Tusa, 1999; Spoto, 2002). In Scandinavia, archaeological findings along the Skagerrak coast indicate Atlantic bluefin exploitation as early as the Scandinavian Mesolithic and Neolithic periods (5800- 2350 BCE) (ICCAT, 2009; S. V. Nielsen and Persson, 2020).

The earliest known fisheries used hooks and lines to hunt tuna, but fishing became more efficient as early as the sixth century BCE, when beach seines and traps replaced hooks and lines in the Phoenician tuna fisheries in the eastern Mediterranean (Di Natale, 2012; Fromentin & Powers, 2005). The industry was further developed by the Greeks and Romans, with written records from around 300 BCE and documented salting plants and factories from the Byzantine era (Block, 2019; Puncher, Onar, et al., 2015). As the fishing industry developed, catches increased. Trap data recovered from 1512-2009 CE suggests catches of around 14’000 tons from Spanish traps alone during the mid-1500’s (Pagá Garcia et al., 2017). In 1880, 22’000 tons were registered in Spanish, Italian, Portuguese and Tunisian traps, but many more traps with unregistered catches are believed to have existed at this time (Pagá Garcia et al., 2017; Ravier & Fromentin, 2001). Indeed, the total catch of bluefin tuna during the 1500-1800’s could be in the same order of magnitude as modern catches, as the actual numbers may be twice as high as reported by these incomplete records (Block, 2019). Thus, historical tuna catches were large enough that they must be taken into consideration when estimating a natural baseline for the population size of the Atlantic bluefin tuna.

In the Americas, the earliest recorded commercial catches date from the early 1900s, when Atlantic bluefin tuna was harpooned for fish oil production and largely viewed as an inconvenience for damaging mackerel- and herring traps (Bigelow & Schroeder, 1953; Block, 2019). Yet, archaeological evidence shows that indigenous Americans caught Pacific bluefin on the west coast as early as 3000 BCE (Crockford, 1997). This suggest that, despite the lack of historical records, Atlantic bluefin tuna fishing prior to the 20th century in the Americas cannot be ruled out. During the early 1900s, the price of Atlantic bluefin gradually increased as the bluefin meat became more popular, and catches increased almost tenfold along the coast of New England and Nova Scotia during the 1940's (Bigelow & Schroeder, 1953).

During the 1950-60's, the total reported catches for the Eastern stock was between 25'000-40'000 tons per year, compared to less than 2'000 tons per year for the western stock (Block, 2019). The Eastern stock was mainly targeted by traps near the Strait of Gibraltar, where adult spawners were intercepted on their migration routes in and out of the Mediterranean, and by Norwegian purse seine fishers in the North Sea (Block, 2019). From 1950-1964, The Norwegian fishing fleet was one of the largest in the Northeast Atlantic, with around 470 purse seine ships targeting bluefin along the Norwegian coast (Nøttestad et al., 2020). In the late 1960s, Atlantic bluefin became absent in the North Sea, which together with the collapse in the herring stock caused Norwegian purse seiners to almost disappear (Tangen 2009). Around the same time, catches in the Mediterranean dropped substantially to what was then an all-time low of 10,000 tons in the early 1970s, likely due to heavy fishing of juveniles and/or altered migration patterns (J. Cort & Abaunza, 2016; J. L. Cort & Abaunza, 2015; Fromentin, 2009; Tiews, 1978). In the West Atlantic, catches peaked at 18,608 tons in 1964 before dropping dramatically to less than 700 tons in 1968 as the fisheries along the coast of Brazil collapsed and smaller bluefin, which were preferred by canneries, became scarce (Mather et al. 1995; Barbara A. Block 2019).

In 1966, the International Commission for the Conservation of Atlantic Tunas (ICCAT) was established in response to the recognition of an increased need for international management of Atlantic tuna. By collecting fishery statistics, coordinate research and develop management advice, ICCAT's overarching responsibility is to conserve tunas and tuna-like species in the Atlantic Ocean and adjacent seas. In practice, ICCAT provides an arena for its 52 contracting parties to agree upon management measures. Contracting members include, among others, the EU, Norway, Iceland, USA, Canada, Brazil, Mexico, Guatemala, Nicaragua, Marocco, Tunisia, Libya, Egypt, Turkey, Japan, Korea, China, and Russia.

Despite the dramatic reductions in catches during the 1960's, fisheries expanded in the early 1970s, especially in the west Atlantic, where a decrease in southern bluefin (*Thunnus maccoyii*) catches coincided with the rise of Japan's burgeoning sashimi market, driving price increases for fatty, late-season adult tuna (Block, 2019). Western catches were substantially reduced in 1982 after the Standing Committee on Research and Statistics (SCRS) advised ICCAT to reduce western stock catches to "as near zero as feasible", as the stock had been depleted (SCRS, 1982). In the same report, SCRS estimated a 50% decrease in the number of adult fish between 1960-1979 in the eastern stock, but still concluded that current regulations were sufficient in the east (SCRS, 1982). During the 1980s-90s, farming of adult catches for fattening and export to Japan became increasingly successful in the Mediterranean (Miyake et al., 2003). By 1996, catches had increased to over 50,000 t in the east, compared to 2,500 t in the more strictly regulated western stock (Fromentin, Bonhommeau, et al., 2014). Despite the implementation of a total allowable catch (TAC) policy, limiting the number of tons harvested by the fisheries each season, catches are assumed to have remained high during the 2000s although these catches were largely underreported (Fromentin, Bonhommeau, et al., 2014).

In 2009, Atlantic bluefin was proposed to be listed under Appendix I in the Convention on International Trade in Endangered Species of Wild Fauna and Flora (CITES) (Block, 2019). This designation would prevent international trading if accepted (CITES, 2021). As a response to this preposition, ICCAT hired an independent panel of experts to review its own performance. The panel consisted of three professors, including the Executive Director of the Australian Fisheries Management Authority, a Japanese professor of International Law, and a fisheries scientist (ICCAT, 2009b). After assessing the management of Atlantic bluefin in relation to ICCAT's objectives of conservation, the panel concluded that the management of the Atlantic bluefin, particularly the eastern stock, "is widely regarded as an international disgrace" and that "there are concerns about transparency within ICCAT both in decision making and in resource allocation" (ICCAT, 2009b). ICCAT was pressured to implement stricter surveillance of commercial companies and to reduce in fishing capacity of the eastern fleets to regain control of the stock decrease.

From 2011-2021, the Atlantic bluefin was listed as *Endangered* on the IUCN Red List (B. Collette et al., 2011, 2021). In September 2021, the Atlantic bluefin's Red List status was changed to *Least Concern* as "no major decline in the global size of the Atlantic bluefin tuna population over the past three generation lengths" had been found (B. Collette et al., 2021). This assessment was made based mainly on the low but relatively stable spawning stock

biomass (SSB) of larger Eastern stock since 1966, despite an estimated 83% decline in the western stock over the same three generations (B. Collette et al., 2021).

In their latest report, SCRS conclude that overfishing is currently not indicated in either of the management stocks (SCRS, 2021). The Eastern SSB has increased substantially since the late 2000s, and additionally over the past few years (2017-2020). The Western stock, which experienced overfishing until 2018, is declining with an estimated SSB decrease of 11.7% from 2017-2020. The recommended TAC is currently at 36,000 t for the Eastern stock, compared to peak catches of 50,000 tons in 1996, and 2,350 t for Western stock, compared to peak catches of 18,608 tons in 1964 (SCRS, 2021). However, SCRS emphasizes that "the current perception of the stock status depends on recruitment estimates which are highly unstable and is also closely related to the assumptions made about stock structure and migratory behaviour, which remain poorly known" and that "changes to assessment and management approaches that take explicit account of mixing are a high priority" (SCRS, 2021).

1.2 Intraspecific population structure

Since 1982, Atlantic bluefin tuna management has been delineated across the Atlantic using an equal-distance line at 45°W (Figure 1), resulting in two management units: a western stock and an eastern stock (SCRS, 1982). At the time, the management favored the use of separate stocks to protect the smaller western stock despite weak biological evidence for population subdivision (Fromentin and Powers 2005; SCRS, 1982). Since then, numerous studies have investigated the biological basis for population subdivision across the Atlantic Ocean to support or contradict the management units.

Repeated homing to natal spawning grounds in the Gulf of Mexico and Mediterranean Sea is well documented by electronic tagging (Block, 2001; Block et al., 2005; Boustany et al., 2008) and otolith chemistry (Brophy et al., 2016; Fraile et al., 2015; Rooker et al., 2014). Recent studies using genome-wide nuclear SNPs have also find genetic differentiation between larval and young-of-the-year (YoY) bluefin in the two spawning regions (Andrews et al., 2021; Rodríguez-Ezpeleta et al., 2019; Puncher et al., 2018). However, regular migration and stock intermixing on foraging grounds has led to discussion about whether the management units reflect the true population origin of the catches (Rodríguez-Ezpeleta et al., 2019; Galuardi et al., 2010). Adult bluefin are powerful swimmers, and frequent migration across the 45°W management boundary is known to occur by members of both stocks (Arregui et al., 2018;

Block, 2001; Block et al., 2005; Galuardi et al., 2010; Lutcavage et al., 1999; Rooker et al., 2006, 2014; Wilson et al., 2015).

Today, the general consensus is that two populations do exist, with strong homing behavior to natal spawning grounds, and extensive mixing in the open North Atlantic foraging areas outside of spawning season (ICCAT, 2021; SCRS, 2019b; Barbara A. Block 2019; Gregory N. Puncher et al. 2018; Hanke et al. 2018; Siskey et al. 2016; Schloesser et al. 2010; Rooker et al. 2007; 2008; Barbara A. Block et al. 2005). Several studies also suggest some patterns of natal homing within the Mediterranean Sea in the Eastern stock, based on genetic evidence (Carlsson et al., 2004; Riccioni et al., 2010, 2013; Viñas et al., 2011) and electronic tagging (Cermeño et al., 2015; Fromentin & Lopuszanski, 2014). The presence of (partly) reproductively isolated subpopulations within the Eastern stock, spawning in Eastern-, Central-, and Western Mediterranean, is however still unclear (Andrews et al., 2021; Rodríguez-Ezpeleta et al., 2019; Antoniou et al., 2017; Vella et al., 2016; Viñas et al., 2011) and is not considered by management (ICCAT, 2021).

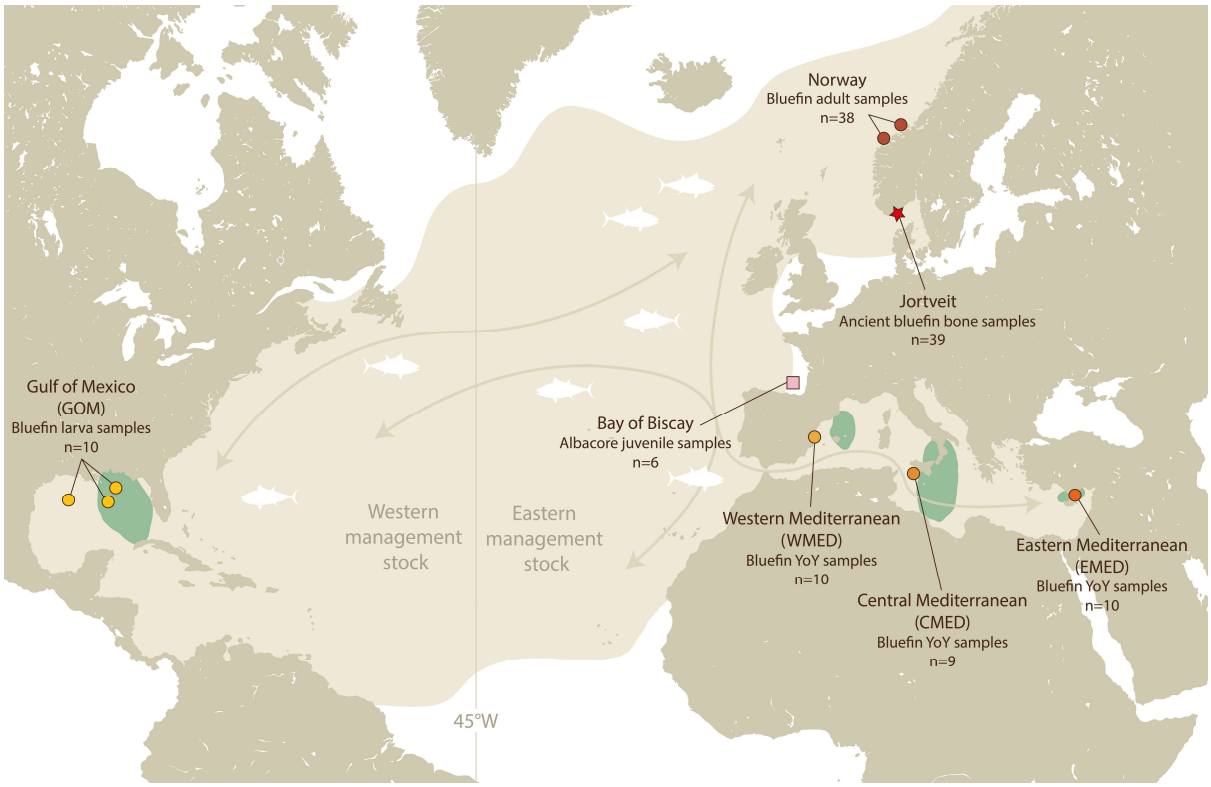

Figure 1: Distribution of the Atlantic bluefin tuna, including spawning areas, adapted from IMR (2021). The equal-distance line (45°W) separates the Eastern and Western stocks for management purposes. Sample locations of tuna studied in this thesis, including number of specimens of both modern and ancient specimens, are indicated on the map. Arrows indicate the main migration routes of adult Atlantic bluefin, adapted from Fromentin, Reygondeau, et al. 2014.

1.3 Interspecific population structure and introgression

Genetic introgression is the integration of genetic material from one parent species into another following hybridization and backcrossing (Rhymer & Simberloff, 1996). The majority of documented introgression in animals appears in the mitochondrial genome (Toews & Brelsford, 2012). Mitochondria are typically inherited maternally in vertebrates, and introgressed mitochondrial genomes will therefore follow the maternal lineage (Brown, 2008). Since the mitochondrial genome is non-recombining, the introgressed genotype remains largely intact over time (Seixas et al., 2018).

Mitochondrial introgression within the *Thunnus* genus, together with the lack of reliable phylogenetically informative markers to distinguish the species, contributed to the phylogeny of the genus being largely unresolved until recently (Alvarado Bremer et al., 1997; Chow et al., 2006; Chow & Kishino, 1995; Díaz-Arce et al., 2016; Santini et al., 2013; Viñas & Tudela, 2009). The Pacific bluefin (*Thunnus thynnus orientalis*), distributed across the North Pacific Ocean, and Atlantic bluefin (*Thunnus thynnus thynnus*) were previously thought to be subspecies of Northern bluefin tuna (*Thunnus thynnus*) but are now regarded as distinct species (Chow et al., 2006; Díaz-Arce et al., 2016) with non-overlapping ranges (Tseng et al., 2011). In mitochondrial phylogenies, the Pacific bluefin tends to form a monophyletic group with the albacore tuna (*Thunnus alalunga*) (Gong et al., 2017; Viñas & Tudela, 2009; Chow et al., 2006). Albacore tuna is found in both the Pacific, Indian and Atlantic Oceans, including the Mediterranean Sea, typically preferring warmer waters than the Pacific and Atlantic bluefins, but with largely overlapping ranges and spawning areas (Chow & Ushiama, 1995; Saber et al., 2015). In the most recent and resolved nuclear phylogeny, the albacore tuna (*Thunnus alalunga*) occurs as the sister-species to the other *Thunnus* species, and the Pacific and Atlantic bluefin form a monophyletic group (Díaz-Arce et al., 2016) (Figure 2).

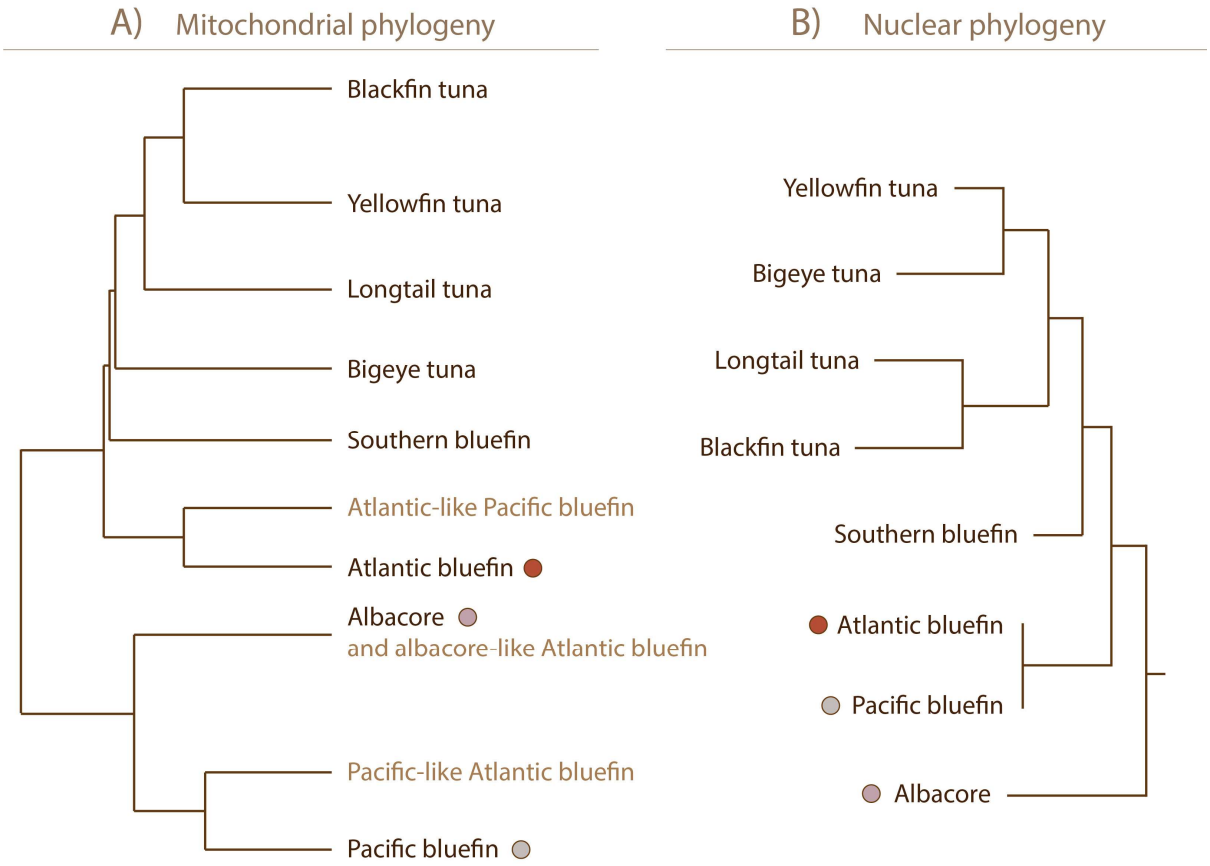

Figure 2: Thunnus phylogenies based on A) the mitochondrial control region adapted from Viñas & Tudela (2009) and B) genome-wide nuclear markers adapted from Díaz-Arce et al. (2016). Tip labels in light brown represent introgressed mitochondrial sequences. The colored circles mark species presented in this thesis.

Introgression is a common phenomenon in fish (Smith, 1992). In tuna, mitochondrial introgression has been demonstrated from both albacore and Pacific bluefin into the Atlantic bluefin (Alvarado Bremer et al., 2005; Carlsson et al., 2004; Chow & Kishino, 1995; Rooker et al., 2007; Viñas et al., 2003, 2011; Viñas & Tudela, 2009). Directional introgression has also been found from the Atlantic bluefin and albacore to the Pacific bluefin (Chow et al., 2006; Chow & Inoue, 1993; Chow & Kishino, 1995; Viñas & Tudela, 2009).

In the Atlantic bluefin, the frequency of introgression from albacore and Pacific bluefin is similar, although relatively rare at around 2-5% (Rooker et al., 2007; Viñas & Tudela, 2009), indicating that cross-species hybridizing occurs with some degree of regularity and between the different species. Interestingly, all introgressed individuals in these studies were sampled from the Eastern Atlantic or Mediterranean Sea, and several studies sampling across the Atlantic find samples with signs of introgression only among the Eastern stock samples (Boustany et al., 2008; Carlsson et al., 2007; Rooker et al., 2007). As of yet, no signs of

introgression have been found in the Western stock, further supporting some trans-Atlantic substructure.

Introgression may indicate range expansion of one or both of the involved species, or alterations in spawning time or location so that hybridization between previously seasonal or geographically separated species becomes possible. Further investigation is needed to clarify whether these introgression events began before, after, or during the most recent glacial period, or if there is a hybridization pattern over time connected to paleoclimatic events. It is not unlikely that the introgression events might be connected to changing climate, as the distribution of Atlantic tuna is thought to have fluctuated corresponding to the Quaternary glacial cycles (Alvarado Bremer et al., 2005). Global warming might alter both migration patterns and preferred locations for spawning for the Atlantic bluefin in the coming years (Faillettaz et al., 2019), which would have implications for stock management.

1.4 Ancient DNA: A useful tool

To investigate the timing of introgression events, as well as potential changes in population structure and genetic subdivision in the stocks over time, ancient samples provide a unique opportunity for inference. For instance, the genetic effects of human exploitation can only be directly compared using ancient DNA, providing non-extrapolated information about past genetic variation and population structure. Methods based on modern DNA depend on backwards-in-time modelling to infer change in genetic variation over time, using underlaying assumptions which may potentially be biased. All models contain uncertainty in their estimates, whereas empirical evidence provide a more solid basis for inference. Direct observation of ancient DNA may for example reveal genetic variation that is no longer present in the modern populations, and which would therefore have been excluded from modern-DNA-based models.

Some analyses of ancient and historical DNA from Atlantic bluefin has been done, including SNP-genotyping (Andrews et al., 2021; Puncher, Cariani, et al., 2015), microsatellite variation of more recent historical samples (Riccioni et al., 2010) and optimalization of laboratory extraction protocols (Puncher, 2015; Puncher et al., 2019). However, these approaches are limited in that a restricted number of molecular markers have been studied. Whole-genome sequencing approaches incorporate genome-wide mutations and structural variation, increasing the statistical power for detection of signatures of selection and population genomic structure (Fuentes-Pardo & Ruzzante, 2017). In addition, the inclusion of a wide diversity of genetic

variations could reduce bias compared to sampling fewer genetic markers. As of yet, whole-genome sequencing of ancient Atlantic bluefin has not been done.

In the past three decades, the field of aDNA has advanced from extraction of small fragments of multicopy DNA to targeted nuclear loci, population scale studies and full genome sequencing (Nistelberger et al., 2019; Willerslev & Cooper, 2005). Most aDNA studies have focused on mammals, whose bones are physiologically different from fish. Although teleost fish bones are often more brittle and lightweight, they do not remodel during growth, do not usually store calcium and some lack osteocytes (Ferrari et al., 2021). These qualities likely increase the likelihood of finding well preserved DNA (Ferrari et al., 2021; Kontopoulos et al., 2019; Szpak, 2011) allowing the application of whole genome aDNA approaches targeting fish (e.g., Star et al., 2017).

One of the challenges of analyzing archaeological and archival specimens is the degradation of DNA over time. Low, stable temperatures likely aid the preservation of DNA (Wayne et al., 1999), thus sequencing of ancient DNA from high-latitude sites may be more successful than analyses of specimens exposed to warmer climates and higher extreme temperatures. Scandinavia is therefore a region in which archaeological specimens have a higher chance of yielding useable and high-quality ancient DNA sequences. In Scandinavia, Atlantic bluefin remains have been excavated from several archaeological sites including Neolithic Skipshelleren (Olsen, 1976), Alveberget (Mansrud & Berg-Hansen, 2021), Ånneröd (Alin, 1955), Gröninge (Särlvik, 1976), Sandhem (Jonsson, 2007), Hakeröd (Jonsson, 2002), Stora Förvar (Ericson, 1989; Knape & Ericson, 1983) and late Mesolithic settlements in Italiensvej and Tågerup (Enghoff et al., 2007; Karsten & Knarrström, 2003) (Figure 3). Many more wetland sites in the South of Norway remain poorly investigated (Nielsen & Persson, 2020). None of the Atlantic bluefin specimens from these sites have yet been analyzed for DNA or other biomolecular markers, but the low and less extreme temperatures along these northern temperate coastal sites makes for promising molecular preservation.

1.5 The Jortveit archaeological site

New findings from recent excavations at Jortveit, a wetland agricultural field in the municipality of Grimstad in the south of Norway, show signs of seasonal fishing of Atlantic bluefin in the Scandinavian Early and Middle Neolithic period (3900-2350 BCE) (Nielsen & Persson, 2020). The Jortveit findings include tools such as arrow heads, axes, toggling harpoons, torches, and fishing hooks, as well as bones from Atlantic bluefin and orca (*Orcinus*

orca), all dating back to a time interval where the Jortveit wetland site was a saltwater lagoon (3900-2500 BCE). The water turned brackish ca. 500 BCE due to continued post-glacial isostatic rebound (Nielsen & Persson, 2020). Nielsen and Persson (2020) propose the hypothesis that tuna and orca chased schools of herring into the lagoon, where the tuna was pierced with toggling harpoons attached to long ropes. Trying to free itself from the fishing gear, some of the tuna presumably swam down, dragging the gear with it and subsequently died at the sea bottom. This location represents the first ever recorded use of toggling harpoons in Norway, previously only dated back to the mid-18th century CE (Lindquist, 1994; Nielsen & Persson, 2020). Containing more tuna bones than any other known sites in Scandinavia, the Jortveit excavations provide a unique opportunity for a population scale study and comparative analyses of ancient and modern tuna.

Figure 3: The Jortveit site, and other Neolithic sites along the Skagerrak coast where Atlantic bluefin tuna bones have been found.

1.6 Project aim

This thesis aims to determine whether there is loss of genetic variation in the heavily exploited modern population compared to the pre-historic natural population of Atlantic bluefin tuna. Focusing on population genomic approaches on whole mitochondrial data, I investigate if and how human exploitation has affected the genetic diversity and evolution of this commercially important species. Understanding the population dynamics in a larger timeframe will provide better context when assessing the natural baseline for comparison to modern management practices. Through genetic investigations of Atlantic bluefin specimens from before the abundance and possibly the genetic variation in the population was reduced, a more solid basis can be provided for conservation and management decisions.

The use of ancient DNA (aDNA) can provide an opportunity for novel insights into bluefin population structure and demographic history, past introgression events and responses to oscillating ocean temperatures. Side-by-side comparison of modern and ancient DNA sequences liberates this study from potentially biased assumptions and uncertainties associated with backwards-in-time modelling by revealing a direct glimpse into the past. Few studies have investigated aDNA from fish on a population size scale, and the tuna bones from Jortveit will be the amongst the oldest fish genomes yet sequenced. In recent years, sequencing technologies and laboratory techniques have drastically improved, resulting in a rapid expansion of aDNA studies. However, few studies have focused on ancient fish, although abundant bone material is expected to accelerate the work in the coming years (Ferrari et al., 2021). By successfully retrieving mitochondrial genomes of Atlantic bluefin tuna from the Jortveit wetland site and comparing to modern conspecifics from across the Atlantic Ocean, I provide the oldest population scale mitogenomic baseline comparison of Atlantic bluefin tuna.

In this study, 39 Neolithic bluefin specimens from the Jortveit excavation are compared to 78 modern bluefin specimens from the coast of Norway, and the Mediterranean and Gulf of Mexico spawning areas (Figure 1). To ensure known spawning origin, the Mediterranean and Gulf of Mexico samples are all larval or young-of-the-year (YoY) samples. Covering each of the three major spawning areas within the Mediterranean allows for population structure investigations also within the Mediterranean Sea. The modern specimens from Norway are foraging adult fish, sampled from commercial fisheries. Mitochondrial genomes were favored over whole-genome nuclear sequence data in this study, as these are more economically obtained, especially from the ancient samples, and a higher number of samples could therefore be included in the analyses.

1.7 Interdisciplinary collaboration

Interdisciplinary work depends on a lot of people, and during this project I've had the pleasure of working with archaeologists, fisheries scientists, and biologists from a handful of different institutions.

Svein Vatsvåg Nielsen and Per Åke Persson at the Cultural history museum, UiO, performed the excavation at the Jortveit wetland site, and collected all ancient specimens used in this project.

The modern samples from Norway were provided by the Institute of Marine Research (IMR), in collaboration with Ørjan Sørensen, Keno Ferter, Martin Wiech, Adam Custer, Christine Djønne and Leif Nøttestad.

The modern young-of-the-year (YoY) samples from across the Mediterranean Sea were provided through collaboration with Adam J. Andrews, Fausto Tinti, Alessia Cariani and the GenoDREAM Group at the Department of Biological, Geological and Environmental Sciences, at the University of Bologna (Ravenna, Italy).

The modern larval samples from the Gulf of Mexico were provided by Estrella Malca and Glenn Zapfe at NOAA Early Life History Unit (Miami, USA) and the NOAA Restore Project.

The Atlantic bluefin samples from the Mediterranean Sea and the Gulf of Mexico, as well as the albacore samples from the Bay of Biscay were processed by Adam J. Andrews, Federica Piattoni, Elisabetta Cilli and Sara De Fanti at the Departments of Biological, Geological and Environmental Sciences, and Cultural Heritage at the University of Bologna (Ravenna, Italy), who performed the genomics laboratory work prior to sequencing for these samples.

2. Material and Methods

2.1 Collection and processing of ancient specimens

All ancient samples were obtained from three archaeological excavations at Jortveit from 2018 to 2020. These excavations were led by Svein Vatsvåg Nielsen and Per Persson from the Cultural History Museum in Oslo. Nine shafts, each approximately 1-1.5 meter in depth and with similar stratigraphical profiles, were excavated. Tuna bones were found at varying depths (42-130 cm) in six of the shafts. Based on carbon dating of wood and charcoal from the sediment profiles, the tuna bones were estimated to be from 4095-4930 BP (2020). Three of the ancient tuna bones were directly carbon dated (Nielsen, 2020b) to approximately 4600 years old (BP 2020). Coordinates, shaft and layer ID, sample depth and sampling date can be found in Appendix A (Table A). Detailed information about the excavation, including sediment dating and stratigraphy, can be found in the archaeological reports (Nielsen, 2020a, 2020b, 2020c) and published paper (Nielsen & Persson, 2020).

All laboratory protocols prior to PCR were performed in a dedicated aDNA laboratory at the Institute of Biosciences, University of Oslo, following strict anti-contamination protocols (Cooper & Poinar, 2000; Gilbert et al., 2005; Llamas et al., 2017).

Upon introduction to the aDNA lab, bones were photographed (Appendix B, Figure S1) and brush-cleaned using a clean toothbrush. Bones were then exposed to UV light for 10 minutes on each side, receiving a total dosage of 4800 J/m^2, to destroy surface DNA from contaminants. The bones were then cut using an electric dentistry tool with an attached cutting disc. Some of the samples were sandblasted prior to cutting (Appendix A, Table S4) using a Renfert Basic Quattro IS sandblasting machine with grainsize 25µm, to remove surface contamination on the bone and again UV-ed at a total dosage of 4800 J/m^2. The cut fragment from each bone was then crushed using a custom designed stainless-steel mortar in the milling room, as described in Gondek, Boessenkool, and Star 2018. Two tubes of milled bone-powder, each 200mg, were set aside for extraction for each sample.

All samples were extracted using a standard extraction protocol adapted from (Dabney et al., 2013). Before extraction, all samples went through a pre-digestion step (DD from Damgaard et al. 2015). Several of the samples also underwent a bleach treatment using the BLEDD protocol from Boessenkool et al. 2017 (Appendix A, Table S4). MinElute purification was performed on a vacuum manifold system (QIAvac 24 Plus, Qiagen).

Sequencing libraries were built following Meyer and Kircher (2010) with modifications, or the Santa Cruz Reaction (SCR) single-stranded library protocol from Kapp, Green, and Shapiro (2021) (Appendix A, Table S4). The double stranded, blunt-end libraries described in Meyer and Kircher 2010 were built using modifications from Schroeder et al. (2015), and all reactions were performed in half volumes to reduce the use of chemical enzymes. These libraries were all built from 20 µL of ligated DNA extract or extraction blanks.

The single stranded libraries were built from 3-20 µL of ligated DNA extract (depending on the DNA concentration) or 20 µL extraction blanks following the SCR protocol using dilution tier 4, which is the second lowest adapter dilution tier described in Kapp, Green, and Shapiro 2021. Titration of the adapters according to input DNA concentration is necessary to reduce adapter dimers in the final library, and Kapp et al. provides an adapter dilution series with five levels of adapter concentrations to be used across given ranges of DNA. However, using higher concentrations of adapters (tier 1-3) resulted in many dimers in the finished libraries of even high concentration samples (Appendix B, Figure S2), and therefore tier 4 was preferred for all samples TUN034-57.

Sample extracts were subject to 12 cycles of PCR, while extraction blanks were subject to 30 cycles of PCR to increase the chance of detecting contamination. Libraries were amplified and cleaned using the Agencourt AMPure XP PCR purification kit (Bronner et al., 2013). Libraries were then examined on a Fragment Analyzer™ (Advanced Analytical) using the High Sensitivity NGS Fragment Analysis Kit to determine suitability for sequencing. Sequencing and demultiplexing, allowing for zero mismatches, was performed at the Norwegian Sequencing Center on a combination of the HiSeq 2500, HiSeq 4000 and NovaSeq SP Illumina sequencing platforms.

2.2 Collection and processing of modern specimens

2.2.1 Norway

Modern tuna tissue samples from Norway were collected by the Norwegian Institute of Marine Research (IMR) from commercial catch off the coast of Møre og Romsdal. Two batches were obtained: The first batch of modern samples (M-TUN002 to M-TUN014) were collected in September 2018, while the remaining samples were collected in September 2020. Each batch of samples were taken from the same fishing net, and the individuals in each net are assumed to belong to the same school.

The 2018 batch of modern samples were freeze dried muscle tissue samples, frozen and powdered on site by the IMR. Samples M-TUN002, 3 and 4 were sampled from the same individuals as M-TUN005, 6 and 7 respectively and were therefore not processed in the lab or sequenced. The 2020 batch of modern samples were skin samples cut out between the spines of the dorsal fin and submerged immediately in RNAlater. The RNAlater reagent acts to stabilize and protect RNA and DNA in the cells of unfrozen samples, eliminating the need to freeze the samples in liquid nitrogen. By inactivating RNAse and DNAse enzymes, RNAlater preserves RNA and DNA in tissues for up to 1 day at 37°C, 1 week at 25°C, 1 month at 4°C, or long-term at -20 °C (ThermoFisher, 2022). After collection, the sample tubes with the fin clips were stored in a fridge for less than one week before being shipped to the laboratory in Oslo where they were placed directly in a -20°C freezer.

Total weight (TW) and curved fork length (CFL) was estimated for the 2020-batch of modern samples, after the tunas were weighed and sampled onshore. As the head and intestines had been removed by the fishers during harvesting, the weight was multiplied with a factor of 1.26 to estimate the total weight (TW) of each fish. Curved fork length (CFL) was calculated based on ICCAT's official formula for CFT-TW conversion as listed in the international sampling report form (ICCAT, 2022):

$$CFL = 2.7901\sqrt{\frac{TW}{0.000050265}}$$

The modern samples from Norway were all extracted in the modern DNA isolation laboratories at CEES, UiO, using the DNeasy Blood & Tissue kit (Qiagen), and following the "Purification of Total DNA from Animal Tissues (Spin-Column Protocol)" from the manufacturer (DNeasy Blood & Tissue Handbook 07/2006, page 28-30) with modifications for optimal lysis and DNA yield. Modifications to the extraction protocol are described in Appendix C.

After extraction, determination of DNA concentration was done for all eluates by fluorescence spectrometry on a Qubit® Flurometer (Invitrogen), using a Qubit™ dsDNA BR (Broad Range) Assay Kit (Thermo Fisher Scientific, USA). The DNA quality was assessed in selected samples, using gel electrophoresis to determine the length of the DNA fragments and a UV spectrophotometer (NanoDrop® ND-1000 V3.1.0) to determine the presence of contaminants. During gel electrophoresis, 3 µL of DNA isolate with 1 µL of gel loading buffer was run on a 1% Agarose gel at 100 Volt for 40 min, and the gel was inspected in a VWR® Smart3 Gel

Documentation system, comparing the samples to a GeneRuler 1 kb 0.1 µg/µL DNA ladder (ThermoFisher). After quantity and quality assessment, only first elutions were used for sequencing as these had higher quality DNA (Appendix B, Figures S3-S4).

Before sequencing, most of the extracts were diluted with EB buffer to achieve a concentration of 20 ng/µl, ensuring that all samples had a similar concentration to enable automated processing. Five low-concentration samples were concentrated using a Savant DNA120 SpeedVac concentrator (Thermo Scientific) (Appendix A, Table S5). Libraries were built by the Norwegian Sequencing Centre using a TruSeq DNA Nano200 preparation kit (Illumina), before sequencing and demultiplexing, allowing for zero mismatches on a combination of the HiSeq 2500, HiSeq 4000 and NovaSeq SP Illumina sequencing platforms.

2.2.2 Mediterranean, Western Atlantic, and Bay of Biscay

In addition to the modern and ancient samples from Norway, I received DNA sequence data from various locations, including: young-of-the-year (YoY) Atlantic bluefin from the Central-, Eastern-, and Western Mediterranean; Atlantic bluefin larval samples from the Gulf of Mexico (GOM); and juvenile albacore (*Thunnus alalunga*) samples from the Bay of Biscay. The Mediterranean samples were obtained by commercial fisheries and scientific surveys, and were all sampled in the context of the Rodríguez-Ezpeleta et al. 2019 study. These samples were all collected from "YoY" bluefin, meaning individuals which had hatched within the same year of sampling. Sampling individuals that are too young to migrate ensured that the sampling site reflected the true spawning origin. The GOM-samples were obtained in the context of the Johnstone et al. 2021 study, and detailed sampling information can be found there. The juvenile albacore samples from the Bay of Biscay were caught by commercial vessel trolling in the summer months between June and September of 2010 and stored in ethanol at sea and have not been published in other studies. All available metadata for the Mediterranean, GOM and albacore samples can be found in Appendix A (Table S3), and the sampling locations are shown in Figure 1.

The samples mentioned above were all extracted at the University of Bologna by a modified salt-based extraction protocol, as per Cruz et al. (2017), using SSTNE extraction buffer (Blanquer, 1990), and treated with RNase to remove residual RNA. After extraction, the total DNA obtained from each extraction was quantified using a Qubit® dsDNA BR Assay Kit (Thermo Fisher Scientific, USA). Negative controls employed for each batch of samples extracted indicated an undetectable level of contamination. Samples were diluted to 10 ng/ul

and 100 ul of DNA was sheared to target sizes of 550 bp using Medium 30 on /90 off for 10 minutes using a Bioruptor ® Pico sonication device (Diagenode). Samples were precipitated using isopropanol, following the suggested procedure from Qiagen (FAQ-ID-2953). Single stranded libraries were built from 20 µL of ligated DNA extract, following the SCR library protocol (Kapp et al., 2021). QPCR was used to decide number of required cycles for indexing (as per the SCR method), and extracts were subject to 10-14 cycles of PCR for double-index barcoding using standard Illumina barcodes. Sequencing and demultiplexing, allowing for zero mismatches, was performed at the Norwegian Sequencing Center on a combination of the HiSeq 2500, HiSeq 4000 and NovaSeq SP Illumina sequencing platforms.

Pacific bluefin whole genome raw sequence data from a recently published study (Suda et al., 2019) was downloaded and used for interspecific population structure analyses. Sample-ID's, databank identifier code and URL are listed in Appendix A (Table S6). The Pacific bluefin samples were collected by the Nansei Islands, between Japan and Taiwan, in 2015 (Suda et al., 2019).

2.3 Bioinformatic processing of ancient and modern sequence data

Both modern and ancient reads were processed using the Paleomix pipeline v.1.2.14 (Schubert et al., 2014). Using AdapterRemoval v.2.3.1 (Schubert et al., 2016), adapters were removed and forward and reverse reads were collapsed and trimmed, discarding collapsed reads shorter than 25 bp. Reads were aligned to an unpublished Atlantic bluefin reference genome provided by a collaborator, and the NCBI Thunnus thynnus mitochondrial reference sequence (GenBank accession nr NC_014052.1) using BWA v.0.7.17 (Li & Durbin, 2009). BWA-mem, which is designed for longer Illumina sequence reads (70bp-1Mbp) was used for mapping in the modern samples, and BWA-aln, which is designed for shorter Illumina sequence reads (<100bp), was used for mapping in the ancient samples. For the modern samples, seeding was used to decrease the running time, while for the ancient samples seeding was disabled to improve the alignment of damaged DNA.

All reads were filtered to a minimum Phred score quality of 25, so that only reads with higher mapping quality to the reference genome were considered endogenous and used for subsequent analyses. PCR duplicates were removed in Picard Tools v.2.18.27 and indel realignment (*GATKs IndelRealigner*) was preformed to produce final BAM files. DNA post-mortem damage patterns were assessed in mapDamage v.2.0.9 (Ginolhac et al., 2011; Jónsson et al., 2013) after downsampling to 100,000 randomly selected reads.

The mitochondrial bamfiles were further processed in GATK v.4.1.4.0 following GATK best practices (McKenna et al., 2010). Individual genotypes were called (GATK v.4.1.4.0 *HaplotypeCaller -ploidy 1*) and then combined into a joint gvcf (GATK v.4.1.4.0 *CombineGVCFs*) before genotyping (GATK v.4.1.4.0 *GenotypeGVCFs*). Genotypes were hard-filtered in BCFtools v.1.9 (Li et al., 2009) (*-i 'FS<60.0 && SOR<4 && MQ>30.0 && QD > 2.0' --SnpGap 10*) and VCFtools v.0.1.16 (Danecek et al., 2011) (*--minGQ 15 --minDP 2 --remove-indels*). The filtering options are described in Appendix A (Table S7).

Filtered VCFs were indexed using Tabix v.0.2.6 (Li, 2011) and consensus sequences created as individual fasta files in BCFtools v.1.9 (bcftools consensus *-H 1*). Outgroup sequences (Appendix A, Table S8) were downloaded from GenBank (Clark et al., 2016) and curated using SeqKit v. 0.11.0 (*restart -i*) (Shen et al., 2016) so that all sequences started at position 1 in the D-loop, to correspond with the sample sequences. After renaming the fasta headers to their appropriate sample-IDs using BBMap v.38.50b (Bushnell, 2014) and combining the files to a multiple sequence alignment (MSA), the joint fastas were aligned using MAFFT v.7.453 (Katoh et al., 2002) (*--auto*).

2.4 Exploratory analyses

The genotyping and filtering process in the GATK pipeline is affected by the haplotype variants present in the analyses. Calling and filtering samples separately and later combining them together in a multiple-fasta, or jointly calling and filtering samples and later excluding specific samples or variants may therefore introduce inaccurate patterns in subsequent analyses (GATK, 2016). This is because genotype likelihoods and variant recalibration are calculated based on the observed haplotypes during variant discovery (Poplin et al., 2018). To accurately present the variation within each dataset, only samples within the chosen datasets should be called and filtered together (GATK, 2016). Joint calling of the samples within each dataset improves sensitivity at low coverage positions and makes the filtering process more statistically accurate, compared to calling individual samples or subsets (Poplin et al., 2018).

Dividing samples into subsets based on location and patterns of introgression prior to calling and filtering was preferred so that the variation within each subset would be accurately presented. Before these subsets could be determined, exploratory analyses were preformed to look for samples with high missingness, identical samples, and highly divergent or introgressed mitochondrial genomes. Such samples may be excluded from certain analyses, in which instance they should also be excluded from the calling and filtering process prior to those

analyses as to not affect the GATK variant discovery calculations among the remaining samples.

Preliminary analyses to determine datasets were performed on a jointly called and filtered multiple-fasta, which included all samples. Missingness and depth was assessed for all samples using VCFtools v.0.1.16 (Danecek et al., 2011) (*--freq2, --depth, --site-mean-depth, --missing-site, --missing-indv*), and plotted in with R v.4.1.2 (R Core Team 2021) in RStudio (Rstudio Team 2021) using ggplot in tidyverse (Wickham et al., 2019). Principal Component analyses (PCA) (Adegenet (Jombart, 2008) in R v.4.1.2) and a Maximum Likelihood (ML) tree (IQTREE v. 1.6.12 (Nguyen et al., 2015), *-m MFP -bb 1000 -BIC*) was used to investigate clustering patterns and assess the presence of introgressed mitochondrial genomes. A skipjack tuna (*Katsuwonus pelamis*) individual obtained from GenBank (Clark et al., 2016) (pelamis_NC_005316_1, Appendix A Table S8) was used as outgroup in the ML analysis. To look for identical haplotypes, a unique-SNPs evaluation was done using custom python3.9 (Rossum and Drake 2009) script (Atmore, 2021) which calculated the number of SNP differences between all individuals, using differently filtered multiple-fasta files as input and outputting distance matrixes.

After discovering several identical samples in the dataset, different filtering values were explored to determine the threshold of when these samples become identical. The most significant change occurred between VCFtools filtering at *minDP2* versus *minDP3*. After thoroughly assessing the number of SNPs separating the similar samples at different filtering settings, ancient samples were discarded if they showed zero SNP differences at minDP2 *or* if they had less than 2 SNP differences at minDP3 *and* came from the same archaeological layer in the same shaft (Appendix A, Table S1). When selecting which of two or more identical samples to discard, the specimen with the highest endogenous DNA content was kept. Identical modern samples (6 pairs, listed in Appendix C) were kept due to the modern sampling method ensuring capture of distinct individuals. All samples with missingness above 50% (VCFtools v.0.1.16 *--missing-indv*, F_MISS) were also discarded.

The exploratory analyses revealed several samples showing strong signs of introgression by clustering with either the albacore or pacific bluefin samples in the PCA (Appendix B, Figure S13). This was supported by the ML tree, which revealed the same individuals falling into highly supported monophyletic clades with the same outgroup species (Appendix B, Figure S14). To allow for investigations of mitogenomic variation within and between locations, both

with and without the presence of introgressed mitochondrial genomes, 15 final datasets were created. Such datasets with and without introgressed genomes were created as these genomes can have a disproportionate impact on the outcome of specific genetic analyses. These introgressed genomes are also fairly rare, which means that randomness due to sampling (or not sampling) these may affect results.

Final datasets were created for each modern sampling location (**NorwayAll**, Eastern Mediterranean (**EMED**), Central Mediterranean (**CMED**), Western Mediterranean (**WMEDAll**) and the Gulf of Mexico (**GOM**) and for the ancient samples from Jortveit (**AncientAll**). Where individuals with likely introgressed mitochondrial genomes were found, a second dataset excluding the introgressed individuals were created (**NorwayExIntrog**, **WMEDExIntrog**, **AncientExIntrog**). In addition, a dataset combining all modern Atlantic bluefin samples (**modernABFT**), a dataset combining all modern Atlantic bluefin samples except the introgressed individuals (**modernExIntrog**), a dataset combining both modern and ancient Atlantic bluefin samples (**AllABFT**) and a dataset combining modern and ancient Atlantic bluefin samples except the introgressed individuals (**AllExIntrog**) were created. Lastly, a dataset including all the Atlantic bluefin specimens and the albacore samples from Bay of Biscay (**All_alb**) and a dataset including all the Atlantic bluefin specimens and both the albacore samples and the Pacific bluefin samples from Suda et al. (2019) (**All_alb_pac**) were created. An overview of the datasets can be found in Table 1. The datasets were separately genotyped, filtered, and aligned as described in Section 2.3 to create respective multiple-fastas for subsequent analyses.

Table 1: Jointly called and filtered datasets, used in population genomic analyses (N = number of samples in each dataset).

		Location	Subset Code	N
Containing samples with signs of introgression	Modern	Norway	**NorwayAll**	38
		Western Mediterranean	**WMEDAll**	10
		All modern ABFT locations	**modernABFT**	77
	Ancient	Jortveit excavation	**AncientAll**	21
	Both modern and ancient	All ABFT locations	**AllABFT**	98
No introgressed samples present	Modern	Norway	**NorwayExIntrog**	35
		Eastern Mediterranean	**EMED**	10
		Central Mediterranean	**CMED**	9
		Western Mediterranean	**WMEDExIntrog**	9
		Gulf of Mexico	**GOM**	10
		All modern ABFT locations	**modernExIntrog**	73
	Ancient	Jortveit excavation	**AncientExIntrog**	20
	Both modern and ancient	All ABFT locations	**AllExIntrog**	93
Datasets with jointly called and filtered outgroup species	All samples in AllABFT + All albacore samples	All ABFT locations + Bay of Biscay	**All_alb**	104
	All samples in AllABFT + All albacore samples + All Pacific bluefin samples	All ABFT locations + Bay of Biscay + Nansei Islands	**All_alb_pac**	113

2.5 Population genomic analyses

2.5.1 Population structure and introgression

Genetic population structure was investigated using Principal Component analyses (PCA) as implemented in the Adegenet package (Jombart, 2008) in R v.4.1.2 (R Core Team 2021). Two datasets were used in the PCA analysis: **All_alb_pac** was used to investigate the interspecific structure between Atlantic bluefin, Pacific bluefin and albacore, and **AllExIntrog** was used to investigate the intraspecific structure within the non-introgressed Atlantic bluefin samples. A map of missing loci and alleles diverging from the reference genome across all SNPs within the **AllABFT** dataset, was created to assess missing genotypes in both ancient and modern samples and better visualize introgressed specimens. All plots were designed in RStudio

(Rstudio Team 2021), using various packages for data loading, analyses, and visualization (Appendix C).

2.5.2 Mitogenomic variation

Genetic diversity was investigated using a range of standard population genetic measurements. The number of haplotypes (Nh) and haplotype diversity (hD) (Nei 1987) was calculated in pegas (Paradis, 2010) with R v.4.1.2 (R Core Team 2021) for all Atlantic bluefin datasets (Section 2.4, Table 1). Nh was independently assessed in Fitchi (Matschiner, 2016). A haplotype is the set of genes inherited from a single parent. In mitochondrial analyses the whole mitochondrial genome can be viewed as a single haplotype. The number of segregating sites (S), nucleotide diversity (π) (Nei 1987), Tajima's D (TD) (Tajima, 1989) with statistical significance, and Fu and Li's F statistic (F) (Fu & Li, 1993) with statistical significance, using skipjack tuna (pelamis_NC_005316_1, Appendix A, Table S8) as an outgroup, were calculated in DnaSP v.6 (Rozas et al., 2017) for all Atlantic bluefin datasets (Section 2.4, Table 1). S, π, TD values were also confirmed in pegas for all Atlantic bluefin datasets (Section 2.4, Table 1). To account for differences in sample sizes across sites when calculating π and TD, an additional analysis using 1000 bootstrap replicates and subsampling n=5 individuals per round without replacement, was performed in pegas on the datasets consisting of non-introgressed samples from separate locations (**AncientExIntrog**, **NorwayExIntrog**, **EMED**, **CMED**, **WMEDExIntrog**, and **GOM**, Section 2.4, Table 1).

As mentioned earlier, the genotyping and filtering process in the GATK pipeline is affected by the haplotype variants present in the analyses. It is recommended that each dataset should be separately called and filtered, so that the calculation of genotype likelihoods is not affected by haplotypes that are not part of the focal dataset (GATK, 2016). However, using fewer samples may reduce sensitivity at low coverage positions and make the filtering process less statistically accurate (Poplin et al., 2018). To investigate whether using jointly versus separately called and filtered datasets affected the statistics, S, π, TD and F were also calculated on the jointly called and filtered dataset **AllABFT** with populations specified in DnaSP v.6 using the *DNA Polymorphism/Divergence Analysis* option in *BatchMode*, with *K. pelamis* (NC_005316.1, Appendix A, Table S8) as an outgroup.

Evolutionary relationships were visualized using haplotype networks created in Fitchi (*--haploid*) (Matschiner, 2016), using two datasets: **All_alb** using all outgroups (Appendix A, Table S8) and **AllExIntrog** using one Pacific bluefin individual as outgroup (NC_008455.1,

Appendix A, Table S8). Fitchi takes a Nexus file format input containing sequence alignments and a phylogenetic tree. IQTREE v. 1.6.12 (Nguyen et al., 2015) was used to generate a ML input tree, using ModelFinderPlus (MFP) (Kalyaanamoorthy et al., 2017) to search for and select the best-fit model according to the Bayesian Information Criterion (BIC) (Schwarz, 1978) for both datasets. Bootstrap values were removed from the ML-tree in ape (Paradis et al., 2004) with R v.4.1.2 (R Core Team 2021), and the fasta-files of the two datasets were converted to Nexus format in AliView v.1.27 (Larsson, 2014) before each phylogenetic tree was manually added to the bottom of the respective Nexus files. Subpopulations and outgroups were defined in Fitchi (*-p*). For the **All_alb** dataset, a minimum edge length of 7 substitutions was defined (*-e 7*) so that haplotypes separated by 7 or less substitutions were collapsed into one node. For the **AllExIntrog** dataset, each node was defined as a unique haplotype (*-e 1*).

2.5.3 Divergence analyses

Genetic distance between sample locations was assessed using measures of absolute (Dxy) and relative (Φst) divergence, calculated using DnaSP v.6 (Rozas et al., 2017) and Arlequin v.3.5 (Excoffier & Lischer, 2010) respectively. Both analyses were preformed using jointly called and filtered datasets **AllABFT** and **AllExIntrog** (Section 2.4, Table 1), with populations specified in DnaSP v.6. Prior to analysis in Arlequin, the MSAs were in edited DnaSP v.6 (*Genome=Haploid, Chomosome Location=Mitochondrial, Sites with gaps = not considered, invariable sites = included*), and the MSAs were converted to Arlequin file formats. In Arlequin, pairwise Φst was calculated based on a distance matrix computed by Arlequin based on Tamura & Nei (1993) and assuming no rate heterogeneity, as suggested for both data subsets by jModelTest v.2.1.10 (Darriba et al., 2012) and bModelTest (R. R. Bouckaert & Drummond, 2017) (implemented in BEAST 2 v.2.6.4 (R. Bouckaert et al., 2014)). To test the significance of Φst, p-values were generated in Arlequin using 1000 permutations.

2.5.4 Phylogenetic analyses

Evolutionary relationships between specimens were investigated using both ML and Bayesian approaches as implement in IQTREE v. 1.6.12 (Nguyen et al., 2015), MrBayes v.3.2.7a (Ronquist et al., 2012; Ronquist & Huelsenbeck, 2003) and BEAST 2 v.2.6.4 (R. Bouckaert et al., 2014). Two datasets, **All_alb** using all outgroups (Appendix A, Table S8) and **AllExIntrog** using one Pacific bluefin individual as outgroup (orientalis_NC_008455_1, Appendix A, Table S8), were used to create phylogenetic trees. ML trees for each of the two datasets with 100 nonparametric bootstrap replicates were created in IQTREE v. 1.6.12. ModelFinder Plus

(MFP) (Kalyaanamoorthy et al., 2017) was used to search all available models, and best-fit models were selected according to the Bayesian Information Criterion (BIC) (Schwarz, 1978).

Bayesian trees were created in MrBayes v.3.2.7a and BEAST 2 v.2.6.4. For the MrBayes analyses, jModelTest v.2.1.10 (Darriba et al., 2012) *(-s 11 -f)* was used to search for and select the best fit model according to BIC. Two independent MCMC analyses ran for 6'000'000 generations using one cold and three heated chains and sampling every 100 generations (*nchains=4 nruns=2 samplefreq=100*). The average standard deviation of split frequencies between the two runs were manually evaluated every 1'000'000 generations (*ngen=1000000*), and the runs were terminated when reaching 0.013 for the **All_alb** dataset and 0.029 for the **AllExIntrog** dataset. Convergence between the pairwise runs and effective sample size (ESS) values were inspected in Tracer v1.7.2 (Rambaut et al., 2018).

Bayesian trees in BEAST 2 were created using the Yule model prior under a strict clock with mutation rate 3.6×10^{-8} substitutions per site per year as per Donaldson and Wilson (1999), running MCMC over 800'000'000 generations and sampling every 1000 generation. bModelTest (R. R. Bouckaert & Drummond, 2017) was used to assess available site models, and the resulting logfile was inspected in Tracer v1.7.2 (Rambaut et al., 2018). Trees were downsampled in LogCombiner (implemented in BEAST 2 v.2.6.4), resampling every 100'000 trees for the **All_alb** dataset and every 10'000 trees for the **AllExIntrog** dataset. TreeAnnotator (implemented in BEAST 2 v.2.6.4) was used to remove the first 10% of the trees (burnin) and create a target maximum clade credibility tree for each of the two datasets, using 7201 trees for the **All_alb** dataset, and 72001 trees for the **AllExIntrog** dataset. Nodes with less than 50% posterior support was excluded from the summary analysis in TreeAnnotator, so that only nodes present in the majority the trees were annotated. The final trees in all phylogenetic analyses were visualized and curated in FigTree v.1.4.4 (Rambaut, 2018).

2.5.5 Demographic reconstruction

Female effective population size (Ne) was modelled back in time using BEAST 2 v.2.6.4 (R. Bouckaert et al., 2014), applying the Coalescent Bayesian Skyline (CBS) prior under a strict clock with mutation rate 3.6×10^{-8} substitutions per site per year as reported for the mtDNA control region in Teleost fish (Donaldson & Wilson, 1999) and commonly used across mitochondrial regions in tunas (Kasim et al., 2020; Kunal et al., 2013; Kumar et al., 2012; Carlsson et al., 2004).

First, the modelling was performed only using modern samples, investigating the effects of introgressed individuals being present in the analysis, using datasets **modernABFT** and **modernExIntrog**. To assess the effect of adding dated ancient samples to the analyses, and whether this would contradict or support the results from the modern datasets, **AllABFT** and **AllExIntrog** were used for modelling, dating all ancient specimens to 4600 BP (using *TipDates*). These datasets were then rerun without dating the ancient samples, to investigate how the model was altered when the ancient samples were assumed to be modern. Finally, analyses of only ancient samples, using the **AncientAll** and **AncientExIntrog** datasets, were performed to examine whether the genetic information in the ancient samples would support the pattern provided by the other models. For all runs, MCMC sampling was done every 1000 generation over a chain length of 800'000'000 and female Ne was calculated over 4 segments (*bPopSizes=bGroupSizes=5*).

All analyses were run independently twice to test for chain convergence. bModelTest (R. R. Bouckaert & Drummond, 2017) was used to select the site model and the chosen model was inspected in Tracer v1.7.2 (Rambaut et al., 2018) along with the traceplots, ESS values, and convergence between the pairwise runs. Bayesian skyline reconstruction was done in Tracer v1.7.2 (*maximum time = lower 95% HPD, root height = TreeHeight*), plotting using the stepwise (constant) Bayesian skyline variant with 100 bins, and the final plots were visualized in RStudio (Rstudio Team 2021) with R v.4.1.2 (R Core Team 2021), using ggplot in tidyverse (Wickham et al., 2019).

3. Results

3.1 DNA yield and library success

The ancient samples showed remarkable DNA preservation with 100% library success and samples yielding, on average, 24% endogenous DNA. A total of 795 million reads were sequenced across the 39 ancient specimens, resulting in 20-fold mt coverage and 0.5-fold nuclear coverage on average. The reads showed those postmortem degradation patterns expected for authentic ancient DNA (Figure 4). The samples that had been through single stranded library preparation yielded higher mt and nuclear coverage, longer reads and average clonality of only 6% compared to 18% for the double stranded library. Paleomix summary statistics for quality are described in Appendix A (Tables S9, S10, S11, S12, S13), and key statistics are summarized in Table 2.

Table 2: Average clonality, endogenous DNA content, mitochondrial and nuclear coverage, and mean fragment lengths for differently processed ancient and modern sample subsets. The clonality and endogenous contents are calculated from the alignment to the nuclear reference genome.

	Average Reads per sample (millions)	Average Clonality (%)	Average Endogenous DNA (fraction)	Average Mitochondrial coverage	Average Nuclear coverage	Average Mean fragment length (bp)
Ancient DS	17	18	0.3	14	0.4	71
Ancient SS	22	6	0.2	25	0.6	101
Norway modern	36	9	0.76	702	9	169
Remaining modern ABFT	38	2.4	0.60	721	2.5	97
albacore	24	2	0.65	221	2	101

A total of 3034 million reads were sequenced across the 83 modern specimens, resulting in 711-fold mt coverage on average for the 77 Atlantic bluefin specimens and 221-fold mt coverage on average for the six albacore samples mapped to the same Atlantic bluefin reference genomes. The nuclear coverage was on average three times higher in the specimens from Norway, which had been processed in the laboratory almost directly after sampling. The Mediterranean and Atlantic specimens from lower latitudes, which had been stored over multiple years before DNA-extraction, had shorter mean fragment length and lower endogenous DNA content than the specimens sampled in Norway. The dried muscle tissue samples from Norway (M-TUN05 – M-TUN014) were sequenced with higher effort, resulting in higher coverage.

The degradation of ancient DNA after death leaves specific, non-random patterns in the sequencing data that was used to authenticate that DNA had been obtained from archaeological specimens. Nonetheless, these patterns are also affected by the type of library preparation used for generating the data (see BOX 1). For instance, the fragmentation plots produced by mapDamage (upper panels in Figure 4) for double stranded libraries reveals an inverse pattern of fragmentation with sequencing the opposite strand (Figure 4a). This pattern is symmetrical for single stranded library preparation, as reads are not filled in using enzymatic approaches based on the opposite strand. Similarly, the bottom panels in Figures A shows the misincorporations, or substitutions, along the forward and reverse strands, relative to the reference. Again, where double stranded libraries show an inverse pattern, this pattern is absent from single stranded libraries. Regardless of the method, all the ancient samples display those

fragmentation and substitution profiles for the reads that are typical for ancient DNA (see BOX 1).

Ancient DNA fragmentation patterns and deamination rates is not expected for modern DNA, as the modern samples are extracted from fresh tissues and have not degraded over time. While the natural fragmentation process is expected to cause non-random variation in the base frequency in and around the ancient reads, the modern fragments have been mechanically sheared at random breakpoints and will have no consistent pattern in the fragmentation plots. The dataset from Norway has very low variation in base frequency, reflecting the high quality of this dataset, while the larger variation in the base frequency along the reads in remaining modern samples is a consequence of the lower nuclear coverage (Table 2). The misincorporation plots of the modern samples indicate no pattern of nucleotide substitutions along the read-ends, as the fragments have remained chemically stable until extraction and sequencing, as opposed to the typically single stranded ends of ancient samples being more exposed to degradation. Fragmentation and misincorporation plots for the albacore and Pacific bluefin samples show a similar profile as the other modern samples (Appendix B, Figure S5).

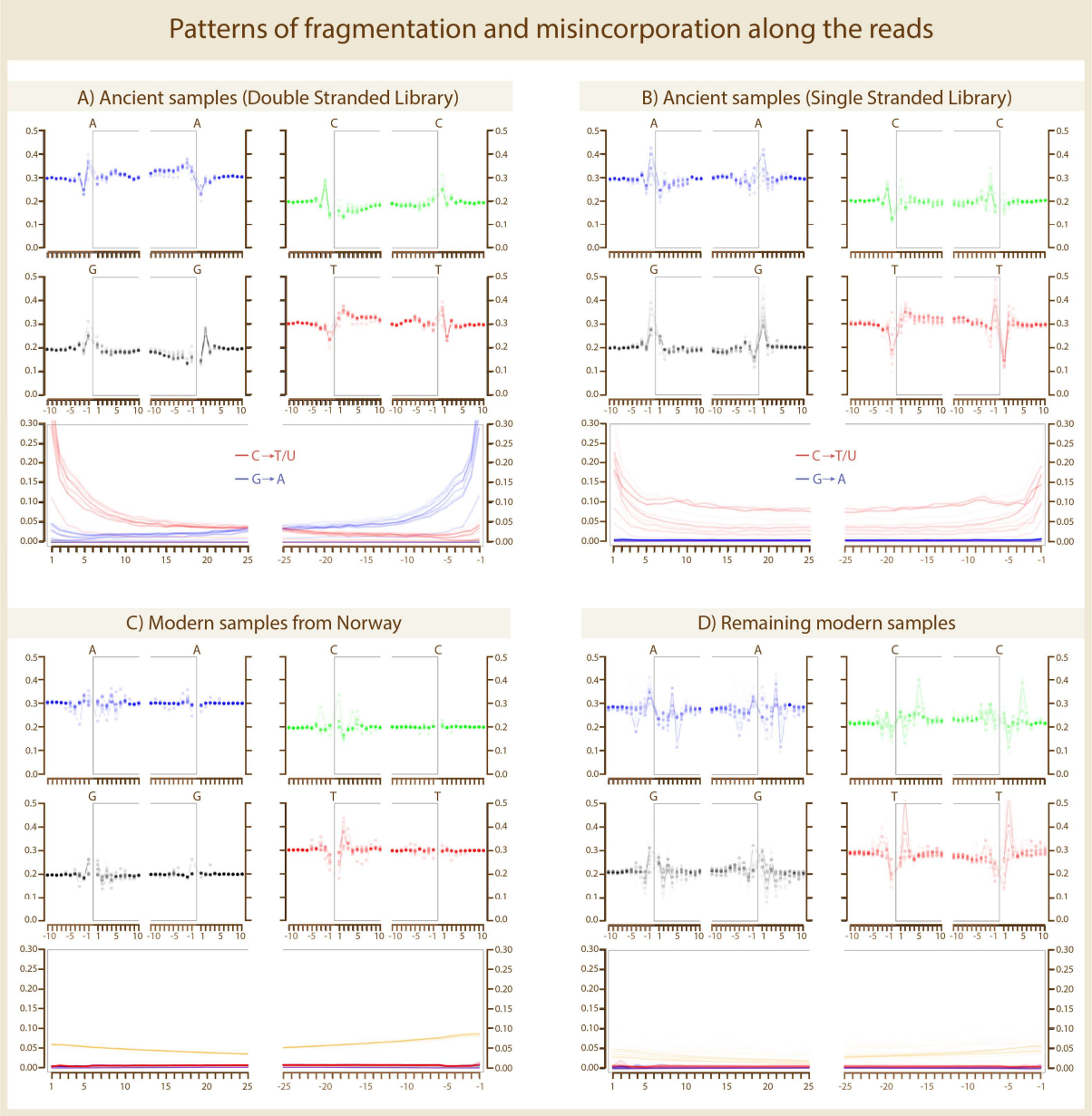

Figure 4: Fragmentation (upper panels) and misincorporation (lower panels) plots from mapDamage v.2.0.9. The fragmentation plots show the base frequency inside and surrounding the read, where the grey box indicates the location of where the reads have mapped to the reference. The misincorporation plots show the rate of substitutions along the positions of the read ends, relative to the reference (Red: C to T. Blue: G to A. Grey: All other substitutions. Green: Deletions. Purple: Insertions. Orange: Soft-clipped bases)

BOX 1: Interpreting mapDamage plots for ancient DNA

Over time, the quality of the DNA decreases due to fragmentation (breaking of the DNA molecule into shorter fragments) and misincorporation (change/replacement of nucleotides in the DNA molecule). During fragmentation, breaking of the forward and reverse strand in different locations often result in fragments with an overhang of single stranded DNA on each side. The DNA breakpoint during fragmentation tends to be located next to an Adenosine (A) or Guanine (G) nucleotide, so that the base closest to the location of our read ends on the reference genome has a higher probability of being an A or a G.

This pattern will be visible as a peak in A or G on both sides of the read if the sample has been through single stranded library preparation, as the reads with their original breakpoints are mapped to a reference so that closest base on the reference to a breakpoint location is A or G on both sides of each read. Low frequency of Cytosine (C) and Thymine (T) on each side of these reads is a statistical consequence of the high frequency of the two other bases. During double stranded library preparation however, the DNA fragments are modified to have blunt ends. On one side of the fragment, the single strand overhang is removed, while on the other side a complementary strand is added to the single stranded overhang to stabilize the fragment. The resulting fragment will have two strands which end in the original breakpoint on one end but are modified on the other end. The modified end will be complementary to the opposite, original strand.

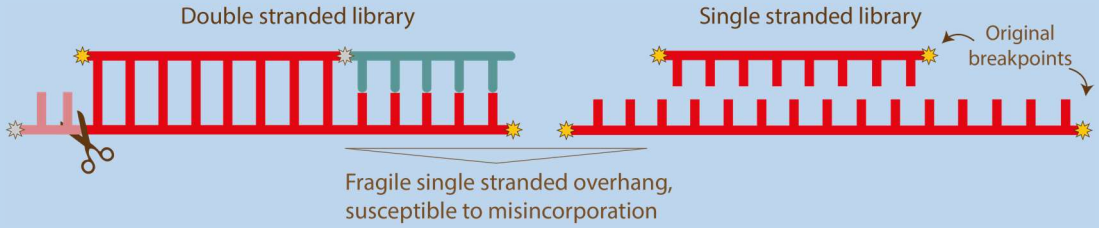

After double stranded library, the reads will therefore show corresponding proportions of the complementary bases; so that when the probability of having an A as the closest base to the read is high on the forward strand, the probability of having a T on the same location in the reverse strand is equally lower. This makes an artificial peak in the frequency of T close to the read-ends, which actually reflects the frequency of A on the complementary strand. Same for G and C.

The single stranded ends that occur during the fragmentation process are more susceptible to misincorporation than the more stable double stranded, middle part of the fragments. During degradation of DNA over time, C is typically replaced with Uracil (U), which is interpreted as T in the sequencing process. The higher rate of degradation in the fragile single stranded ends becomes visible in the misincorporation-plots as an increase in C→T/U substitution rate in positions closer to the read ends. This misincorporation pattern will be visible on both reverse and forward strands of samples that have been though single stranded library protocol. For samples that have been through double stranded library preparation, the G→A substitutions on the reverse strands in the double stranded library protocol is an effect of the higher frequency of C→T/U substitutions on the forward strand.

Source: Jónsson et al., 2013 and references herein

3.2 Population structure and introgression

Inter and intra level population structure was hierarchically investigated using Principal Component Analyses (PCA). The interspecific PCA of dataset **All_alb_pac** (Figure 5) show one Norway- (M-TUN009) and one WMED- (MA-IEO-BA-0-113) specimen clustering with the albacore samples and two Norway- (M-TUN023 and M-TUN041) and one ancient sample (TUN044) clustering with the Pacific bluefin. The remaining Atlantic bluefin samples fall together in a separate cluster. Three ancient samples (TUN031, TUN040 and TUN047) in the Atlantic bluefin cluster, and the ancient individual in the Pacific bluefin cluster (TUN044) fall slightly away from the other samples. Rather than indicating diverging haplotypes, this tendency of ancient samples to fall towards the center of the plot (PC1=0) may be explained by a higher degree of missingness than the modern samples and therefore lack of descriptive SNPs that might otherwise have settled them closer to their respective clusters.

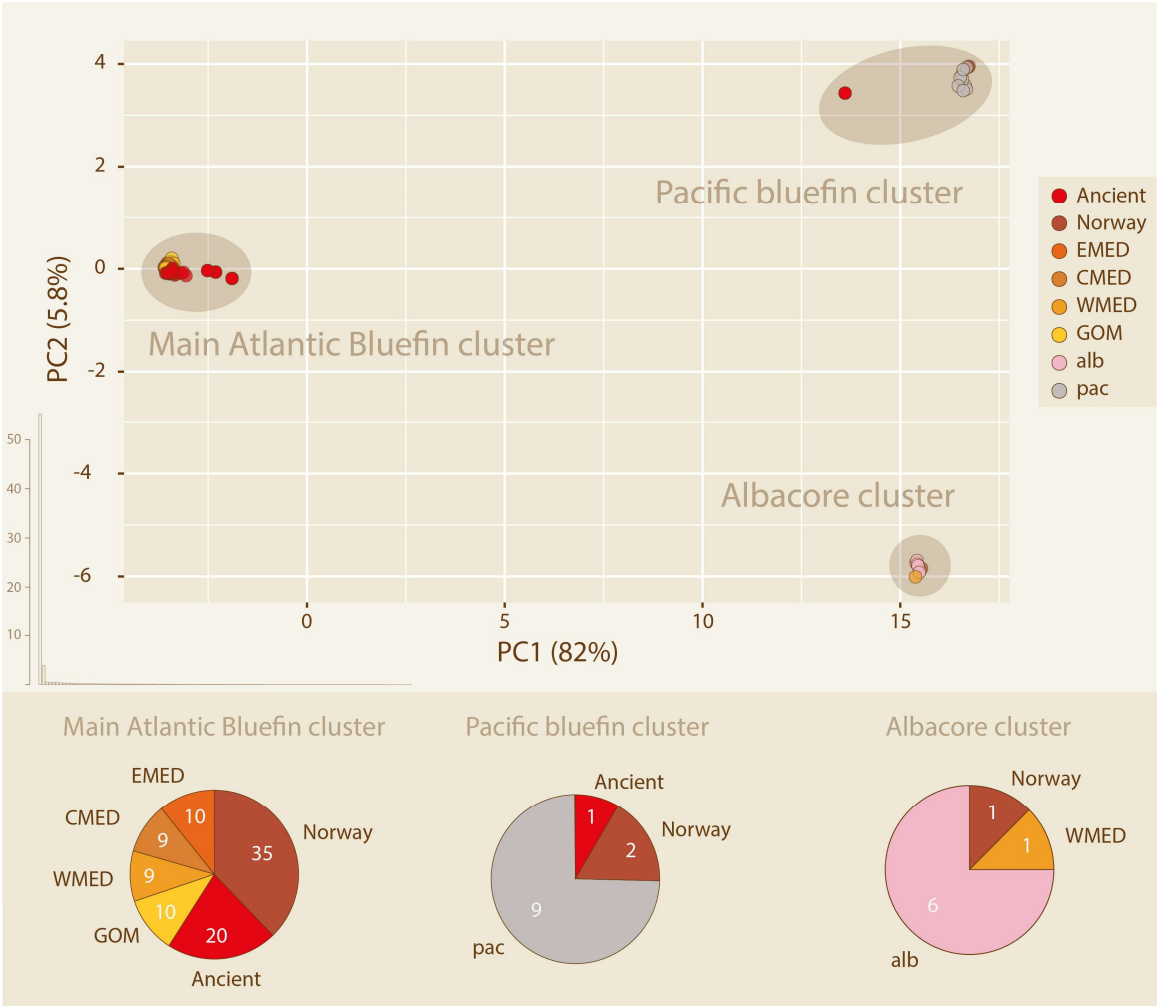

*Figure 5: Interspecific PCA of all samples, including albacore and pacific bluefin, using dataset **All_alb_pac**. The samples in the three PCA-clusters are visualized as pie-charts on the lower panel, with the number of samples indicated on the slices. Eigenvalues are shown in the left corner of the upper panel.*

A more fine-scaled PCA analysis selecting only non-introgressed, interspecific Atlantic bluefin samples (dataset **AllExIntrog**) shows three additional clusters (Figure 6). Modern samples from the Eastern Atlantic (Norway and Mediterranean) are present in all three clusters, while the Western Atlantic samples (GOM) are only observed in the upper right cluster. The far-left cluster contains individuals from all Mediterranean areas as well as three Norwegian samples but lack both Western Atlantic and ancient samples. The bottom panel (Figure 6) highlights the ancient individuals, falling in the center of both right clusters, and the Mediterranean samples scattered across all three clusters with no visible population structure. The PC1-axis here only explains 8.6% of the total variance in the dataset, compared to 82% in the interspecific PCA (Figure 5), and the samples presented in the intraspecific PCA (Figure 6), all fell in the main Atlantic bluefin cluster of the interspecific PCA (Figure 5)

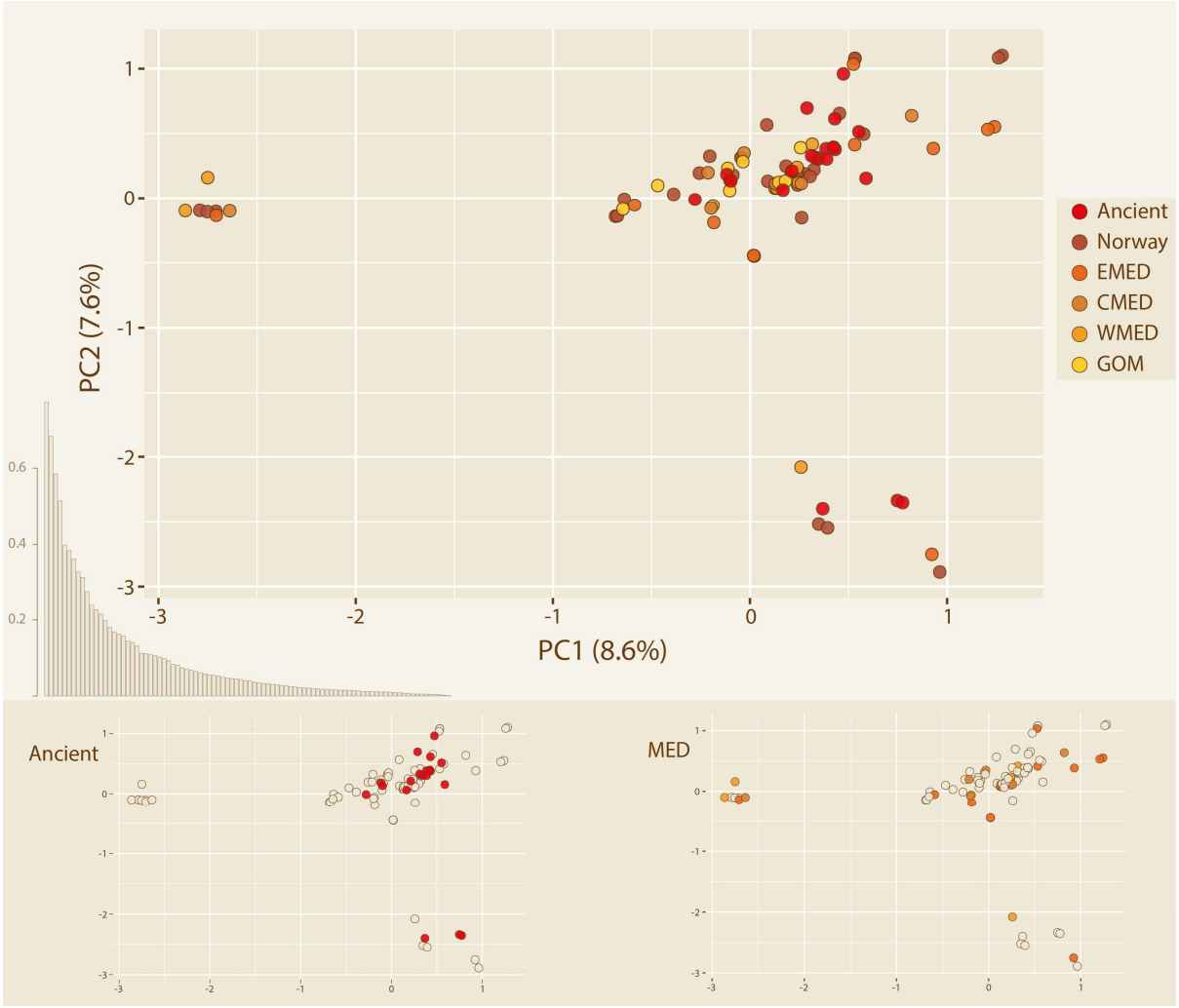

Figure 6: Intraspecific PCA of non-introgressed Atlantic bluefin samples, showing three scattered clusters. The ancient and Mediterranean samples are highlighted in the bottom panel. Eigenvalues are shown in the left corner of the upper panel.

To assess missing genotypes in both ancient and modern samples and to better visualize introgressed specimens, missing and diverging loci were plotted across all Atlantic bluefin specimens (**AllABFT** dataset). The plot revealed higher missingness among the ancient samples, and five samples heavily marked with the presence of second alleles diverging from the reference genome (Figure 5). The samples with high amounts of second alleles are those which clustered with the albacore and pacific bluefin in Figure 5, and therefore have greater genetic divergence from the Atlantic bluefin reference genome.

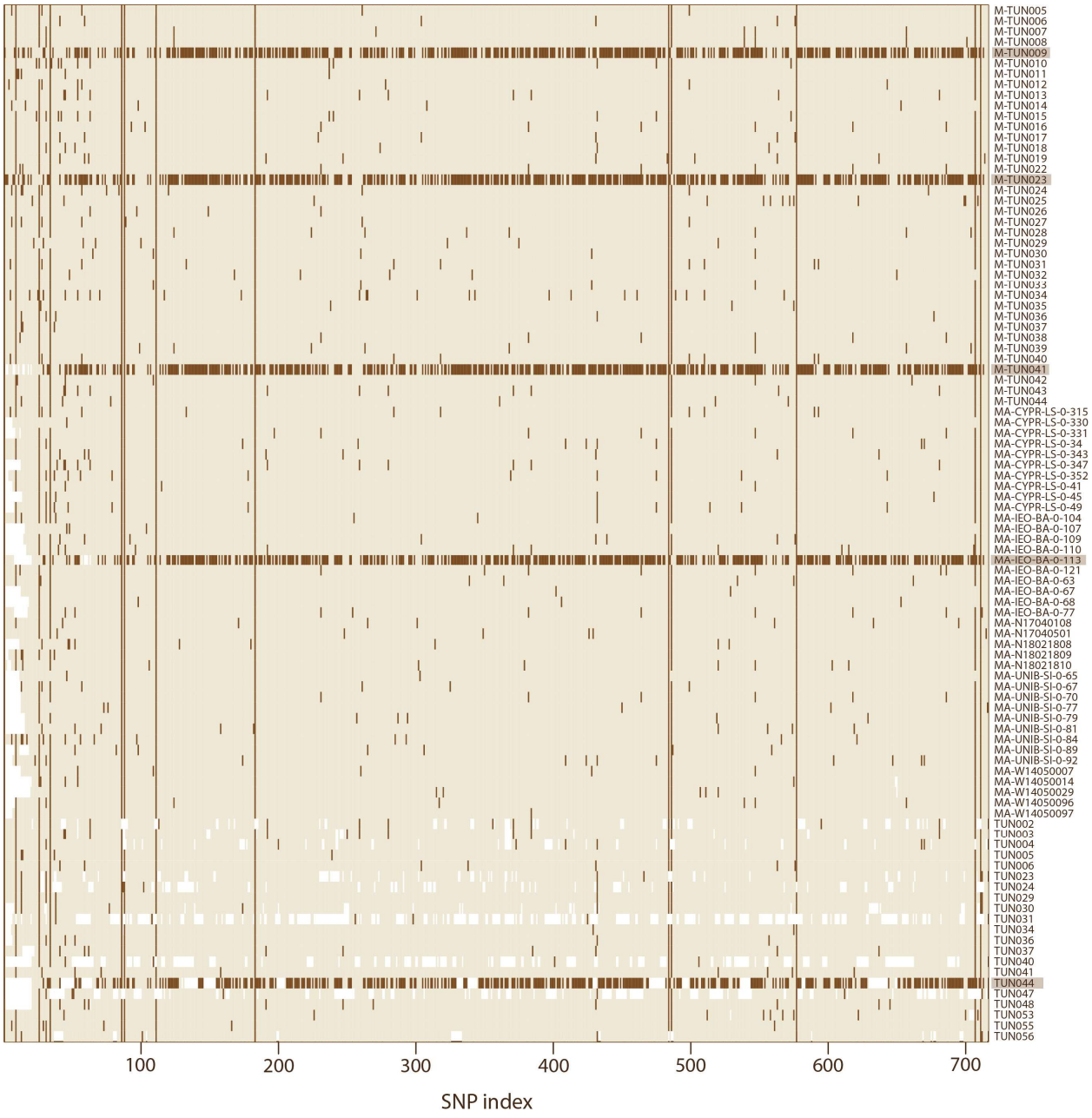

*Figure 7: Loci missingness (white) and presence of second alleles (dark brown) in the **AllABFT** dataset, which includes all Atlantic bluefin samples used in the population genomic analyses.*

3.3 Mitogenomic variation

3.3.1 Population genomic statistics

Patterns of genetic diversity within samples were calculated using a range of genomic statistics for each Atlantic bluefin dataset (Table 3). The subsets including introgressed individuals (**AncientAll**, **NorwayAll**, **WMEDAll**, **modernABFT** and **AllABFT**) have higher π and S. Segregating sites are differences, or polymorphisms, between the sequences in a dataset, while the nucleotide diversity (π) is the average number of pairwise base pair differences per site between the sequences (Nei 1987). Including a largely divergent haplotype in a dataset adds new variation which increases the S and π. The introgressed mitochondrial genomes contain a high amount of divergent alleles (Section 3.2, Figure 7), and therefore cause a strong increase in S and π when included (Table 3).

The haplotype diversity (hD), however, remains high and stable across all subsets and is not affected by the inclusion of introgressed individuals. The haplotype diversity is the probability of obtaining unique haplotypes when drawing two random samples from a population (Nei 1987). The datasets containing only unique samples (N=Nh) will therefore have a hD of 1, meaning 100% probability of obtaining unique samples during random sampling. Four of the samples from Norway were pairwise identical, which of one pair was the two introgressed Pacific-like samples. The **NorwayAll** dataset therefore has two fewer haplotypes than the number of samples, while the **NorwayExIntrog** has one less haplotype than the number of samples. A similar pattern can be seen in the other datasets containing identical samples, for example the **AllABFT** dataset, which includes all twelve pairwise identical samples, has six fewer haplotypes than the number of samples. As all identical haplotypes within the ancient dataset were removed, the hD is 1 (Table 3).

Tajima's D (TD) and Fu & Li's F statistic (F) are both neutrality statistics, testing the observed variation for deviation against the model of neutral selection, and values close to 0 indicate that the sequences in question are close to meeting the neutrality assumptions of no selection (Holt, 2006; Mishmar et al., 2003; Fu & Li, 1993; Tajima, 1989). When common alleles are frequent, TD becomes positive, while an excess of rare alleles gives a negative TD (Tajima, 1989). Generally, a positive TD is interpreted as an indication of balancing selection or decrease in population size, causing genetic variation to be maintained in the population, while a negative TD suggests positive selection or population expansion (Fijarczyk & Babik, 2015; Delph & Kelly, 2014).

F calculates the difference between the number of singletons (mutations that are present only once across all sequences) and the average number of pairwise nucleotide differences between the sequences, with positive values indicating balancing or positive selection and negative values indicating purifying selection, selective sweeps or rapid population growth (Fu & Li, 1993; Krutovsky & Neale, 2005). In all datasets, TD and F were both negative, indicating an excess of low frequency polymorphisms (TD) and singletons (F) likely resulting from population expansion (Biswas & Akey, 2006; Krutovsky & Neale, 2005; Fu & Li, 1993; Tajima, 1989).

The jointly called and filtered dataset with populations defined in DnaSP v.6 (Appendix A, Table S14) show a similar pattern, and is further discussed in Section 4.2.

Table 3: Population genomic statistics of the separately called and filtered datasets.
*N = number of samples, hD = haplotype diversity, Nh = number of haplotypes, S = number of segregating sites, π = nucleotide diversity, TD = Tajima's D, F = Fu & Li's F statistic. Significance levels (**=0.01, *=0.05, n.s.=not significant) are indicated for the TD and F values.*

Subset	N	hD	Nh	S	π	TD	F
AncientAll	21	1.000	21	54	0.0003	-2.562 (**)	-3.731 (**)
AncientExIntrog	20	1.000	20	16	0.0001	-2.177 (**)	-2.687 (*)
NorwayAll	38	0.997	36	608	0.0049	-1.714 (n.s.)	-0.3191 (n.s.)
NorwayExIntrog	35	0.998	34	182	0.0012	-2.109 (*)	-2.522 (*)
EMED	10	1.000	10	86	0.0013	-1.464 (n.s.)	-1.636 (n.s.)
CMED	9	1.000	9	79	0.0012	-1.703 (n.s.)	-1.804 (n.s.)
WMEDAll	10	1.000	10	460	0.0059	-2.059 (**)	-2.374 (**)
WMEDExIntrog	9	1.000	9	68	0.0011	-1.497 (n.s.)	-1.605 (n.s.)
GOM	10	1.000	10	67	0.0009	-1.754 (*)	-1.980 (n.s.)
modernABFT	77	0.998	71	664	0.0034	-2.080 (*)	-0.796 (n.s.)
modernExIntrog	73	0.998	69	268	0.0011	-2.378 (*)	-3.888 (**)
AllABFT	98	0.998	91	112	0.0005	-2.058 (*)	-1.418 (n.s.)
AllExIntrog	93	0.999	89	54	0.0002	-2.477 (**)	-3.644 (*)

TD and F do not vary consistently between datasets including and excluding introgressed individuals. Including introgressed mitochondrial genomes in a dataset will however impact neutrality statistics by increasing S and π, and calculations of neutrality statistics between different species is not recommended as they were developed for within-population comparisons (Fu & Li, 1993; Tajima, 1989). Within the non-introgressed datasets, the sample size may also affect the neutrality statistics as 1) stochasticity in the smaller sample sizes may

introduce sampling bias and 2) larger datasets have a higher probability of including individual variation.

To account for sample size differences when comparing π and TD, a bootstrap simulation was performed on each of the separately called and filtered datasets of non-introgressed Atlantic bluefin from different locations, randomly drawing five individuals 1000 independent times and calculating the statistics for each round in every subset. To avoid inflated estimates, introgressed samples were excluded from the simulations. The resulting variation in TD and π was low between the modern populations, although the GOM samples from the smaller Western stock had slightly lower TD and π than the other modern populations (Section 3.3, Figure 8-9). Lower π in the **GOM** dataset is consistent with the non-bootstrap calculation (Section 3.3, Table 3). The largest of the modern subsets, **NorwayExIntrog**, showed large deviation in TD between the calculated statistics and the bootstrap simulation (Section 3.3, Table 3 and Figure 9). Among the modern subsets, **NorwayExIntrog** had the largest difference between S and π (Section 3.3, Table 3), yielding a low and significant TD value, which was reduced when fewer samples and thereby fewer segregating sites were present in the bootstrap simulation. The high S in the **NorwayExIntrog** dataset is likely a consequence of the larger sample size, however one sample (M-TUN034) in this dataset was also highly divergent and may have been contaminated (see Section 3.3.2), likely contributing to an increase in S.

The ancient dataset (**AncientExIntrog**) had the lowest TD and π of all non-introgressed datasets in both the statistical calculations and the bootstrap simulations. In the statistical calculations (Section 3.3, Table 3) however, the difference in TD between the **AncientExIntrog** and **NorwayExIntrog** was slim. Neutrality statistics are highly sensitive to sequencing effort, and interpretations of absolute values should be avoided when analyzing low-depth Next Generation Sequencing (NGS) data (Korneliussen et al., 2013). The low S in the **AncientExIntrog**, affecting the TD statistic, may be explained by the lower sequencing depth and should therefore be interpreted with caution. The negative and significant TD and F statistics in the ancient population does however indicate population growth prior to the Neolithic (3900-2350 BCE) period.

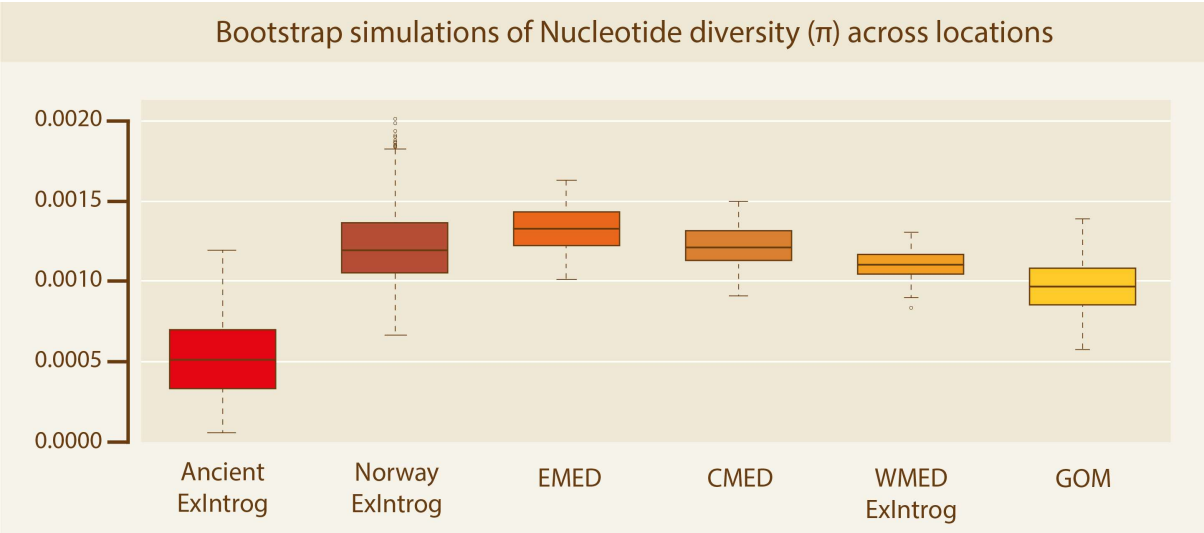

Figure 8: Results of bootstrap simulations (sample size =5, 1000 replicates) of nucleotide diversity (π) in separately called and filtered datasets.

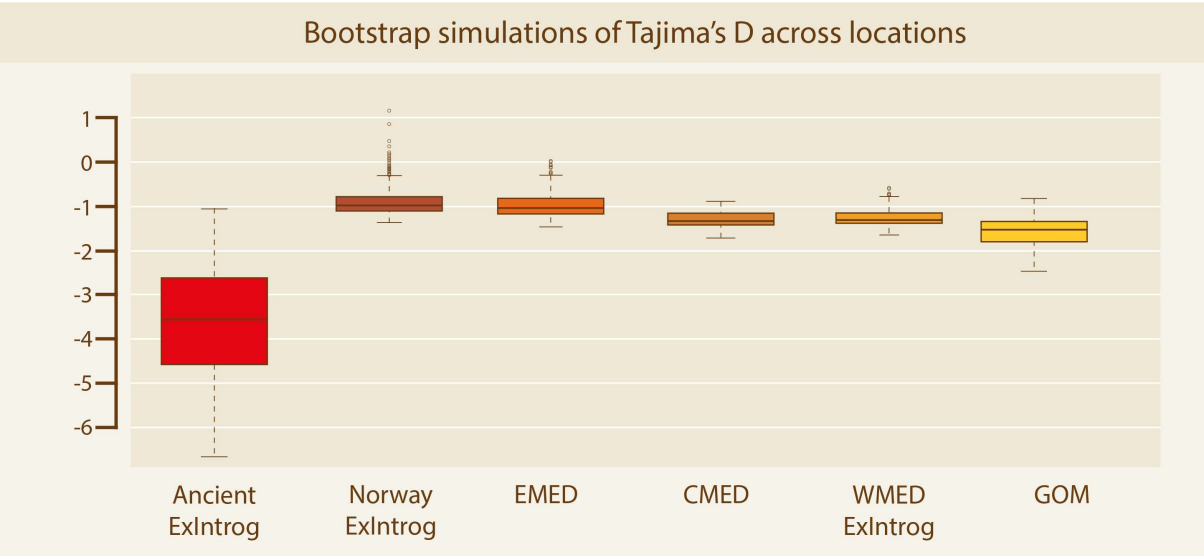

Figure 9: Results of bootstrap simulations (sample size =5, 1000 replicates) of Tajima's D (TD) in separately called and filtered datasets.

3.3.2 Haplotype networks and identical samples

The intraspecific haplotype network with a unique haplotype in each node reveals a star-like pattern among the non-introgressed individuals (Figure 10), corroborating population expansion as newer haplotypes are derived from a shared, central haplotype. One outlier individual from Norway (M-TUN034) branches out from the orientalis outgroup, rather than the center of the star, with branch lengths indicating an accumulation of substitutions in this sample. This sample may be a highly diverging haplotype within the non-introgressed Atlantic bluefin group, or alternatively the sample may have been contaminated.

The total number of substitutions in the network (Fitch distance) is 963, including the orientalis outgroup, and the network contains in total 138 nodes and 137 edges. The Norway and Mediterranean (EMED, CMED, WMED) samples are scattered evenly across the network, while the GOM samples occupy the upper left side of the network, consistent with their affiliation to only one of the three clusters in the intraspecific PCA (Figure 6). The middle-lower part of the network has a higher density of ancient samples, consistent with the ancient clustering on one side of the intraspecific PCA (Figure 6). The ancient samples also tend to fall slightly towards the center of the network.

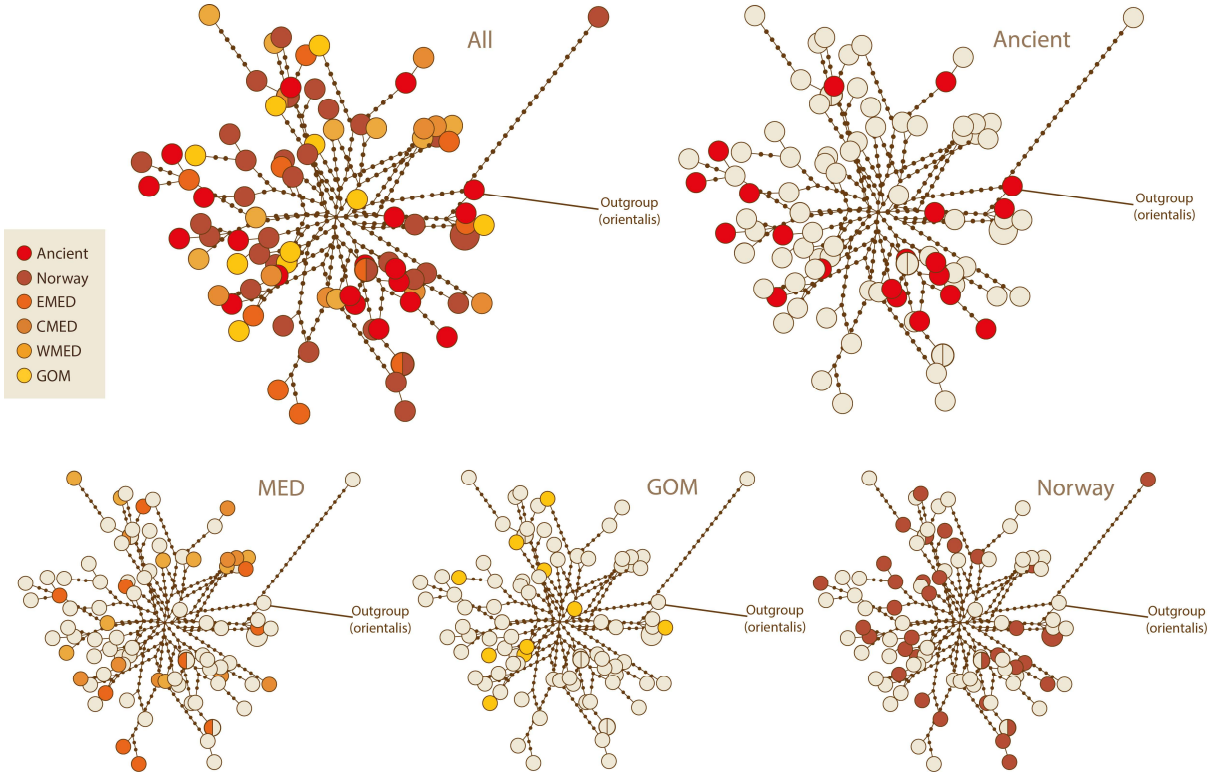

*Figure 10: Intraspecific haplotype network of all non-introgressed Atlantic bluefin individuals, using dataset **AllExIntrog** and a Pacific bluefin outgroup. Each node represents a unique haplotype.*

Several identical haplotypes appear in the intraspecific haplotype network (Figure 10). Two Norway samples have identical haplotypes (M-TUN043 = M-TUN013), two EMED samples are identical to two of the other Norway samples (MA-CYPR-LS-0-315 = M-TUN031 and MA-CYPR-LS-0-45 = M-TUN036), and one CMED sample is identical to another Norway sample (MA-UNIB-SI-0-70 = M-TUN038). This is consistent with the unique-SNPs evaluation from the python script (Appendix C).

Including introgressed individuals and outgroups in the haplotype network shows one ancient sample (TUN044) and two Norway samples (M-TUN023, M-TUN041) clustering with the

Pacific bluefin (orientalis) outgroup and one WMED (MA-IEO-BA-0-113) and one Norway sample (M-TUN009) clustering with the albacore (alalunga) outgroup (Figure 11). This corresponds to the PCA clustering of the same samples (Figure 5) and the configuration of the interspecific phylogeny (Figure 13). The albacore samples from Bay of Biscay also clearly clusters with the alalunga outgroup but seems more closely related with the introgressed bluefin samples than with the alalunga outgroup individuals from GenBank. In this network, seven substitutions or less are accepted within each node. The largest node contains 79 individuals (29 Norway, 8 EMED, 8 WMED, 9 GOM, 6 CMED, 19 Ancient). The total number of substitutions in the network (Fitch distance) is 2830, including the pelamis outgroup, and the network contains in total 42 nodes and 41 edges. The outlier sample (M-TUN034), branching away from the other samples in the intraspecific haplotype network (Figure 10), can be recognized as branching further from the main node than the other non-introgressed Atlantic bluefin in the upper right interspecific haplotype network (Figure 11).

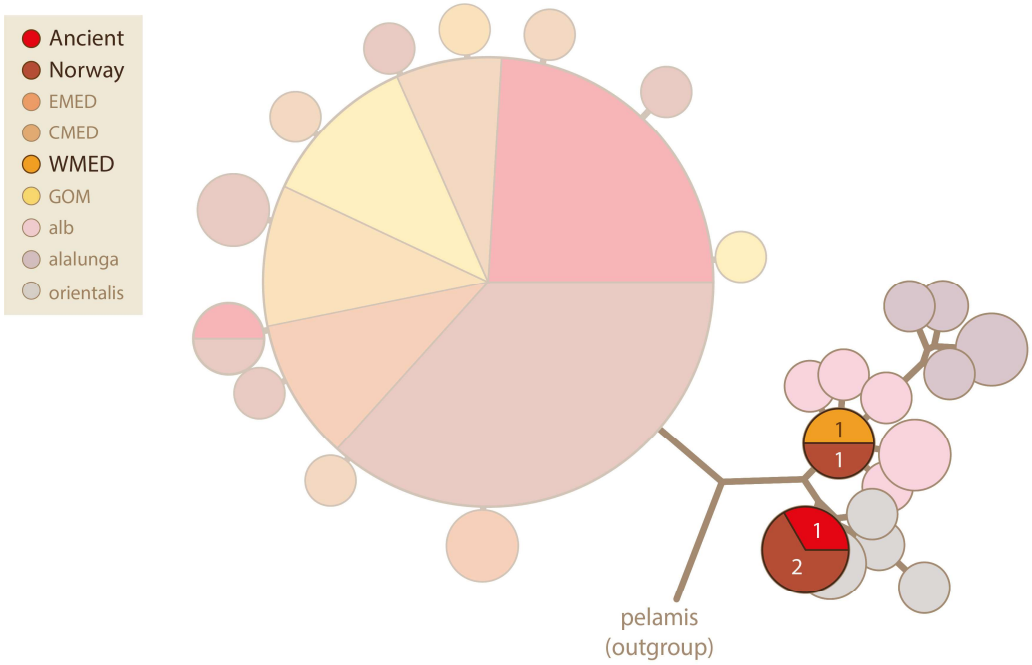

Figure 11: Interspecific haplotype network of all Atlantic bluefin and albacore samples, using the All_alb dataset and outgroups listed in Appendix A, Table S8. Introgressed haplotypes of Atlantic bluefin samples are highlighted and marked with the number of samples represented in the node. Each node represents haplotypes with 7 or fewer nucleotide substitutions between them.

3.4 Population divergence

Pairwise genetic distance between sample locations shows low absolute (Dxy) and relative (Φst) divergence across all populations (Figure 12). The absolute nucleotide divergence (Dxy) becomes larger when introgressed samples are included in the population, which is expected when highly divergent haplotypes and new alleles are added to the calculation. Including the introgressed mitogenomes also increases the nucleotide diversity. The relative nucleotide divergence (Φst) is low and non-significant across all populations. The Φst p-values can be found in Appendix A (Table S15). Comparing the two heatmaps (Figure 12), the Φst-values vary between the analyses, also when comparing the populations which have no introgressed individuals (EMED, CMED, GOM). Some variation is expected as the two datasets are called and filtered separately, and the distance matrix is computed for each joint dataset by Arlequin v.3. using the TN93 (Tamura & Nei, 1993) substitution model (Appendix A, Table S16).

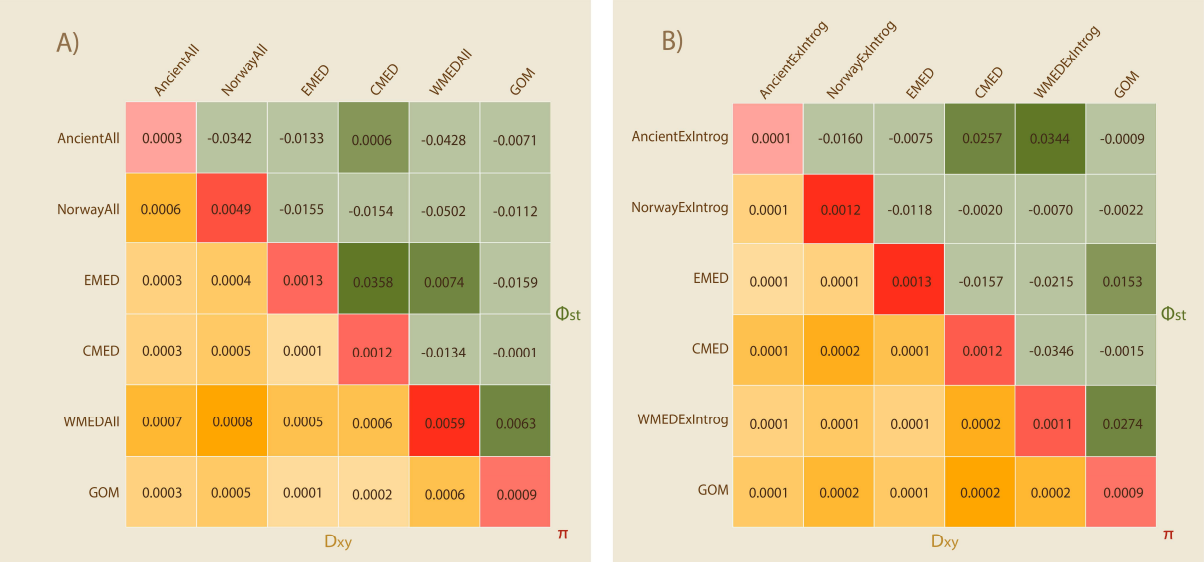

Figure 12: Results from population divergence analyses, presented as a heatmap showing absolute (Dxy) and relative (Φst) divergence between populations when A) including and B) excluding the introgressed individuals. The nucleotide diversity within each population is shown on the diagonal.

3.5 Phylogenetic analyses

Interspecific evolutionary relationships were investigated using ML and Bayesian phylogenetic analyses. The outgroup species, skipjack tuna, formed a paraphyletic group in the ML analysis (Figure 13) and in the Bayesian analysis in MrBayes (Appendix B, Figure S6), but a monophyletic group in the BEAST 2 Bayesian tree (Appendix B, Figure S7). In all phylogenetic analyses, the Pacific bluefin individuals (orientalis_*) obtained from GenBank (Clark et al., 2016), form a monophyletic group, while the albacore tuna (alalunga_* and alb_*)

fall as polyphyletic (Figure 13, Appendix B Figures S2 and S14). Within the albacore group, the individuals obtained from GenBank (alalunga_*) form a highly supported monophyletic group, while the albacore samples from the Bay of Biscay (alb_*) form a paraphyletic group with two albacore-like Atlantic bluefin samples (MA-IEO-BA-0-113 and M-TUN009). Three Atlantic bluefin individuals (TUN044, M-TUN041, M-TUN023) form a sister group to the Pacific bluefin, supported by 100% bootstrap in the ML analysis and 100% Bayesian posterior probability in both Bayesian phylogenetic analyses (Figure 13).

Within the non-introgressed Atlantic bluefin group, samples from different locations are scattered across the tree, with no pattern of population clustering of Eastern- and Western Atlantic, or Eastern-, central or Western Mediterranean samples (upper panels Figure 13). Additional investigations of intraspecific evolutionary relationship within the non-introgressed Atlantic bluefin samples, using ML and Bayesian phylogenetic analyses on the **AllExIntrog** dataset, corroborate the lack of population structure with the non-introgressed Atlantic bluefin samples (upper panels Figure 14, Appendix B Figures S9, S8). However, the PCA-clusters 1 and 3 from the intraspecific PCA (Figure 6) fall as monophyletic clades with high posterior probability from BEAST 2 (cluster 1) and MrBayes (cluster 3) in the intraspecific phylogeny (lower panels Figure 14). One cluster of ancient samples is present with low support in all analyses (Figures 13-14, and Appendix B Figures S6, S7, S8, S9).

Norway sample M-TUN034 stands out with a long branch length in both ML phylogenies (Figures 13-14), indicating several substitutions separating this individual from the other samples in the same clade. In both BEAST 2 phylogenies (Figure S7-S8), this sample falls as a sister-group to all the other non-introgressed Atlantic bluefin samples. This is also the case in the MrBayes analysis when introgressed samples are included (Figure S6). GOM sample MA-N17040108 forms a sister lineage to M-TUN034 in the ML phylogenies (Figures 13-14) and the MrBayes phylogeny excluding introgressed samples (Figure S9), while falling as a sister lineage to the non-introgressed Atlantic bluefin main group in two of the Bayesian trees (Appendix B Figures S6 and S8).

Substitution models selected by the different programs varied to some degree between the datasets (Appendix A, Table S16). However, all selected models assumed unequal base frequencies, different rates of transversions and transitions, and equal substitution rates among sites (i.e., no gamma rate heterogeneity). The selected models are listed in Appendix A (Table S16), and described in detail by Posada (2003).

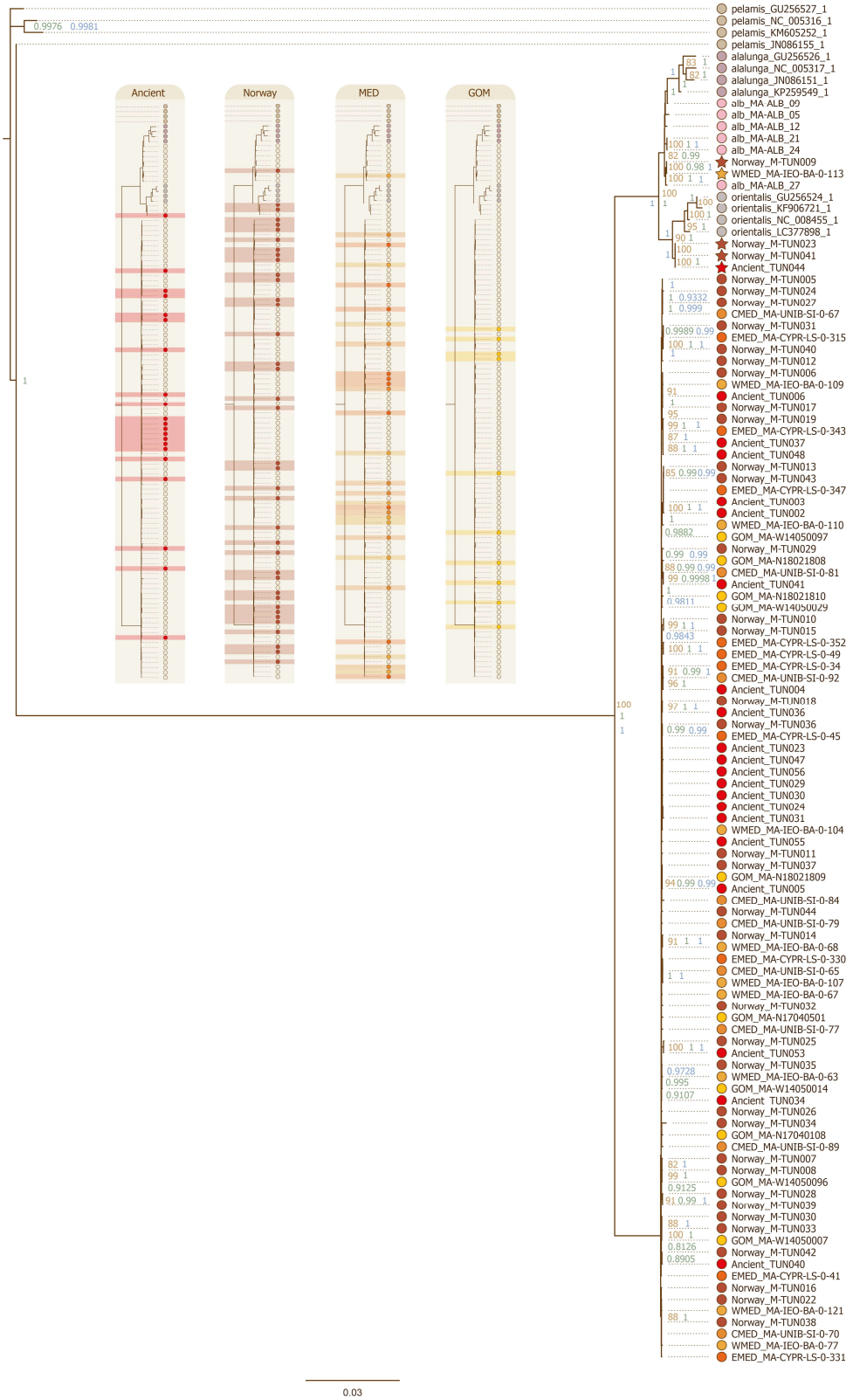

*Figure 13: Interspecific Maximum Likelihood (ML) phylogeny of all samples (dataset **All_alb**) and outgroups (Appendix A, Table S8). Introgressed individuals are highlighted (stars). Bootstrap values over 80 are shown in brown, posterior probability values over 0.8 from MrBayes (see also Appendix B, Figure S6) are added in green, and posterior probability values over 0.8 from BEAST 2 (see also Appendix B, Figure S7) are added in blue. The upper panel highlights how the populations fall in the tree.*

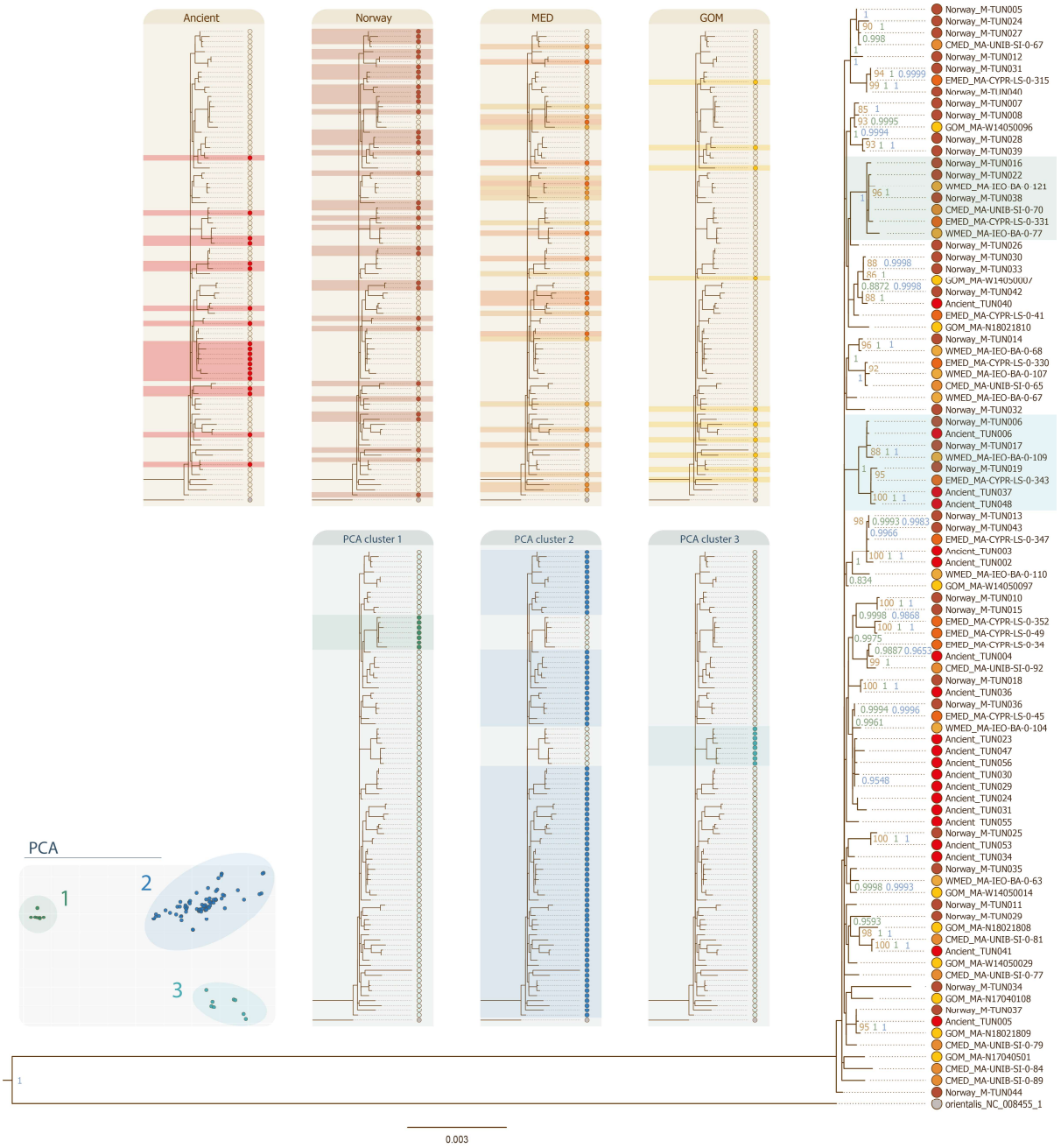

*Figure 14: Intraspecific Maximum Likelihood (ML) phylogeny of non-introgressed Atlantic bluefin individuals (dataset **AllExIntrog**), using a Pacific bluefin individual as outgroup. Bootstrap values over 80 are shown in brown, posterior probability values over 0.8 from MrBayes (see also Appendix B, Figure S9) are added in green, and posterior probability values over 0.8 from BEAST 2 (see also Appendix B, Figure S8) are added in blue. The upper and lower panel highlights how the populations and intraspecific PCA clusters respectively fall in the tree.*

3.6 Demographic reconstruction

Female effective population size (Ne) was modelled over time, and Coalescent Bayesian Skyline (CBS) plots were created for different datasets of modern and ancient individuals. When only modern samples are included in the analysis, the Ne is stable over the past 5000 years at around 300,000 individuals, both when including (**modernABFT**) and excluding (**modernExIntrog**) introgressed individuals (Figure 15). However, going further back in time, the CBS profiles differ between the two modern datasets. The **modernExIntrog** dataset shows a steep decrease in Ne down to less than 10,000 individuals during the Last Glacial Maximum (LGM) while the **modernABFT** dataset shows the lowest Ne, with approximately 50,000 individuals, around 10,000 years ago.

Including the ancient samples in the analysis greatly increase the 95% confidence intervals and corroborate the increase in Ne after the Late Glacial Interstadial (LGI) warming period with a subsequent stable Ne over the past 5000 years (Figure 15). However, combining the modern and ancient samples increases the median Ne to an estimated 3,000,000 individuals over the past 5000 years and over 1,000,000 individuals during the LGM. The CBS profile is similar in the modern and ancient combined datasets including (**AllABFT**) and excluding (**AllExIntrog**) introgressed individuals. Modelling the Ne over time only using ancient specimens (**AncientAll**, **AncientExIntrog**) (Appendix B, Figure S10), shows a steady increase in Ne during and after the LGI with a subsequent stabilization in Ne around 5000 years ago. The estimated Ne is however consistently lower than in any of the other CBS analyses, with the increase from around 30,000 individuals to stabilization at a little more than 100,000 individuals. The CBS profile is similar in the ancient datasets including (**AllABFT**) and excluding (**AllExIntrog**) introgressed individuals.

Large confidence intervals in the combined modern and ancient datasets (**AllABFT** and **AllExIntrog**) may be explained by the genetic similarity between modern and ancient specimens. If this is the case, treating the ancient samples as if they were modern when modelling Ne over time will result in a CBS profile similar to the profile generated by the modern datasets (**modernABFT**, **modernExIntrog**). These plots including non-dated ancient samples (Appendix B, Figure S11) do in fact show a very similar profile to the CBS plots generated by the modern datasets (Figure 15). However, the slight depression in Ne at around 0 CE (modern plots in Figure 15) becomes more pronounced when non-dated ancient samples are included (Appendix B, Figure S11), which may be explained by the increase in Ne

experienced by the ancient specimens approximately 2000 years prior to sampling (Appendix B, Figure S10).

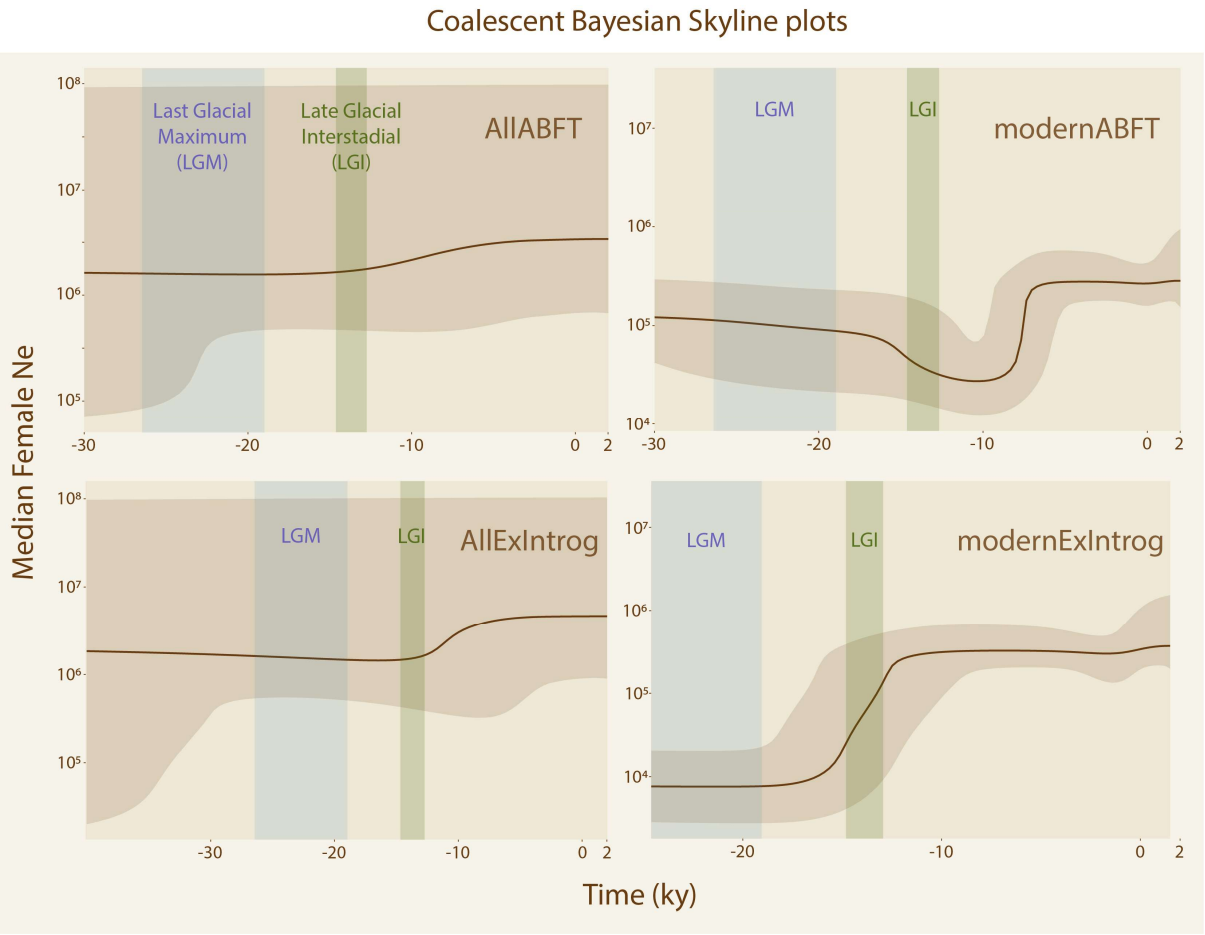

Figure 15: Female effective population size (Ne) modelled back in time, showing coalescent Bayesian Skyline (CBS) plots of only modern samples (right panels), and with ancient samples added to the analysis (left panels). Two major climatic periods are marked in the plot: The Last Glacial Maximum (LGM) and the Late Glacial Interstadial (LGI). The 95% confidence intervals are marked in dark brown.

4. Discussion

4.1 Material and Methods discussion

4.1.1 Preservation and dating

Analysis of 39 ancient Atlantic bluefin samples from the Early and Middle Neolithic period (3900-2350 BCE) revealed excellent ancient DNA preservation, with 100% library success and samples yielding 24% endogenous DNA on average. These are exceptionally preserved bones, compared to typical aDNA yield observed in the field (Carpenter et al., 2013). Low and stable temperatures, as well as favorable soil profile conditions of marine mud and silty clay (Nielsen, 2020a; Nielsen & Persson, 2020), has likely aided the biomolecular preservation (Bollongino et al., 2008; Gugerli et al., 2005). While three of the ancient tuna bones were directly carbon dated (Nielsen, 2020b) to approximately 4600 years old (BP 2020), the remaining bones were not dated, leading to some uncertainty in the timeframe of the other specimens. Nonetheless, apart from one surface stray find (TUN036), all the bones were dated by context as these were found in soil layers that were carbon dated using wood and charcoal. The carbon dates obtained from wood and charcoal where bones were found all fall in the range of 4135-4890 BP (2020) (Nielsen & Persson, 2020). Thus, the dated samples from the context layers correspond well with the three, individually carbon dated tuna bones, indicating high consistency in obtained age estimates.

4.1.2 Contamination and identical samples

Prior to laboratory processing, the ancient samples were handled without gloves and stored together in collective bags, increasing the risk of human contamination and cross-contamination between samples. Fragmentation patterns and deamination rates did, however, confirm the samples yielded authentic ancient DNA, and bioinformatic analyses showed the sequences belong to tuna. Cross-contamination between ancient samples may have occurred during storing or laboratory procedures, and several of the ancient samples produced indistinguishable DNA sequences. During the archaeological excavation, all bones from the same layer and shaft were jointly stored. Several of the identical ancient samples were found close together in the field and stored in the same bags (Appendix A, Table S1) and may therefore have been vertebrae from the same individuals or experienced cross-contamination during storage.

Of the 18 ancient samples that were excluded after exploratory analyses due to high missingness or indistinguishable mitochondrial genomes, nine contained an identical introgressed Pacific-like haplotype (Appendix B, Figures S12-S14). The frequency of directional introgression from Pacific-to Atlantic bluefin is relatively rare at around 2-5% (Rooker et al., 2007; Viñas & Tudela, 2009), thus the probability of finding such a high number of introgressed Pacific-like individuals was assumed to be low. A more likely scenario is that these were all vertebrae from the same individual. Four of the remaining 9 identical specimens were found close together in the same shaft and layer (TUN025-28, Appendix A, Table S1) and are also likely sampled from the same fish, although this time a non-introgressed individual. Identical samples were discarded to ensure that only unique individuals were included in the population genomic analyses.

Among the modern samples from Norway, two samples from the same extraction experiment (M-TUN023 and M-TUN041) and two samples from different extraction experiments (M-TUN013 and M-TUN043) produced indistinguishable DNA sequences. These identical modern samples could be included, as the modern sampling method ensured different individuals and the risk of contamination dominating the DNA yield was assumed to be low. Five of the modern Norway samples were also identical to Mediterranean and GOM samples (Appendix C), which had all been sampled independently, extracted in different laboratories, and sequenced on different flow cells, indicating that identical mitochondrial DNA sequences do occur naturally.

4.1.3 Library success

Ancient samples yielded lower coverage, endogenous DNA, and shorter read length than the modern samples (Appendix A, Tables S9, S10, S11), which is expected for authentic ancient DNA. Ancient libraries created using the SCR library protocol (Kapp et al., 2021) – here referred to as 'SS' libraries – generated more and longer reads while keeping the average clonality much lower than the double stranded (DS) library protocol from Meyer and Kircher (2010). Clonality is a relative measure of how many reads align to the same first base in the reference genome. Increasing the sequencing effort generally increases the clonality as 1) more PCR duplicates are sequenced and 2) a higher number of reads generates a higher random chance of aligning to the same first base in the reference genome (Boessenkool et al., 2017; Schubert et al., 2014). When comparing libraries, lower clonality combined with equal or higher coverage indicates a more complex library with a higher fraction of unique reads (Kapp et al., 2021; Euclide et al., 2020; Boessenkool et al., 2017).

The low clonality in the SS library may be partly explained by the fact that overlapping single strands of different length are not considered clonal if they do not start in the same position (Kapp et al., 2021). However, the considerably lower clonality despite the higher number of reads indicates complex SS libraries. Future investigations will therefore benefit from using the SS library protocol to generate high coverage at lower sequencing effort, compared to the DS library protocol.

4.1.4 Calling and filtering stochasticity

Hard filtering thresholds were thoroughly investigated on a jointly called dataset including all samples and re-evaluated after identical and high-missingness samples were excluded. The selected read depth filtering threshold (*--minDP 2*) in VCFtools v.0.1.16 (Danecek et al., 2011) is however lower than commonly used for whole genome ancient DNA (e.g. Ferrari et al., 2022; Martínez-García et al., 2021). At the selected threshold, sites sequenced twice or more were included in subsequent analyses, introducing the possibility of sequencing errors being presented as genetic variation in the datasets. Increasing the depth filtering threshold would increase the confidence in the presented variants. However, using a low filtering threshold was preferred to ensure that existing variation in the low coverage ancient specimens was included.

The sample datasets (Section 2.4, Table 1) were separately called and filtered so that only variants within each dataset were included in the GATK variant discovery calculations. Due to some stochasticity in the calling and filtering process, separately calling and filtering the datasets could introduce variation between the subsets that would otherwise have been held constant. In addition, larger datasets tend to have better statistical accuracy during filtering and higher sensitivity at low coverage positions (Poplin et al., 2018), leading to some of the smaller datasets likely having more stochastic variability than the larger datasets. To ensure that this did not have major impacts on the variant composition in the datasets, mitogenomic variation analyses were performed on both separately and jointly called datasets. The resulting Nh and the hD remained equal, and the π and S did not vary considerably, although both became generally lower in the joint dataset (Appendix A, Table S14). As expected, the larger datasets remained more similar than the smaller datasets.

The lower π and S indicate that more variants were filtered in the jointly called and filtered dataset. Singletons have a larger chance of being removed during filtering (GATK, 2022a), and a higher chance of occurring in a smaller dataset. This is because adding more samples to a dataset increase the probability of mutations being present in more than one of the samples by

chance, and the mutation will then no longer be counted as a singleton. The F statistic, which calculates the number of differences between singletons and π, may therefore be expected to be slightly skewed toward more negative values in the smaller datasets where a higher number of singletons are counted. Indeed, this was the case for most of the datasets (Appendix A, Table S14). In addition, the non-significant F statistics tended to vary more than the significant F values, and three of the F values became less significant in the jointly called and filtered dataset.

TD did not vary considerably between the jointly and separately called and filtered datasets. However, three of the TD values became more significant, and there was a tendency toward more negative TD values. TD uses the relationship between S and π (Tajima, 1989) to test for signs of selection. An excess of low frequency polymorphisms, or variable loci (S), compared to π, leads to negative TD. More pairwise differences between specimens within the same population (π) than segregating sites, as well as lack of variation both in S and π, gives positive TD values. The tendency toward more negative TD values in the jointly called and filtered datasets is likely due to a greater decrease in π than in S. The only exception to the decrease in S and π was the **AllAncient** dataset. Here, TD still became more negative, despite the increase in π, which can be explained by the even greater increase in S (Appendix A, Table S14). Low sequencing coverage is known to strongly affect neutrality statistics (Korneliussen et al., 2013), and the absolute values of TD, as well as F, should therefore be interpreted with caution.

Overall, defining datasets before or after calling and filtering did not have major impacts on the mitogenomic variation. The statistical patterns were similar in both analyses and indicated the same population genomic trends (see also Section 4.3 and 4.4). Still, the separation of samples into subsets based on location and patterns of introgression prior to calling and filtering, was preferred so that the variation within each subset would be accurately presented in subsequent analyses.

4.2 Interspecific population structure and introgression

A wide range of genomic analyses was used to investigate interspecific population structure across three tuna species; albacore, Pacific and Atlantic bluefin, which are known to hybridize (Chow & Kishino, 1995; Viñas & Tudela, 2009). Ordination analysis revealed three Atlantic bluefin samples clustering with Pacific bluefin, and two Atlantic bluefin samples clustering with albacore (Section 3.2, Figure 5). No patterns of introgression were found among western Atlantic studies, which is consistent with previous studies (Boustany et al., 2008; Carlsson et al., 2007; Rooker et al., 2007). Four of the introgressed individuals were modern, resulting in

a mitochondrial introgression frequency of 5.97% among the modern Eastern Atlantic samples (n=67), with 2.99% directional introgression from both albacore and Pacific bluefin. This is consistent with previous studies (Rooker et al., 2007; Viñas & Tudela, 2009). The introgressed individuals were also heavily marked with presence of second alleles in the loci missingness plot (Section 3.2, Figure 7), and grouped with albacore or Pacific bluefin in both the interspecific phylogeny (Section 3.5, Figure 13) and haplotype network (Section 3.3, Figure 11).

One ancient sample clustered with Pacific bluefin in all interspecific population structure analyses, indicating the presence of natural hybridization between Atlantic and Pacific bluefin in the Neolithic (3900-2350 BCE) period. The one introgressed ancient sample leads to a calculated introgression frequency from Pacific to Atlantic of 4.8% in the ancient population (n=21), but the low sample size leads to high stochasticity. No sign of hybridization with albacore was found in the ancient population, however, the low introgression frequency (2-5%) estimated for directional mitochondrial introgression from albacore (Rooker et al., 2007; Viñas & Tudela, 2009) would be difficult to detect without a larger sample size. The absence of albacore introgression in the ancient Atlantic bluefin population does therefore not disprove natural hybridization between the two species in the Neolithic period. The presence of an introgressed Pacific-like haplotype among the ancient specimens, however, confirms Pacific- and Atlantic- bluefin hybridization prior to major anthropogenic activity. These introgression patterns are therefore likely explained by natural migration of Pacific bluefin into the Atlantic Ocean, rather than human transportation, bluefin farming activities or ongoing climate change.

In mitochondrial phylogenies of the *Thunnus* genus, albacore and Pacific bluefin tend to group as sister species, which together form the sister group of the remaining thunnus species, including the Atlantic bluefin (Alvarado Bremer et al., 1997; Chow et al., 2006; Chow & Kishino, 1995; Gong et al., 2017; Viñas & Tudela, 2009). This pattern was also observed for all interspecific phylogenetic analyses in this thesis (Section 3.5, Figure 13, Appendix B Figures S6-S7). While the introgressed Pacific-like Atlantic bluefins form a monophyletic sister group to the true Pacific samples, the introgressed albacore-like Atlantic bluefins intermix with the true albacore samples from the Bay of Biscay. This same pattern was found by Viñas & Tudela (2009), who used a methodology which took the presence of mitochondrial introgression between albacore, Pacific and Atlantic tuna into consideration (see Section 1.3, Figure 2A).

Within the albacore group, the sequences downloaded from GenBank (Clark et al., 2016) diverged from the albacore samples from the Bay of Biscay with high support (Section 3.5, Figure 13), and were separated in the interspecific haplotype-network (Section 3.3, Figure 11). Although the albacore sequences from GenBank are unpublished, the branch length in the interspecific haplotype network and high support separating these specimens from the Bay of Biscay albacore and introgressed Atlantic samples, could indicate that they were sampled in the Pacific Ocean.

Overall, the interspecific phylogenies indicate some genetic divergence between the Pacific bluefin and the Pacific-like introgressed mitochondrial genomes, but no clear divergence between the albacore and the albacore-like introgressed mitochondrial genomes. This could indicate post-hybridization selection in the Pacific-like individuals, for instance adaptation to abiotic conditions or biotic factors (e.g., prey or disease variety) in the Atlantic Ocean, or neutral genetic drift. To investigate the effects of selection or drift over time, a larger number of both recent and derived hybrid individuals should be analyzed at both nuclear and mitochondrial level. Since mitochondrial genomes are non-recombining, determination of the number of generations since the hybridization event occurred is not possible without nuclear analyses. The intermixing of albacore-like introgressed mitochondrial genomes with the Atlantic albacore samples may therefore either be explained by recent hybridization events, low selection pressure over time, or genetic drift. Further investigations may reveal differential selection pressures in Pacific-like and albacore-like introgressed mitochondrial genomes or disclose the observed variation as a result of individual differences in time since hybridization and exposure to genetic drift.

4.3 Intraspecific population structure and divergence

Determination of loci for stock assignment has been a focus in population genomics of Atlantic bluefin over the past few years (Andrews et al., 2021; B. B. Collette, 2017; Hanke et al., 2018, pp. 1975–2015; Rodríguez-Ezpeleta et al., 2019). Stock intermixing on foraging grounds and frequent migration across the 45°W management boundary has led to discussion about whether the management units reflect the true population origin of the catches (Arregui et al., 2018; Block, 2001; Block et al., 2005; Galuardi et al., 2010; Lutcavage et al., 1999; Rooker et al., 2006, 2014; Wilson et al., 2015). Post-mortem determination of stock affiliation during harvest of Atlantic bluefin in foraging areas or outside of spawning season, would enable accurate registration of catches and closer observation of the SSB's.

In this study, spatial population structure within the Atlantic bluefin datasets was investigated using a series of genomic tools and common population statistics. Pairwise genetic distance between sample locations showed low absolute (Dxy) and relative (Φst) divergence across all populations (Section 3.4, Figure 12B), with no significant Φst-values (Appendix A, Table S15). This indicates conservation of the mitochondrial genome, despite natal homing to geographically separated spawning grounds in the Western- and Eastern Atlantic Ocean (Block et al., 2005; Boustany et al., 2008; Brophy et al., 2016). Genetic divergence between the Western and Eastern Atlantic stock has been found by previous studies, but only using nuclear markers (Andrews et al., 2021; Rodríguez-Ezpeleta et al., 2019; Puncher et al., 2018).

The mitochondrial genome likely lack SNPs indicative of spawning origin, and previous studies using mitochondrial data find no significant divergence between the two stocks (Alvarado Bremer et al., 2005; Ely et al., 2002; Pujolar et al., 2003). However, the intraspecific PCA revealed three clusters of which only one contained the GOM samples (Section 3.2, Figure 6), and in the intraspecific haplotype network, GOM samples only occupied half of the network (Section 3.3, Figure 10). Together with the lower π (Section 3.3 Table 3 and Figure 8), and the only positive Φst-values among non-introgressed modern population comparisons (Section 3.4, Figure 12B), this may be a reflection of a smaller and less genetically diverse population spawning in the Gulf of Mexico. Still, the lack of unique or diverging sites in the mitochondrial genome suggest that nuclear DNA should be the focus of future investigations to determine loci for stock assignment.

No evidence of population structure was found between the Mediterranean spawning locations, consistent with recent genetic studies (Andrews et al., 2021; Rodríguez-Ezpeleta et al., 2019; Puncher et al., 2018; Antoniou et al., 2017; Di Natale et al., 2017). Within the non-introgressed Atlantic bluefin group, samples from different locations were scattered across the trees in all phylogenetic analyses (Section 3.5, Figures H-I), with no pattern of population clustering of Eastern- and Western Atlantic, or Eastern-, central or Western Mediterranean samples, corroborating the lack of mitogenomic signatures for population structure. The lack of unique or diverging mitochondrial loci suggest that future research on post-mortem stock assignment of catches should be directed at nuclear genetic markers or otolith shape and isotope analyses, where signatures of stock affiliation has been found (Andrews et al., 2021; Brophy et al., 2020; Rodríguez-Ezpeleta et al., 2019; Brophy et al., 2016; Puncher et al., 2018; Fraile et al., 2015; Rooker et al., 2014).

4.4 Temporal genetic divergence and demographic reconstruction

Comparison between ancient and modern Atlantic bluefin revealed mitogenomic stability, despite centuries of human exploitation. High hD, S and π across modern sampling locations indicate no loss of mitochondrial genetic diversity over the past ~4600 years. Preservation of mitochondrial haplotypes was further supported by intermixing of modern and ancient specimens in ordination-, network- and phylogenetic analyses.

The difference in S and π between ancient and modern datasets should however be interpreted with caution, as the sequencing and processing methodologies impact these statistics. Lower sequencing effort and degraded and fragmented DNA tend to reduce S and π. This is due to several factors, including: 1) polymorphic sites not being sequenced in all samples (lower sequencing coverage) and/or 2) fewer reads covering a polymorphic site (lower sequencing depth) and thereby increasing the probability of the site getting removed during bioinformatic processing and filtering after sequencing (De Summa et al., 2017; Yu & Sun, 2013). Ancient DNA can therefore be expected to have lower S and π than high-quality modern DNA, which was the case for the ancient datasets in this study (Section 3.3, Table 3). All identical ancient haplotypes were removed from the analyses as the resampling of the same individual could not be ruled out. Because of this, the genetic diversity in the ancient population may be overestimated, and especially the hD may be inflated. Despite this, the S and π was higher in all modern datasets and the hD remained high across modern sampling locations. The temporal increase in genetic diversity is however likely an effect of ancient DNA degradation, rather than biological diversification.

Coalescent Bayesian Skyline models of Ne over time using only modern samples, or both modern and dated ancient samples, show no increase in Ne over the past 5,000 years (Section 3.6 Figure 15). The largely similar ancient and modern sequences result in high confidence intervals when the ancient samples are dated in the priors (see Section 3.6). This supports the lack of temporal genetic divergence indicated by the low absolute (Dxy) and relative (Φst) pairwise genetic distance analyses (Section 3.4, Figure 12) and intermixing of ancient and modern samples in the PCA's (Section 3.2 Figures E-F), haplotype networks (Section 3.3 Figure 10-11), and phylogenetic trees (Section 3.5 Figures H-I).

Negative and significant TD and F values indicate population expansion in both ancient and modern Atlantic bluefin tuna (Section 3.3, Table 3). The intraspecific haplotype network is also consistent with population expansion as newer haplotypes are derived from a common

ancestral, central haplotype in a star-like constellation (Section 3.3, Figure 10). Female effective population size (Ne) was modelled over time under the Coalescent Bayesian Skyline (CBS) prior, resulting in temporal demographic plots showing population size increase over the past 10,000 years in all analyses (Section 3.6 Figure 15, Appendix B Figures S10-S11). This corroborates population expansion as indicated by the star-like haplotype network (Figure 10), and negative and significant TD and F statistics (Section 3.3, Table 3 and Figure 9). In all CBS plots using non-introgressed Atlantic bluefin, the expansion begins around the time of the late glacial interstadial (LGI), which was the first extensive warming period after the last glacial maximum (LGM) (Ammann et al., 2013).

Previous scientific studies have found genomic signatures of population expansion in the Atlantic bluefin mitochondrial genome (Boustany et al., 2008; Alvarado Bremer et al., 2005; Carlsson et al., 2004). Bremer et al. (2005) suggest re-colonization of the Mediterranean spawning area after the last glacial maximum (LGM) as a possible explanation for the population expansion. This period coincides with warming ocean temperatures and likely increased prey abundance; therefore Bremer et al. suggest habitat expansion for Atlantic bluefin. Unfavorable spawning conditions in the Mediterranean likely limited Atlantic bluefin reproduction to the Gulf of Mexico during the LGM (Cury et al., 1998), as the summer sea surface temperature was too cold for spawning (Cury et al., 1998; Schaefer, 2001; Thiede, 1978). Subsequent invasion of the Mediterranean Sea and population growth during the Holocene (12,000-0 BP) may explain the genomic signatures of population expansion

5. Conclusion

A comparison between ancient and modern Atlantic bluefin genomes may provide information about changes in genetic diversity and population structure, the time of introgression events and the genetic impacts of over-exploitation. In this study, mitochondrial genomes from Neolithic (3900-2350 BCE) Atlantic bluefin fishbone remains were compared against modern samples from all major spawning regions and the Norwegian coast foraging area, revealing no clear genetic divergence between ancient and modern populations and no loss in genetic diversity in the mitochondrial genome over the past ~4600 years.

Intermixing of modern and ancient specimens in ordination-, network- and phylogenetic analyses, as well as high haplotype diversity across modern sampling locations indicate the preservation of mitochondrial haplotypes through time. The modern specimens had higher π and S, which was likely an effect of ancient DNA (aDNA) degradation and lower sequencing

depth. Analyses of intraspecific population structure did not support a clear pattern of population subdivision between the Eastern- and Western Atlantic stocks, indicating a lack of mitogenomic signatures for stock assignment. In addition, young of the year (YoY) bluefin samples from Mediterranean Sea indicated no genetic divergence between the three major spawning areas. Negative and significant Tajima's D and Fu & Li's F statistics across modern and ancient datasets and a star-like pattern in the intraspecific haplotype network signify population expansion. Coalescent Bayesian skyline analyses timed the expansion around the Late Glacial Interstadial (LGI), which was the first pronounced warming period after the Last Glacial Maximum (LGM).

Interspecific analyses revealed patterns of hybridization and directional mitochondrial introgression from albacore and Pacific bluefin into the Atlantic bluefin at a low and similar rate of close to 3% among the modern samples from the Eastern management stock, which is consistent with previous studies (Rooker et al., 2007; Viñas & Tudela, 2009). No sign of introgression was found among the Western stock samples. One ancient specimen with an introgressed Pacific bluefin mitochondrial genome provides evidence for natural hybridization between Atlantic and Pacific bluefin in the Neolithic period.

In summary, these result highlight the mitogenomic stability in Atlantic bluefin tuna over the past ~4600 years despite centuries of human exploitation. Similar results have been found in other marine predators with large distributions and intraspecific high geneflow, for example in recently published genomic studies of the Atlantic cod (Pinsky et al., 2021; Martínez-García et al., 2021). Further investigations are needed to establish or disprove fisheries-induced evolution or reductions nuclear genetic diversity, but conservation of mitochondrial haplotypes through time suggest that ecosystem impacts and reduced abundance may be more acute effects of the overfishing of Atlantic bluefin tuna.

Funding

This thesis is partly funded by RCN project 262777 "*Catching the Past"*, a Young Research Talent Grant awarded to my main supervisor Dr. Bastiaan Star. The aim of the project is to investigate the impacts of past exploitation in the marine environment. In addition to this funding, I have received financing by Naturviternes Legat, a fund providing scholarships for both students and working members of the Naturviterne organization.

Competing interests

I declare that I have no competing interests.

References

Albaina, A., Iriondo, M., Velado, I., Laconcha, U., Zarraonaindia, I., Arrizabalaga, H., Pardo, M. A., Lutcavage, M., Grant, W. S., & Estonba, A. (2013). Single nucleotide polymorphism discovery in albacore and Atlantic bluefin tuna provides insights into worldwide population structure. *Animal Genetics*, *44*(6), 678–692. https://doi.org/10.1111/age.12051

Alin, J. 1955. Förteckning över stenåldersboplatser i norra Bohuslän. Göteborgs och Bohusläns Fornminnesförening, Göteborg

Alvarado Bremer, J. R., Naseri, I., & Ely, B. (1997). Orthodox and unorthodox phylogenetic relationships among tunas revealed by the nucleotide sequence analysis of the mitochondrial DNA control region. *Journal of Fish Biology*, *50*(3), 540–554. https://doi.org/10.1111/j.1095-8649.1997.tb01948.x

Alvarado Bremer, J. R., Viñas, J., Mejuto, J., Ely, B., & Pla, C. (2005). Comparative phylogeography of Atlantic bluefin tuna and swordfish: The combined effects of vicariance, secondary contact, introgression, and population expansion on the regional phylogenies of two highly migratory pelagic fishes. *Molecular Phylogenetics and Evolution*, *36*(1), 169–187. https://doi.org/10.1016/j.ympev.2004.12.011

Ammann, B., van Leeuwen, J. F. N., van der Knaap, W. O., Lischke, H., Heiri, O., & Tinner, W. (2013). Vegetation responses to rapid warming and to minor climatic fluctuations during the Late-Glacial Interstadial (GI-1) at Gerzensee (Switzerland). *Palaeogeography, Palaeoclimatology, Palaeoecology*, *391*, 40–59. https://doi.org/10.1016/j.palaeo.2012.07.010

Andrews, A. J., Puncher, G. N., Bernal-Casasola, D., Di Natale, A., Massari, F., Onar, V., Toker, N. Y., Hanke, A., Pavey, S. A., Savojardo, C., Martelli, P. L., Casadio, R., Cilli, E., Morales-Muñiz, A., Mantovani, B., Tinti, F., & Cariani, A. (2021). Ancient DNA SNP-panel data suggests stability in bluefin tuna genetic diversity despite centuries of fluctuating catches in the eastern Atlantic and Mediterranean. *Scientific Reports*, *11*(1), 20744. https://doi.org/10.1038/s41598-021-99708-9

Antoniou, A., Kasapidis, P., Kotoulas, G., Mylonas, C. C., & Magoulas, A. (2017). Genetic diversity of Atlantic Bluefin tuna in the Mediterranean Sea: Insights from genome-wide SNPs and microsatellites. *Journal of Biological Research-Thessaloniki*, *24*(1), 3. https://doi.org/10.1186/s40709-017-0062-2

Aristotelis, 1635, De Animalibus. In: Stagiritae peripatetico rum. Principis de Historia Animalium. Edited by Theodoro Goza, Venezia, Italy: 1-843.

Arregui, I., Galuardi, B., Goñi, N., Lam, C. H., Fraile, I., Santiago, J., Lutcavage, M., & Arrizabalaga, H. (2018). Movements and geographic distribution of juvenile bluefin tuna in the Northeast Atlantic, described through internal and satellite archival tags. *ICES Journal of Marine Science*, *75*(5), 1560–1572. https://doi.org/10.1093/icesjms/fsy056

Atmore, L. M. (2021). *Nucleotide_differences* [Python3]. https://github.com/laneatmore/nucleotide_differences

Auguie, B., & Antonov, A. (2017). gridExtra: miscellaneous functions for "grid" graphics. R package version, 2(1).

Auton, A., & Marcketta, A. (2015). *VCFtools*. https://vcftools.github.io/man_latest.html

Bigelow, H. B., & Schroeder, W. C. (1953). *Fishes of the Gulf of Maine*. U.S. Government Printing Office.

Biswas, S., & Akey, J. M. (2006). Genomic insights into positive selection. *Trends in Genetics*, *22*(8), 437–446. https://doi.org/10.1016/j.tig.2006.06.005

Blanquer, A. (1990). Phylogéographie intraspécifique d'un poisson marin, le flet Platichthys flesus L. (Heterosomata): Polymorphisme des marqueurs nucléaires et mitochondriaux [Thesis, Montpellier 2]. In *Http://www.theses.fr*. http://www.theses.fr/1990MON20015

Block, B. A. (2001). Migratory Movements, Depth Preferences, and Thermal Biology of Atlantic Bluefin Tuna. *Science*, *293*(5533), 1310–1314. https://doi.org/10.1126/science.1061197

Block, B. A. (2019). *The Future of Bluefin Tunas: Ecology, Fisheries Management, and Conservation*. JHU Press.

Block, B. A., Teo, S. L. H., Walli, A., Boustany, A., Stokesbury, M. J. W., Farwell, C. J., Weng, K. C., Dewar, H., & Williams, T. D. (2005). Electronic tagging and population structure of Atlantic bluefin tuna. *Nature*, *434*(7037), 1121–1127. https://doi.org/10.1038/nature03463

Boessenkool, S., Hanghøj, K., Nistelberger, H. M., Der Sarkissian, C., Gondek, A. T., Orlando, L., Barrett, J. H., & Star, B. (2017). Combining bleach and mild predigestion improves ancient DNA recovery from bones. *Molecular Ecology Resources*, *17*(4), 742–751. https://doi.org/10.1111/1755-0998.12623

Bollongino, R., Tresset, A., & Vigne, J.-D. (2008). Environment and excavation: Pre-lab impacts on ancient DNA analyses. *Comptes Rendus Palevol*, *7*(2), 91–98. https://doi.org/10.1016/j.crpv.2008.02.002

Bouckaert, R., Heled, J., Kühnert, D., Vaughan, T., Wu, C.-H., Xie, D., Suchard, M. A., Rambaut, A., & Drummond, A. J. (2014). BEAST 2: A Software Platform for Bayesian Evolutionary Analysis. *PLOS Computational Biology*, *10*(4), e1003537. https://doi.org/10.1371/journal.pcbi.1003537

Bouckaert, R. R., & Drummond, A. J. (2017). bModelTest: Bayesian phylogenetic site model averaging and model comparison. *BMC Evolutionary Biology*, *17*(1), 42. https://doi.org/10.1186/s12862-017-0890-6

Boustany, A. M., Reeb, C. A., & Block, B. A. (2008). Mitochondrial DNA and electronic tracking reveal population structure of Atlantic bluefin tuna (Thunnus thynnus). *Marine Biology*, *156*(1), 13–24. https://doi.org/10.1007/s00227-008-1058-0

Bronner, I. F., Quail, M. A., Turner, D. J., & Swerdlow, H. (2013). Improved Protocols for Illumina Sequencing. *Current Protocols in Human Genetics*, *79*(1), 18.2.1-18.2.42. https://doi.org/10.1002/0471142905.hg1802s79

Brophy, D., Haynes, P., Arrizabalaga, H., Fraile, I., Fromentin, J. M., Garibaldi, F., Katavic, I., Tinti, F., Karakulak, F. S., Macías, D., Busawon, D., Hanke, A., Kimoto, A., Sakai, O., Deguara, S., Abid, N., & Santos, M. N. (2016). Otolith shape variation provides a marker of stock origin for north Atlantic bluefin tuna (Thunnus thynnus). *Marine and Freshwater Research*, *67*(7), 1023–1036. https://doi.org/10.1071/MF15086

Brophy, D., Rodríguez-Ezpeleta, N., Fraile, I., & Arrizabalaga, H. (2020). Combining genetic markers with stable isotopes in otoliths reveals complexity in the stock structure of Atlantic bluefin tuna (Thunnus thynnus). *Scientific Reports*, *10*(1), 1–17. https://doi.org/10.1038/s41598-020-71355-6

Brown, K. H. (2008). Fish mitochondrial genomics: Sequence, inheritance and functional variation. *Journal of Fish Biology*, *72*(2), 355–374. https://doi.org/10.1111/j.1095-8649.2007.01690.x

Bushnell, B. (2014). *BBMap: A Fast, Accurate, Splice-Aware Aligner* (LBNL-7065E). Lawrence Berkeley National Lab. (LBNL), Berkeley, CA (United States). https://www.osti.gov/biblio/1241166

Cantu, C., Bucheli, S., & Houston, R. (2022). Comparison of DNA extraction techniques for the recovery of bovine DNA from fly larvae crops. *Journal of Forensic Sciences*, *n/a*(n/a). https://doi.org/10.1111/1556-4029.15010

Carey, F. G., & Lawson, K. D. (1973). Temperature regulation in free-swimming bluefin tuna. *Comparative Biochemistry and Physiology Part A: Physiology*, *44*(2), 375–392. https://doi.org/10.1016/0300-9629(73)90490-8

Carlsson, J., McDowell, J. R., Carlsson, J. E. L., & Graves, J. E. (2007). Genetic Identity of YOY Bluefin Tuna from the Eastern and Western Atlantic Spawning Areas. *Journal of Heredity*, *98*(1), 23–28. https://doi.org/10.1093/jhered/esl046

Carlsson, J., McDOWELL, J. R., Díaz-Jaimes, P., Carlsson, J. E. L., Boles, S. B., Gold, J. R., & Graves, J. E. (2004). Microsatellite and mitochondrial DNA analyses of Atlantic bluefin tuna (Thunnus thynnus thynnus) population structure in the Mediterranean Sea. *Molecular Ecology*, *13*(11), 3345–3356. https://doi.org/10.1111/j.1365-294X.2004.02336.x

Carpenter, M. L., Buenrostro, J. D., Valdiosera, C., Schroeder, H., Allentoft, M. E., Sikora, M., Rasmussen, M., Gravel, S., Guillén, S., Nekhrizov, G., Leshtakov, K., Dimitrova, D., Theodossiev, N., Pettener, D., Luiselli, D., Sandoval, K., Moreno-Estrada, A., Li, Y., Wang, J., … Bustamante, C. D. (2013). Pulling out the 1%: Whole-Genome Capture for the Targeted Enrichment of Ancient DNA Sequencing Libraries. *The American Journal of Human Genetics*, *93*(5), 852–864. https://doi.org/10.1016/j.ajhg.2013.10.002

Cermeño, P., Quílez-Badia, G., Ospina-Alvarez, A., Sainz-Trápaga, S., Boustany, A. M., Seitz, A. C., Tudela, S., & Block, B. A. (2015). Electronic Tagging of Atlantic Bluefin Tuna (Thunnus thynnus, L.) Reveals Habitat Use and Behaviors in the Mediterranean Sea. *PLOS ONE*, *10*(2), e0116638. https://doi.org/10.1371/journal.pone.0116638

Chow, S., & Inoue, S. (1993). *Intra and interspesific restriction fragment length polymorphism in mitochondrial genes of Thunnus tuna species*.

Chow, S., & Kishino, H. (1995). Phylogenetic relationships between tuna species of the genus Thunnus (Scombridae: Teleostei): Inconsistent implications from morphology, nuclear and mitochondrial genomes. *Journal of Molecular Evolution*, *41*(6). https://doi.org/10.1007/BF00173154

Chow, S., Nakagawa, T., Suzuki, N., Takeyama, H., & Matsunaga, T. (2006). Phylogenetic relationships among Thunnus species inferred from rDNA ITS1 sequence. *Journal of Fish Biology*, *68*(A), 24–35. https://doi.org/10.1111/j.0022-1112.2006.00945.x

Chow, S., & Ushiama, H. (1995). Global population structure of albacore (Thunnus alalunga) inferred by RFLP analysis of the mitochondrial ATPase gene. *Marine Biology*, *123*(1), 39–45. https://doi.org/10.1007/BF00350321

CITES. (2021, June 22). *Appendices I, II and III*. https://cites.org/eng/app/appendices.php

Clark, K., Karsch-Mizrachi, I., Lipman, D. J., Ostell, J., & Sayers, E. W. (2016). GenBank. *Nucleic Acids Research*, *44*(Database issue), D67–D72. https://doi.org/10.1093/nar/gkv1276

Collette, B., Amorim, A. F., Boustany, A., Carpenter, K. E., de Oliveira Leite Jr., N., Di Natale, A., Die, D., Fox, W., Fredou, F. L., Graves, J., Viera Hazin, F. H., Hinton, M., Juan Jorda, M., Kada, O., Minte Vera, C., Miyabe, N., Nelson, R., Oxenford, H., Pollard, D., … Uozumi, Y. (2011, February 18). *IUCN Red List of Threatened Species: Atlantic Bluefin Tuna*. IUCN Red List of Threatened Species. https://www.iucnredlist.org/en

Collette, B. B. (2017). Bluefin tuna science remains vague. *Science*, *358*(6365), 879–880. https://doi.org/10.1126/science.aar3928

Collette, B., Fox, W., Jorda, M. J., Graves, J., Boustany, A., & Restrepo, V. (2021). IUCN Red List of Threatened Species: Thunnus thynnus. *IUCN Red List of Threatened Species*. https://www.iucnredlist.org/en

Cooper, A., & Poinar, H. N. (2000). Ancient DNA: do it right or not at all. *Science*, *289*(5482), 1139–1139.

Cort, J., & Abaunza, P. (2016). *The impact of massive fishing of juvenile Atlantic bluefin tunas on the spawning population (1949-2010)*.

Cort, J., Deguara, S., Galaz, T., Melich, B., Artetxe, I., Arregui, I., Neilson, J., Andrushchenko, I., Hanke, A., Santos, M., Estruch, V., Lutcavage, M., Knapp, J., Compeán-Jiménez, G., Solana-Sansores, R., Belmonte, A., Martínez, D., Piccinetti, C., Kimoto, A., & Idrissi, M. (2013). Determination of L max for Atlantic Bluefin Tuna, Thunnus thynnus (L.), from Meta-Analysis of Published and Available Biometric Data. *Reviews in Fisheries Science*, *21*, 181–212. https://doi.org/10.1080/10641262.2013.793284

Cort, J. L., & Abaunza, P. (2015). The Fall of the Tuna Traps and the Collapse of the Atlantic Bluefin Tuna, Thunnus thynnus (L.), Fisheries of Northern Europe from the 1960s. *Reviews in Fisheries Science & Aquaculture*, *23*(4), 346–373. https://doi.org/10.1080/23308249.2015.1079166

Crockford, S. J. (1997). Archeological evidence of large northern bluefin tuna, Thunnus thynnus, in coastal waters of British Columbia and northern Washington. *Oceanographic Literature Review*, *11*(44), 1359.

Cruz, V. P., Vera, M., Pardo, B. G., Taggart, J., Martinez, P., Oliveira, C., & Foresti, F. (2017). Identification and validation of single nucleotide polymorphisms as tools to detect hybridization and population structure in freshwater stingrays. *Molecular Ecology Resources*, *17*(3), 550–556. https://doi.org/10.1111/1755-0998.12564

Cury, P., Anneville, O., Bard, F. X., Fontenau, A., & Roy, C. (1998). Obstinate North Atlantic bluefin tuna (Thunnus thynnus thynnus): An evolutionary perspective to consider spawning migration. *Col. Vol. Sci. Pap. ICCAT*, *50*, 239–247.

Dabney, J., Knapp, M., Glocke, I., Gansauge, M.-T., Weihmann, A., Nickel, B., Valdiosera, C., Garcia, N., Paabo, S., Arsuaga, J.-L., & Meyer, M. (2013). Complete mitochondrial genome sequence of a Middle Pleistocene cave bear reconstructed from ultrashort DNA fragments. *Proceedings of the National Academy of Sciences*, *110*(39), 15758–15763. https://doi.org/10.1073/pnas.1314445110

Damgaard, P. B., Margaryan, A., Schroeder, H., Orlando, L., Willerslev, E., & Allentoft, M. E. (2015). Improving access to endogenous DNA in ancient bones and teeth. *Scientific Reports*, *5*(1), 11184. https://doi.org/10.1038/srep11184

Danecek, P., Auton, A., Abecasis, G., Albers, C. A., Banks, E., DePristo, M. A., Handsaker, R. E., Lunter, G., Marth, G. T., Sherry, S. T., McVean, G., Durbin, R., & 1000 Genomes Project Analysis Group. (2011).

The variant call format and VCFtools. *Bioinformatics*, *27*(15), 2156–2158. https://doi.org/10.1093/bioinformatics/btr330

Darriba, D., Taboada, G. L., Doallo, R., & Posada, D. (2012). jModelTest 2: More models, new heuristics and parallel computing. *Nature Methods*, *9*(8), 772–772. https://doi.org/10.1038/nmeth.2109

De Summa, S., Malerba, G., Pinto, R., Mori, A., Mijatovic, V., & Tommasi, S. (2017). GATK hard filtering: Tunable parameters to improve variant calling for next generation sequencing targeted gene panel data. *BMC Bioinformatics*, *18*(5), 119. https://doi.org/10.1186/s12859-017-1537-8

Delph, L. F., & Kelly, J. K. (2014). On the importance of balancing selection in plants. *The New Phytologist*, *201*(1), 10.1111/nph.12441. https://doi.org/10.1111/nph.12441

Di Natale, A. (2012). Literature On The Eastern Atlantic And Mediterranean Tuna Trap Fishery. *ICCAT Coll.*, 46.

Di Natale, A. (2014). *The ancient distribution of bluefin tuna fishery: How coins can improve our knowledge*. 17.

Di Natale, A., Tensek, S., & Pagá García, A. (2017). ICCAT Atlantic-wide research programme for bluefin tuna (GBYP) activity report for the last part of phase 6 and the first part of phase 7 (2016-2017). *SCRS*, *Collect. Vol. Sci. Pap. ICCAT, 74(6): 3100-3171 (2018)*, 72.

Díaz-Arce, N., Arrizabalaga, H., Murua, H., Irigoien, X., & Rodríguez-Ezpeleta, N. (2016). RAD-seq derived genome-wide nuclear markers resolve the phylogeny of tunas. *Molecular Phylogenetics and Evolution*, *102*, 202–207. https://doi.org/10.1016/j.ympev.2016.06.002

Donaldson, K. A., & Wilson, R. R. (1999). Amphi-Panamic Geminates of Snook (Percoidei: Centropomidae) Provide a Calibration of the Divergence Rate in the Mitochondrial DNA Control Region of Fishes. *Molecular Phylogenetics and Evolution*, *13*(1), 208–213. https://doi.org/10.1006/mpev.1999.0625

Edwards, S. M. (2017). lemon: Freshing Up your'ggplot2'Plots.

Ely, B., Stoner, D. S., Bremer, A. J. R., Dean, J. M., Addis, P., Cau, A., Thelen, E. J., Jones, W. J., Black, D. E., Smith, L., Scott, K., Naseri, I., & Quattro, J. M. (2002). Analyses of Nuclear ldhA Gene and mtDNA Control Region Sequences of Atlantic Northern Bluefin Tuna Populations. *Marine Biotechnology*, *4*(6), 583–588. https://doi.org/10.1007/s10126-002-0040-y

Enghoff, I. B., B. R. MacKenzie, and E. E. Nielsen. 2007. "The Danish Fish Faune During the Warm Atlantic Period (ca. 7000-3900 bc): Forerunner of Future Change?" Fisheries Research 87: 167–180

Ericson, P. G. P. 1989. "Faunahistoriskt Intressanta Stenålderfynd Från Stora Karlsö." Flora och Fauna 84: 192–198.

Euclide, P. T., McKinney, G. J., Bootsma, M., Tarsa, C., Meek, M. H., & Larson, W. A. (2020). Attack of the PCR clones: Rates of clonality have little effect on RAD-seq genotype calls. *Molecular Ecology Resources*, *20*(1), 66–78. https://doi.org/10.1111/1755-0998.13087

Excoffier, L., & Lischer, H. E. L. (2010). Arlequin suite ver 3.5: A new series of programs to perform population genetics analyses under Linux and Windows. *Molecular Ecology Resources*, *10*(3), 564–567. https://doi.org/10.1111/j.1755-0998.2010.02847.x

Faillettaz, R., Beaugrand, G., Goberville, E., & Kirby, R. R. (2019). Atlantic Multidecadal Oscillations drive the basin-scale distribution of Atlantic bluefin tuna. *Science Advances*, *5*(1), eaar6993. https://doi.org/10.1126/sciadv.aar6993

Ferrari, G., Atmore, L. M., Jentoft, S., Jakobsen, K. S., Makowiecki, D., Barrett, J. H., & Star, B. (2022). An accurate assignment test for extremely low-coverage whole-genome sequence data. *Molecular Ecology Resources*, *22*(4), 1330–1344. https://doi.org/10.1111/1755-0998.13551

Ferrari, G., Cuevas, A., Gondek-Wyrozemska, A. T., Ballantyne, R., Kersten, O., Pálsdóttir, A. H., van der Jagt, I., Hufthammer, A. K., Ystgaard, I., Wickler, S., Bigelow, G. F., Harland, J., Nicholson, R., Orton, D., Clavel, B., Boessenkool, S., Barrett, J. H., & Star, B. (2021). The preservation of ancient DNA in archaeological fish bone. *Journal of Archaeological Science*, *126*, 105317. https://doi.org/10.1016/j.jas.2020.105317

Fijarczyk, A., & Babik, W. (2015). Detecting balancing selection in genomes: Limits and prospects. *Molecular Ecology*, *24*(14), 3529–3545. https://doi.org/10.1111/mec.13226

Fjelstrup, S., Andersen, M. B., Thomsen, J., Wang, J., Stougaard, M., Pedersen, F. S., Ho, Y.-P., Hede, M. S., & Knudsen, B. R. (2017). The Effects of Dithiothreitol on DNA. *Sensors (Basel, Switzerland)*, *17*(6), 1201. https://doi.org/10.3390/s17061201

Fraile, I., Arrizabalaga, H., & Rooker, J. R. (2015). Origin of Atlantic bluefin tuna (Thunnus thynnus) in the Bay of Biscay. *ICES Journal of Marine Science*, *72*(2), 625–634. https://doi.org/10.1093/icesjms/fsu156

Fromentin, J.-M. (2009). Lessons from the past: Investigating historical data from bluefin tuna fisheries. *Fish and Fisheries*, *10*(2), 197–216. https://doi.org/10.1111/j.1467-2979.2008.00311.x

Fromentin, J.-M., Bonhommeau, S., Arrizabalaga, H., & Kell, L. T. (2014). The spectre of uncertainty in management of exploited fish stocks: The illustrative case of Atlantic bluefin tuna. *Marine Policy*, *47*, 8–14. https://doi.org/10.1016/j.marpol.2014.01.018

Fromentin, J.-M., & Lopuszanski, D. (2014). Migration, residency, and homing of bluefin tuna in the western Mediterranean Sea. *ICES Journal of Marine Science*, *71*(3), 510–518. https://doi.org/10.1093/icesjms/fst157

Fromentin, J.-M., & Powers, J. E. (2005). Atlantic bluefin tuna: Population dynamics, ecology, fisheries and management. *Fish and Fisheries*, *6*(4), 281–306. https://doi.org/10.1111/j.1467-2979.2005.00197.x

Fromentin, J.-M., Reygondeau, G., Bonhommeau, S., & Beaugrand, G. (2014). Oceanographic changes and exploitation drive the spatio-temporal dynamics of Atlantic bluefin tuna (Thunnus thynnus). *Fisheries Oceanography*, *23*(2), 147–156. https://doi.org/10.1111/fog.12050

Fu, Y. X., & Li, W. H. (1993). Statistical tests of neutrality of mutations. *Genetics*, *133*(3), 693–709. https://doi.org/10.1093/genetics/133.3.693

Fuentes-Pardo, A. P., & Ruzzante, D. E. (2017). Whole-genome sequencing approaches for conservation biology: Advantages, limitations and practical recommendations. *Molecular Ecology*, *26*(20), 5369–5406. https://doi.org/10.1111/mec.14264

Galuardi, B., Royer, F., Golet, W., Logan, J., Neilson, J., & Lutcavage, M. (2010). Complex migration routes of Atlantic bluefin tuna (Thunnus thynnus) question current population structure paradigm. *Canadian Journal of Fisheries and Aquatic Sciences*, *67*(6), 966–976. https://doi.org/10.1139/F10-033

GATK. (2016). *GATK Hands -On Tutorial: Variant Discovery with GATK*. https://qcb.ucla.edu/wp-content/uploads/sites/14/2016/03/GATK_Discovery_Tutorial-Worksheet-AUS2016.pdf

GATK. (2022a, February). *The logic of joint calling for germline short variants*. GATK. https://gatk.broadinstitute.org/hc/en-us/articles/360035890431-The-logic-of-joint-calling-for-germline-short-variants

GATK. (2022b, April 15). *Hard-filtering germline short variants*. https://gatk.broadinstitute.org/hc/en-us/articles/360035890471-Hard-filtering-germline-short-variants

Gilbert, M. T. P., Bandelt, H.-J., Hofreiter, M., & Barnes, I. (2005). Assessing ancient DNA studies. *Trends in Ecology & Evolution*, *20*(10), 541–544. https://doi.org/10.1016/j.tree.2005.07.005

Ginolhac, A., Rasmussen, M., Gilbert, M. T. P., Willerslev, E., & Orlando, L. (2011). mapDamage: Testing for damage patterns in ancient DNA sequences. *Bioinformatics*, *27*(15), 2153–2155. https://doi.org/10.1093/bioinformatics/btr347

Gondek, A. T., Boessenkool, S., & Star, B. (2018). A stainless-steel mortar, pestle and sleeve design for the efficient fragmentation of ancient bone. *BioTechniques*, *64*(6), 266–269. https://doi.org/10.2144/btn-2018-0008

Gong, L., Liu, L.-Q., Guo, B.-Y., Ye, Y.-Y., & Lü, Z.-M. (2017). The complete mitochondrial genome characterization of Thunnus obesus (Scombriformes: Scombridae) and phylogenetic analyses of Thunnus. *Conservation Genetics Resources*, *9*(3), 379–383. https://doi.org/10.1007/s12686-017-0688-2

Gugerli, F., Parducci, L., & Petit, R. J. (2005). Ancient plant DNA: Review and prospects. *New Phytologist*, *166*(2), 409–418. https://doi.org/10.1111/j.1469-8137.2005.01360.x

Hanke, A., Macdonnell, A., Dalton, A., Busawon, D., Rooker, J., & Secor, D. (2018). *STOCK MIXING RATES OF BLUEFIN TUNA FROM CANADIAN LANDINGS: 1975-2015*. *76*, 2622–2634.

Hasegawa, M., Kishino, H., & Yano, T. (1985). Dating of the human-ape splitting by a molecular clock of mitochondrial DNA. *Journal of Molecular Evolution*, *22*(2), 160–174. https://doi.org/10.1007/BF02101694

Holt, R. D. (2006). Emergent neutrality. *Trends in Ecology & Evolution*, *21*(10), 531–533. https://doi.org/10.1016/j.tree.2006.08.003

ICCAT. (2022). *List of Reporting Requirements for the SCRS in 2022*. ICCAT. https://www.iccat.int/en/submitSTAT.html

ICCAT. 2009. Report of the world symposium for the study into the stock fluctuation of northern bluefin tunas (Thunnus thynnus and Thunnus orientalis), including the historical periods. ICCAT Collective Volume of Scientific Papers 63:1–49.

ICCAT. 2009b. Report of the independent performance review of ICCAT. www.iccat.int /Documents/Other/PERFORM_%20REV_TRI_LINGUAL.pdf

IMR. (2021, October 29). *Makrellstørje*. Havforskningsinstituttet. https://www.hi.no/hi/temasider/arter/makrellstorje

Johnstone, C., Pérez, M., Malca, E., Quintanilla, J. M., Gerard, T., Lozano-Peral, D., Alemany, F., Lamkin, J., García, A., & Laiz-Carrión, R. (2021). Genetic connectivity between Atlantic bluefin tuna larvae spawned in the Gulf of Mexico and in the Mediterranean Sea. *PeerJ*, *9*, e11568. https://doi.org/10.7717/peerj.11568

Jombart, T. (2008). adegenet: A R package for the multivariate analysis of genetic markers. *Bioinformatics*, *24*(11), 1403–1405. https://doi.org/10.1093/bioinformatics/btn129

Jonsson, L. 2007. Djurbenen från Sandhem. Tidigare undersökningar av djurben från kökkenmöddingar i Västsverige, in: Lönn, M., Claesson, P. (Eds.), Vistelser Vid Vatten. Gropkeramiska Platser Och Kokgropar Från Bronsålder Och Järnålder. Riksantikvarieämbetet & Bohusläns museum, Ödeshög, 231–235.

Jonsson, L. 2002. Animal bones from the Middle Neolithic site Hakeröd in Bohuslän, Sweden. ANL-rapport 2002:1, Institutionen för Arkeologi, Göteborgs universitet, Göteborg.

Jónsson, H., Ginolhac, A., Schubert, M., Johnson, P. L. F., & Orlando, L. (2013). mapDamage2.0: Fast approximate Bayesian estimates of ancient DNA damage parameters. *Bioinformatics*, *29*(13), 1682–1684. https://doi.org/10.1093/bioinformatics/btt193

Kalyaanamoorthy, S., Minh, B. Q., Wong, T. K., von Haeseler, A., & Jermiin, L. S. (2017). ModelFinder: Fast Model Selection for Accurate Phylogenetic Estimates. *Nature Methods*, *14*(6), 587–589. https://doi.org/10.1038/nmeth.4285

Kapp, J. D., Green, R. E., & Shapiro, B. (2021). A Fast and Efficient Single-stranded Genomic Library Preparation Method Optimized for Ancient DNA. *Journal of Heredity*, *112*(3), 241–249. https://doi.org/10.1093/jhered/esab012

Karsten, P., and B. Knarrström. 2003. The Tågerup Excavation. National Heritage Board. Lund: National Heritage Board.

Kasim, N. S., Jaafar, T. N. A. M., Piah, R. M., Arshaad, W. M., Nor, S. A. M., Habib, A., Ghaffar, M. A., Sung, Y. Y., Danish-Daniel, M., & Tan, M. P. (2020). Recent population expansion of longtail tuna Thunnus tonggol (Bleeker, 1851) inferred from the mitochondrial DNA markers. *PeerJ*, *8*, e9679. https://doi.org/10.7717/peerj.9679

Katoh, K., Misawa, K., Kuma, K., & Miyata, T. (2002). MAFFT: A novel method for rapid multiple sequence alignment based on fast Fourier transform. *Nucleic Acids Research*, *30*(14), 3059–3066. https://doi.org/10.1093/nar/gkf436

Kimura, M. (1981). Estimation of evolutionary distances between homologous nucleotide sequences. *Proceedings of the National Academy of Sciences*, *78*(1), 454–458. https://doi.org/10.1073/pnas.78.1.454

Knape, A., and P. G. P. Ericson. 1983. "Återupptäckta Fund Från Grotta Stora Förvar." Fornvännen 78: 192–198.

Knaus, B. J., & Grünwald, N. J. (2017). vcfr: A package to manipulate and visualize variant call format data in R. *Molecular Ecology Resources*, *17*(1), 44–53. https://doi.org/10.1111/1755-0998.12549

Kodama, Y., Shumway, M., Leinonen, R., & International Nucleotide Sequence Database Collaboration. (2012). The Sequence Read Archive: Explosive growth of sequencing data. *Nucleic Acids Research*, *40*(Database issue), D54-56. https://doi.org/10.1093/nar/gkr854

Kontopoulos, I., Penkman, K., McAllister, G. D., Lynnerup, N., Damgaard, P. B., Hansen, H. B., Allentoft, M. E., & Collins, M. J. (2019). Petrous bone diagenesis: A multi-analytical approach. *Palaeogeography, Palaeoclimatology, Palaeoecology*, *518*, 143–154. https://doi.org/10.1016/j.palaeo.2019.01.005

Korneliussen, T. S., Moltke, I., Albrechtsen, A., & Nielsen, R. (2013). Calculation of Tajima's D and other neutrality test statistics from low depth next-generation sequencing data. *BMC Bioinformatics*, *14*(1), 289. https://doi.org/10.1186/1471-2105-14-289

Krutovsky, K. V., & Neale, D. B. (2005). Nucleotide Diversity and Linkage Disequilibrium in Cold-Hardiness- and Wood Quality-Related Candidate Genes in Douglas Fir. *Genetics*, *171*(4), 2029–2041. https://doi.org/10.1534/genetics.105.044420

Kucera, A. C., & Heidinger, B. J. (2018). Avian Semen Collection by Cloacal Massage and Isolation of DNA from Sperm. *JoVE (Journal of Visualized Experiments)*, *132*, e55324. https://doi.org/10.3791/55324

Küchelmann, H. C. (2020). Hanseatic fish trade in the North Atlantic: Evidence of fish remains from Hanse cities in Germany. *AmS-Skrifter*, *27*, 75–92. https://doi.org/10.31265/ams-skrifter.v0i27.257

Kumar, G., Kunal, S. P., Menezes, M. R., & Meena, R. M. (2012). Three genetic stocks of frigate tuna Auxis thazard thazard (Lacepede, 1800) along the Indian coast revealed from sequence analyses of mitochondrial DNA D-loop region. *Marine Biology Research*, *8*(10), 992–1002. https://doi.org/10.1080/17451000.2012.702913

Kunal, S. P., Kumar, G., Menezes, M. R., & Meena, R. M. (2013). Mitochondrial DNA analysis reveals three stocks of yellowfin tuna Thunnus albacares (Bonnaterre, 1788) in Indian waters. *Conservation Genetics*, *14*(1), 205–213. https://doi.org/10.1007/s10592-013-0445-3

Larsson, A. (2014). AliView: A fast and lightweight alignment viewer and editor for large datasets. *Bioinformatics*, *30*(22), 3276–3278. https://doi.org/10.1093/bioinformatics/btu531

Li, H. (2011). Tabix: Fast retrieval of sequence features from generic TAB-delimited files. *Bioinformatics*, *27*(5), 718–719. https://doi.org/10.1093/bioinformatics/btq671

Li, H., & Durbin, R. (2009). Fast and accurate short read alignment with Burrows–Wheeler transform. *Bioinformatics*, *25*(14), 1754–1760. https://doi.org/10.1093/bioinformatics/btp324

Li, H., Handsaker, B., Wysoker, A., Fennell, T., Ruan, J., Homer, N., Marth, G., Abecasis, G., Durbin, R., & 1000 Genome Project Data Processing Subgroup. (2009). The Sequence Alignment/Map format and SAMtools. *Bioinformatics*, *25*(16), 2078–2079. https://doi.org/10.1093/bioinformatics/btp352

Lindquist, O. (1994). *Whales, dolphins and porpoises in the economy and culture of peasant fishermen in Norway, Orkney, Shetland, Faroe Islands and Iceland, ca.900—1900 A.D., and Norse Greenland, ca.1000—1500 A.D.* [Thesis, University of St Andrews]. https://research-repository.st-andrews.ac.uk/handle/10023/2953

Llamas, B., Valverde, G., Fehren-Schmitz, L., Weyrich, L. S., Cooper, A., & Haak, W. (2017). From the field to the laboratory: Controlling DNA contamination in human ancient DNA research in the high-throughput sequencing era. *STAR: Science & Technology of Archaeological Research*, *3*(1), 1–14. https://doi.org/10.1080/20548923.2016.1258824

Lutcavage, M. E., Brill, R. W., Skomal, G. B., Chase, B. C., & Howey, P. W. (1999). Results of pop-up satellite tagging of spawning size class fish in the Gulf of Maine: Do North Atlantic bluefin tuna spawn in the mid-Atlantic? *Canadian Journal of Fisheries and Aquatic Sciences*, *56*(2), 173–177. https://doi.org/10.1139/f99-016

Mansrud, A., & Berg-Hansen, I. M. (2021). Animist Ontologies in the Third Millennium BCE? Hunter-Gatherer Persistency and Human–Animal Relations in Southern Norway: The Alveberget Case. *Open Archaeology*, *7*(1), 868–888. https://doi.org/10.1515/opar-2020-0176

Martínez-García, L., Ferrari, G., Oosting, T., Ballantyne, R., van der Jagt, I., Ystgaard, I., Harland, J., Nicholson, R., Hamilton-Dyer, S., Baalsrud, H. T., Brieuc, M. S. O., Atmore, L. M., Burns, F., Schmölcke, U., Jakobsen, K. S., Jentoft, S., Orton, D., Hufthammer, A. K., Barrett, J. H., & Star, B. (2021). *Historical Demographic Processes Dominate Genetic Variation in Ancient Atlantic Cod Mitogenomes*. https://doi.org/10.17863/CAM.71522

Mather, F.J., J.M. Mason, and A.C. Jones. 1995. Historical document: Life history and fisheries of Atlantic bluefin tuna. 1995. NOAA Tech. Memo. NMFS--SEFSC-370

Matschiner, M. (2016). Fitchi: Haplotype genealogy graphs based on the Fitch algorithm. *Bioinformatics*, *32*(8), 1250–1252. https://doi.org/10.1093/bioinformatics/btv717

McKenna, A., Hanna, M., Banks, E., Sivachenko, A., Cibulskis, K., Kernytsky, A., Garimella, K., Altshuler, D., Gabriel, S., Daly, M., & DePristo, M. A. (2010). The Genome Analysis Toolkit: A MapReduce framework for analyzing next-generation DNA sequencing data. *Genome Research*, *20*(9), 1297–1303. https://doi.org/10.1101/gr.107524.110

Meyer, M., & Kircher, M. (2010). Illumina Sequencing Library Preparation for Highly Multiplexed Target Capture and Sequencing. *Cold Spring Harbor Protocols*, *2010*(6), pdb.prot5448. https://doi.org/10.1101/pdb.prot5448

Mishmar, D., Ruiz-Pesini, E., Golik, P., Macaulay, V., Clark, A. G., Hosseini, S., Brandon, M., Easley, K., Chen, E., Brown, M. D., Sukernik, R. I., Olckers, A., & Wallace, D. C. (2003). Natural selection shaped regional mtDNA variation in humans. *Proceedings of the National Academy of Sciences*, *100*(1), 171–176. https://doi.org/10.1073/pnas.0136972100

Miyake, P. M., Katavic, I., Miyabe, N., & Ticina, V. (2003). General review of Bluefin Tuna farming in the Mediterranean area. *SCRS*, 11.

Nei, M. (1987). Molecular Evolutionary Genetics. Columbia Univ. Press, New York.

Nguyen, L.-T., Schmidt, H. A., von Haeseler, A., & Minh, B. Q. (2015). IQ-TREE: A Fast and Effective Stochastic Algorithm for Estimating Maximum-Likelihood Phylogenies. *Molecular Biology and Evolution*, *32*(1), 268–274. https://doi.org/10.1093/molbev/msu300

Nielsen, S. V. (2020a). *Myrfunn fra Jortveit. Rapport 1 av 3. Jortveit, 172/2, Grimstad, Agder.* https://www.duo.uio.no/handle/10852/85693

Nielsen, S. V. (2020b). *Myrfunn fra Jortveit. Rapport 2 av 3. Jortveit, 172/2, Grimstad, Agder.* https://www.duo.uio.no/handle/10852/85694

Nielsen, S. V. (2020c). *Myrfunn fra Jortveit. Rapport 3 av 3. Jortveit, 172/2, Grimstad, Agder.* https://www.duo.uio.no/handle/10852/85695

Nielsen, S. V., & Persson, P. (2020). The Jortveit farm wetland: A Neolithic fishing site on the Skagerrak coast, Norway. *Journal of Wetland Archaeology*, *0*(0), 1–24. https://doi.org/10.1080/14732971.2020.1776495

Nistelberger, H. M., Pálsdóttir, A. H., Star, B., Leifsson, R., Gondek, A. T., Orlando, L., Barrett, J. H., Hallsson, J. H., & Boessenkool, S. (2019). Sexing Viking Age horses from burial and non-burial sites in Iceland using ancient DNA. *Journal of Archaeological Science*, *101*, 115–122. https://doi.org/10.1016/j.jas.2018.11.007

Nøttestad, L., Boge, E., & Ferter, K. (2020). The comeback of Atlantic bluefin tuna (Thunnus thynnus) to Norwegian waters. *Fisheries Research*, *231*, 105689. https://doi.org/10.1016/j.fishres.2020.105689

Olsen, H. 1976. Skipshelleren. Osteologisk materiale. Zoologisk Museum. Universitetet i Bergen, Bergen.

Oppianus, 177 BCE. Halieuticon. In Della Caccia e della Pesca. Edited by A.M. Salvini, 1738. Firenze, Italy.

Pagá Garcia, A., Palma, C., Di Natale, A., Tensek, S., Parrilla, A., & de Bruyn, P. (2017). *Report on Revised Trap Data Recovered by ICCAT GBYP From Phase 1 To Phase 6*. 25.

Paradis, E. (2010). pegas: An R package for population genetics with an integrated–modular approach. *Bioinformatics*, *26*(3), 419–420. https://doi.org/10.1093/bioinformatics/btp696

Paradis, E., Claude, J., & Strimmer, K. (2004). APE: Analyses of Phylogenetics and Evolution in R language. *Bioinformatics*, *20*(2), 289–290. https://doi.org/10.1093/bioinformatics/btg412

Pauly, D. (1995). Anecdotes and the shifting baseline syndrome of fisheries. *Trends in Ecology & Evolution*, *10*(10), 430. https://doi.org/10.1016/S0169-5347(00)89171-5

Plinius, C.S., 65 CE (reedited in 1553). Historia Mundi. In Naturalis Historia, edited by A. Vicentino. Ludguni, Italy

Pinnegar, J. K., & Engelhard, G. H. (2008). The 'shifting baseline' phenomenon: A global perspective. *Reviews in Fish Biology and Fisheries*, *18*(1), 1–16. https://doi.org/10.1007/s11160-007-9058-6

Pinsky, M. L., Eikeset, A. M., Helmerson, C., Bradbury, I. R., Bentzen, P., Morris, C., Gondek-Wyrozemska, A. T., Baalsrud, H. T., Brieuc, M. S. O., Kjesbu, O. S., Godiksen, J. A., Barth, J. M. I., Matschiner, M., Stenseth, N. Chr., Jakobsen, K. S., Jentoft, S., & Star, B. (2021). Genomic stability through time despite decades of exploitation in cod on both sides of the Atlantic. *Proceedings of the National Academy of Sciences*, *118*(15), e2025453118. https://doi.org/10.1073/pnas.2025453118

Poplin, R., Ruano-Rubio, V., DePristo, M. A., Fennell, T. J., Carneiro, M. O., Auwera, G. A. V. der, Kling, D. E., Gauthier, L. D., Levy-Moonshine, A., Roazen, D., Shakir, K., Thibault, J., Chandran, S., Whelan, C., Lek, M., Gabriel, S., Daly, M. J., Neale, B., MacArthur, D. G., & Banks, E. (2018). *Scaling accurate genetic variant discovery to tens of thousands of samples* (p. 201178). bioRxiv. https://doi.org/10.1101/201178

Posada, D. (2003). Using MODELTEST and PAUP* to Select a Model of Nucleotide Substitution. *Current Protocols in Bioinformatics*, *00*(1), 6.5.1-6.5.14. https://doi.org/10.1002/0471250953.bi0605s00

Pujolar, J. M., Roldán, M. I., & Pla, C. (2003). Genetic analysis of tuna populations, Thunnus thynnus thynnus and T. alalunga. *Marine Biology*, *143*(3), 613–621. https://doi.org/10.1007/s00227-003-1080-1

Puncher, G. N. (2015). *Assessment of the population structure and temporal changes in spatial dynamics and genetic characteristics of the Atlantic bluefin tuna under a fishery independent framework.* [Doctoral Thesis, Alma Mater Studiorum - Università di Bologna]. https://doi.org/10.6092/unibo/amsdottorato/7227

Puncher, G. N., Cariani, A., Cilli, E., Massari, F., Leone, A., Morales-Muniz, A., Onar, V., Toker, N. Y., Bernal Casasola, D., Moens, T., & Tinti, F. (2019). Comparison and optimization of genetic tools used for the identification of ancient fish remains recovered from archaeological excavations and museum collections in the Mediterranean region. *International Journal of Osteoarchaeology*, *29*(3), 365–376. https://doi.org/10.1002/oa.2765

Puncher, G. N., Cariani, A., Cilli, E., Massari, F., Martelli, P. L., Morales, A., Onar, V., Toker, N. Y., Moens, T., & Tinti, F. (2015). *Unlocking the evolutionary history of the mighty bluefin tuna using novel paleogenetic techniques and ancient tuna remains*. 12.

Puncher, G. N., Cariani, A., Maes, G. E., Van Houdt, J., Herten, K., Cannas, R., Rodriguez-Ezpeleta, N., Albaina, A., Estonba, A., Lutcavage, M., Hanke, A., Rooker, J., Franks, J. S., Quattro, J. M., Basilone, G., Fraile, I., Laconcha, U., Goñi, N., Kimoto, A., … Tinti, F. (2018). Spatial dynamics and mixing of bluefin tuna in the Atlantic Ocean and Mediterranean Sea revealed using next-generation sequencing. *Molecular Ecology Resources*, *18*(3), 620–638. https://doi.org/10.1111/1755-0998.12764

Puncher, G. N., Onar, V., Toker, N. Y., & Tinti, F. (2015). A multitude of Byzantine Era Bluefin Tuna and Swordfish bones uncovered in Istanbul, Turkey. *ICCAT Coll.* https://doi.org/10.1371/journal.pone.0039998

R Core Team (2021). R: A language and environment for statistical computing. R Foundation for Statistical Computing, Vienna, Austria. URL https://www.R-project.org/.

Rambaut, A. (2018, November 26). *FigTree v1.4.4*. GitHub. https://github.com/rambaut/figtree/releases

Rambaut, A., Drummond, A. J., Xie, D., Baele, G., & Suchard, M. A. (2018). Posterior Summarization in Bayesian Phylogenetics Using Tracer 1.7. *Systematic Biology*, *67*(5), 901–904. https://doi.org/10.1093/sysbio/syy032

Ravier, C., & Fromentin, J.-M. (2001). Long-term fluctuations in the eastern Atlantic and Mediterranean bluefin tuna population. *ICES Journal of Marine Science*, *58*(6), 1299–1317. https://doi.org/10.1006/jmsc.2001.1119

Rhymer, J. M., & Simberloff, D. (1996). Extinction by Hybridization and Introgression. *Annual Review of Ecology and Systematics*, *27*(1), 83–109. https://doi.org/10.1146/annurev.ecolsys.27.1.83

Riccioni, G., Landi, M., Ferrara, G., Milano, I., Cariani, A., Zane, L., Sella, M., Barbujani, G., & Tinti, F. (2010). Spatio-temporal population structuring and genetic diversity retention in depleted Atlantic Bluefin tuna of the Mediterranean Sea. *Proceedings of the National Academy of Sciences of the United States of America*, *107*(5), 2102–2107. https://doi.org/10.1073/pnas.0908281107

Riccioni, G., Stagioni, M., Landi, M., Ferrara, G., Barbujani, G., & Tinti, F. (2013). Genetic Structure of Bluefin Tuna in the Mediterranean Sea Correlates with Environmental Variables. *PLOS ONE*, *8*(11), e80105. https://doi.org/10.1371/journal.pone.0080105

Rodríguez, F., Oliver, J. L., Marín, A., & Medina, J. R. (1990). The general stochastic model of nucleotide substitution. *Journal of Theoretical Biology*, *142*(4), 485–501. https://doi.org/10.1016/S0022-5193(05)80104-3

Rodríguez-Ezpeleta, N., Díaz-Arce, N., Walter, J. F., Richardson, D. E., Rooker, J. R., Nøttestad, L., Hanke, A. R., Franks, J. S., Deguara, S., Lauretta, M. V., Addis, P., Varela, J. L., Fraile, I., Goñi, N., Abid, N., Alemany, F., Oray, I. K., Quattro, J. M., Sow, F. N., … Arrizabalaga, H. (2019). Determining natal origin for improved management of Atlantic bluefin tuna. *Frontiers in Ecology and the Environment*, *17*(8), 439–444. https://doi.org/10.1002/fee.2090

Rohland, N., Siedel, H., & Hofreiter, M. (2010). A rapid column-based ancient DNA extraction method for increased sample throughput. *Molecular Ecology Resources*, *10*(4), 677–683. https://doi.org/10.1111/j.1755-0998.2009.02824.x

Ronquist, F., & Huelsenbeck, J. P. (2003). MrBayes 3: Bayesian phylogenetic inference under mixed models. *Bioinformatics*, *19*(12), 1572–1574. https://doi.org/10.1093/bioinformatics/btg180

Ronquist, F., Teslenko, M., van der Mark, P., Ayres, D. L., Darling, A., Höhna, S., Larget, B., Liu, L., Suchard, M. A., & Huelsenbeck, J. P. (2012). MrBayes 3.2: Efficient Bayesian Phylogenetic Inference and Model Choice Across a Large Model Space. *Systematic Biology*, *61*(3), 539–542. https://doi.org/10.1093/sysbio/sys029

Rooker, J. R., Alvarado Bremer, J. R., Block, B. A., Dewar, H., de Metrio, G., Corriero, A., Kraus, R. T., Prince, E. D., Rodríguez-Marín, E., & Secor, D. H. (2007). Life History and Stock Structure of Atlantic Bluefin Tuna (Thunnus thynnus). *Reviews in Fisheries Science*, *15*(4), 265–310. https://doi.org/10.1080/10641260701484135

Rooker, J. R., Arrizabalaga, H., Fraile, I., Secor, D. H., Dettman, D. L., Abid, N., Addis, P., Deguara, S., Karakulak, F. S., Kimoto, A., Sakai, O., Macías, D., & Santos, M. N. (2014). Crossing the line: Migratory and homing behaviors of Atlantic bluefin tuna. *Marine Ecology Progress Series*, *504*, 265–276. https://doi.org/10.3354/meps10781

Rooker, J. R., Secor, D. H., De Metrio, G., Schloesser, R., Block, B. A., & Neilson, J. D. (2008). Natal Homing and Connectivity in Atlantic Bluefin Tuna Populations. *Science*, *322*(5902), 742–744. https://doi.org/10.1126/science.1161473

Rooker, J. R., Secor, D. H., Metrio, G. D., Rodríquez-marín, E., & Farrugia, A. F. (2006). Evaluation of population structure and mixing rates of Atlantic bluefin tuna from chemical signatures in otoliths. *ICCAT, Col. Vol. Sci. Pa*, 813–818.

Rozas, J., Ferrer-Mata, A., Sánchez-DelBarrio, J. C., Guirao-Rico, S., Librado, P., Ramos-Onsins, S. E., & Sánchez-Gracia, A. (2017). DnaSP 6: DNA Sequence Polymorphism Analysis of Large Data Sets. *Molecular Biology and Evolution*, *34*(12), 3299–3302. https://doi.org/10.1093/molbev/msx248

RStudio Team (2021). RStudio: Integrated Development for R. RStudio, PBC, Boston, MA URL http://www.rstudio.com/.

Saber, S., Urbina, J. O. de, Gómez-Vives, M. J., & Macías, D. (2015). Some aspects of the reproductive biology of albacore Thunnus alalunga from the western Mediterranean Sea. *Journal of the Marine Biological Association of the United Kingdom*, *95*(8), 1705–1715. https://doi.org/10.1017/S002531541500020X

Santini, F., Carnevale, G., & Sorenson, L. (2013). First molecular scombrid timetree (Percomorpha: Scombridae) shows recent radiation of tunas following invasion of pelagic habitat. *Italian Journal of Zoology*, *80*(2), 210–221. https://doi.org/10.1080/11250003.2013.775366

Särlvik, I. 1976. Fornlämning 72 och 116, stenåldersboplats, Gröninge, Tölö sn, Halland. Vol. 9. Riksantikvarieämbetet Rapport 1976 B, Stockholm

Schaefer, K. M. (2001). Reproductive biology of tunas. In *Fish Physiology* (Vol. 19, pp. 225–270). Academic Press. https://doi.org/10.1016/S1546-5098(01)19007-2

Schloesser, R. W., Neilson, J. D., Secor, D. H., & Rooker, J. R. (2010). Natal origin of Atlantic bluefin tuna (Thunnus thynnus) from Canadian waters based on otolith δ13C and δ18O. *Canadian Journal of Fisheries and Aquatic Sciences*, *67*(3), 563–569. https://doi.org/10.1139/F10-005

Schroeder, H., Ávila-Arcos, M. C., Malaspinas, A.-S., Poznik, G. D., Sandoval-Velasco, M., Carpenter, M. L., Moreno-Mayar, J. V., Sikora, M., Johnson, P. L. F., Allentoft, M. E., Samaniego, J. A., Haviser, J. B., Dee, M. W., Stafford, T. W., Salas, A., Orlando, L., Willerslev, E., Bustamante, C. D., & Gilbert, M. T.

P. (2015). Genome-wide ancestry of 17th-century enslaved Africans from the Caribbean. *Proceedings of the National Academy of Sciences*, *112*(12), 3669–3673. https://doi.org/10.1073/pnas.1421784112

Schubert, M., Ermini, L., Sarkissian, C. D., Jónsson, H., Ginolhac, A., Schaefer, R., Martin, M. D., Fernández, R., Kircher, M., McCue, M., Willerslev, E., & Orlando, L. (2014). Characterization of ancient and modern genomes by SNP detection and phylogenomic and metagenomic analysis using PALEOMIX. *Nature Protocols*, *9*(5), 1056–1082. https://doi.org/10.1038/nprot.2014.063

Schubert, M., Lindgreen, S., & Orlando, L. (2016). AdapterRemoval v2: Rapid adapter trimming, identification, and read merging. *BMC Research Notes*, *9*(1), 88. https://doi.org/10.1186/s13104-016-1900-2

Schwarz, G. (1978). Estimating the Dimension of a Model. *The Annals of Statistics*, *6*(2), 461–464.

SCRS. (1982). Report of the Standing Committee on Research and Statistics (SCRS). ICCAT Report for the Biennial Period 1980–81, Part II (1981)

SCRS. (2019). *2019 SCRS Report*. (ICCAT) SCRS Standing Committee on Research and Statistics. https://www.iccat.int/Documents/SCRS/ExecSum/BFT_ENG.pdf

SCRS. (2019b). Report of the Standing Committee on Research and Statistics (SCRS). https://www.iccat.int/Documents/Meetings/Docs/2019/REPORTS/2019_SCRS_ENG.pdf

SCRS. (2021). Report for biennial period 2020-21: 2020 SCRS Advice to the Comission. *ICCAT Biennial Reports*, *1*, 341.

Seixas, F. A., Boursot, P., & Melo-Ferreira, J. (2018). The genomic impact of historical hybridization with massive mitochondrial DNA introgression. *Genome Biology*, *19*(1), 91. https://doi.org/10.1186/s13059-018-1471-8

Shen, W., Le, S., Li, Y., & Hu, F. (2016). SeqKit: A Cross-Platform and Ultrafast Toolkit for FASTA/Q File Manipulation. *PLOS ONE*, *11*(10), e0163962. https://doi.org/10.1371/journal.pone.0163962

Siskey, M. R., Wilberg, M. J., Allman, R. J., Barnett, B. K., & Secor, D. H. (2016). Forty years of fishing: Changes in age structure and stock mixing in northwestern Atlantic bluefin tuna (Thunnus thynnus) associated with size-selective and long-term exploitation. *ICES Journal of Marine Science*, *73*(10), 2518–2528. https://doi.org/10.1093/icesjms/fsw115

Smith, G. R. (1992). Introgression in Fishes: Significance for Paleontology, Cladistics, and Evolutionary Rates. *Systematic Biology*, *41*(1), 41–57. https://doi.org/10.2307/2992505

Sölen, G., Edgren, M., Scott, O. C. A., & Révész, L. (1991). Radioprotection by Dithiothreitol (DTT) at Varying Oxygen Concentrations: Predictions of a Modified Competition Model and Theory Evaluation. *International Journal of Radiation Biology*, *59*(2), 409–418. https://doi.org/10.1080/09553009114550371

Spoto, S. 2002. Sicilia Antica: Usi, costumi e personaggi dalla preistoria alla società greca, nell'isola culla della civiltà europea. Edited by N.E. Compton. Rome: Newton & Compton.

Star, B., Boessenkool, S., Gondek, A. T., Nikulina, E. A., Hufthammer, A. K., Pampoulie, C., Knutsen, H., André, C., Nistelberger, H. M., Dierking, J., Petereit, C., Heinrich, D., Jakobsen, K. S., Stenseth, N. Chr., Jentoft, S., & Barrett, J. H. (2017). Ancient DNA reveals the Arctic origin of Viking Age cod from Haithabu, Germany. *Proceedings of the National Academy of Sciences*, *114*(34), 9152–9157. https://doi.org/10.1073/pnas.1710186114

Stevens, E. D., Kanwisher, J. W., & Carey, F. G. (2000). Muscle temperature in free-swimming giant Atlantic bluefin tuna (Thunnus thynnus L.). *Journal of Thermal Biology*, *25*(6), 419–423. https://doi.org/10.1016/S0306-4565(00)00004-8

Suda, A., Nishiki, I., Iwasaki, Y., Matsuura, A., Akita, T., Suzuki, N., & Fujiwara, A. (2019). Improvement of the Pacific bluefin tuna (Thunnus orientalis) reference genome and development of male-specific DNA markers. *Scientific Reports*, *9*(1), 14450. https://doi.org/10.1038/s41598-019-50978-4

Szpak, P. (2011). Fish bone chemistry and ultrastructure: Implications for taphonomy and stable isotope analysis. *Journal of Archaeological Science*, *38*(12), 3358–3372. https://doi.org/10.1016/j.jas.2011.07.022

Tajima, F. (1989). Statistical method for testing the neutral mutation hypothesis by DNA polymorphism. *Genetics*, *123*(3), 585–595. https://doi.org/10.1093/genetics/123.3.585

Tamura, K., & Nei, M. (1993). Estimation of the number of nucleotide substitutions in the control region of mitochondrial DNA in humans and chimpanzees. *Molecular Biology and Evolution*, *10*(3), 512–526. https://doi.org/10.1093/oxfordjournals.molbev.a040023

Tangen, M. 2009. The Norwegian fishery for Atlantic Bluefin Tuna. ICCAT Collective Volume of Scientific Papers 63:79–93

ThermoFisher. (2022). *RNAlater Solutions for RNA Stabilization and Storage*. ThermoFisher. //www.thermofisher.com/uk/en/home/brands/product-brand/rnalater.html

Thiede, J. (1978). A Glacial Mediterranean. *Nature*, *276*(5689), 680–683. https://doi.org/10.1038/276680a0

Tiews, K. (1978). On the disappearance of Bluefin Tuna in the North Sea and its Ecological Implications for Herring and Mackerel. *Rapp. P.-v. Réun. Cons. Int. Explor.*, *Mer, 172: 301-309.*, 301–309.

Toews, D. P. L., & Brelsford, A. (2012). The biogeography of mitochondrial and nuclear discordance in animals. *Molecular Ecology*, *21*(16), 3907–3930. https://doi.org/10.1111/j.1365-294X.2012.05664.x

Tseng, M.-C., Shiao, J.-C., & Hung, Y.-H. (2011). Genetic identification of Thunnus orientalis, T. thynnus, and T. maccoyii by a cytochrome b gene analysis. *Environmental Biology of Fishes*, *91*(1), 103–115. https://doi.org/10.1007/s10641-010-9764-0

Tusa, S. 1999. La Sicilia nella Preistoria [1983]. Palermo, Italy: Sellerio.

Van Rossum, G., & Drake, F. L. (2009). Python 3 Reference Manual. Scotts Valley, CA: CreateSpace.

Vella, A., Vella, N., Karakulak, F. s., Oray, I., Garcia-Tiscar, S., & de Stephanis, R. (2016). Population genetics of Atlantic bluefin tuna, Thunnus thynnus (Linnaeus, 1758), in the Mediterranean: Implications for its conservation management. *Journal of Applied Ichthyology*, *32*(3), 523–531. https://doi.org/10.1111/jai.13035

Viñas, J., Gordoa, A., Fernández-Cebrián, R., Pla, C., Vahdet, Ü., & Araguas, R. M. (2011). Facts and uncertainties about the genetic population structure of Atlantic bluefin tuna (Thunnus thynnus) in the Mediterranean. Implications for fishery management. *Reviews in Fish Biology and Fisheries*, *21*(3), 527–541. https://doi.org/10.1007/s11160-010-9174-6

Viñas, J., Pla, C., Tawil, M. Y., Hattour, A., & Farrugia, A. F. (2003). *Mitochondrial Genetic Characterization Of Bluefin Tuna (Thunnus Thynnus) From Three Mediterranean (Libya, Malta, Tunisia); And One Atlantic Locations (Gulf Of Cadiz)*. 7.

Viñas, J., & Tudela, S. (2009). A Validated Methodology for Genetic Identification of Tuna Species (Genus Thunnus). *PLoS ONE*, *4*(10), e7606. https://doi.org/10.1371/journal.pone.0007606

Wall, J. D., Tang, L. F., Zerbe, B., Kvale, M. N., Kwok, P.-Y., Schaefer, C., & Risch, N. (2014). Estimating genotype error rates from high-coverage next-generation sequence data. *Genome Research*, *24*(11), 1734–1739. https://doi.org/10.1101/gr.168393.113

Wayne, R. K., Leonard, J. A., & Cooper, A. (1999). Full of Sound and Fury: History of Ancient DNA. *Annual Review of Ecology and Systematics*, *30*(1), 457–477. https://doi.org/10.1146/annurev.ecolsys.30.1.457

Wickham, H., Averick, M., Bryan, J., Chang, W., McGowan, L. D., François, R., Grolemund, G., Hayes, A., Henry, L., Hester, J., Kuhn, M., Pedersen, T. L., Miller, E., Bache, S. M., Müller, K., Ooms, J., Robinson, D., Seidel, D. P., Spinu, V., … Yutani, H. (2019). Welcome to the Tidyverse. *Journal of Open Source Software*, *4*(43), 1686. https://doi.org/10.21105/joss.01686

Willerslev, E., & Cooper, A. (2005). Review Paper. Ancient DNA. *Proceedings of the Royal Society B: Biological Sciences*, *272*(1558), 3–16. https://doi.org/10.1098/rspb.2004.2813

Wilson, S. G., Jonsen, I. D., Schallert, R. J., Ganong, J. E., Castleton, M. R., Spares, A. D., Boustany, A. M., Stokesbury, M. J. W., & Block, B. A. (2015). Tracking the fidelity of Atlantic bluefin tuna released in Canadian waters to the Gulf of Mexico spawning grounds. *Canadian Journal of Fisheries and Aquatic Sciences*. https://doi.org/10.1139/cjfas-2015-0110

Yu, X., & Sun, S. (2013). Comparing a few SNP calling algorithms using low-coverage sequencing data. *BMC Bioinformatics*, *14*(1), 274. https://doi.org/10.1186/1471-2105-14-274

Appendix A: Supplementary tables

Table S1: Metadata for the ancient Atlantic bluefin specimens from Jortveit. The sample-ID's of genetically indistinguishable and high missingness samples that were removed from population genomic analyses are marked with a star.

Sample-ID	Bone element	Layer	Shaft ID	Coordinates	Depth (cm)
TUN001*	Dentary	F9-C61323	1	N 58.27736681 E 8.50065423	95
TUN002	Cleithrum	F15-C61323	2	N 58.27730617 E 8.50075421	125-130
TUN003	Cleithrum	F15-C61323	2	N 58.27730617 E 8.50075421	125-130
TUN004	Atlas	F15-C61323	2	N 58.27730617 E 8.50075421	125-130
TUN005	Vertebrae	F15-C61323	2	N 58.27730617 E 8.50075421	125-130
TUN006	Vertebrae	F15-C61323	2	N 58.27730617 E 8.50075421	125-130
TUN023	Vertebrae	F21-C61777	6	N 58.27733771 E 8.50067349	125-130
TUN024	Vertebrae	F21-C61777	6	N 58.27733771 E 8.50067349	125-130
TUN025*	Vertebrae	F21-C61777	6	N 58.27733771 E 8.50067349	125-130
TUN026*	Vertebrae	F21-C61777	6	N 58.27733771 E 8.50067349	125-130
TUN027*	Vertebrae	F21-C61777	6	N 58.27733771 E 8.50067349	125-130
TUN028*	Vertebrae	F21-C61777	6	N 58.27733771 E 8.50067349	125-130
TUN029	Vertebrae	F21-C61777	6	N 58.27733771 E 8.50067349	125-130
TUN030	Vertebrae	F21-C61777	6	N 58.27733771 E 8.50067349	125-130
TUN031	Vertebrae	F21-C61777	6	N 58.27733771 E 8.50067349	125-130
TUN033*	Vertebrae	F21-C61777	6	N 58.27733771 E 8.50067349	125-130
TUN034	Vertebrae	F47-C62459	8	N 58.27733771 E 8.50067349	122
TUN035*	Vertebrae	F57-C62459	9	N 58.27702482 E 8.50139877	42
TUN036	Vertebrae	F53-C62459	n.a.	N 58.27736916 E 8.50125242	surface
TUN037	Vertebrae	F45-C62459	8	N 58.27618779 E 8.50118548	90-110
TUN038*	Vertebrae	F57-C62459	9	N 58.27702482 E 8.50139877	42
TUN039*	Vertebrae	F57-C62459	9	N 58.27736916 E 8.50125242	42
TUN040	Vertebrae	F38-C62459	7	N 58.27736916 E 8.50125242	35
TUN041	Vertebrae	F21- C61777	6	N 58.27711556 E 8.50163449	125-130
TUN042*	Vertebrae	F57-C62459	9	N 58.27733771 E 8.50067349	42
TUN043*	Vertebrae	F57-C62459	9	N 58.27736916 E 8.50125242	42
TUN044	Vertebrae	F57-C62459	9	N 58.27736916 E 8.50125242	42
TUN045*	Vertebrae	F57-C62459	9	N 58.27736916 E 8.50125242	42
TUN046*	Vertebrae	F57-C62459	9	N 58.27736916 E 8.50125242	42
TUN047	Vertebrae	F21- C61777	6	N 58.27736916 E 8.50125242	125-130
TUN048	Vertebrae	F58-C62459	9	N 58.27733771 E 8.50067349	42
TUN050*	Vertebrae	F47-C62459	9	N 58.27736916 E 8.50125242	57
TUN051*	Vertebrae	F57-C62459	8	N 58.27736916 E 8.50125242	122
TUN052*	Vertebrae	F38-C62459	9	N 58.27702482 E 8.50139877	42
TUN053	Vertebrae	F21- C61777	7	N 58.27736916 E 8.50125242	35
TUN054*	Vertebrae	F21- C61777	6	N 58.27711556 E 8.50163449	125-130
TUN055	Vertebrae	F57-C62459	6	N 58.27733771 E 8.50067349	125-130
TUN056	Vertebrae	F21- C61777	9	N 58.27733771 E 8.50067349	42
TUN057*	Vertebrae	F21- C61777	6	N 58.27736916 E 8.50125242	125-130

* Genetically indistinguishable and/or high missingness samples, excluded from population genomic analyses

Table S2: Metadata for the modern Atlantic bluefin specimens from Norway, including estimated curved fork length (CFL) and total wight (TW) where this was available.

Sample-ID	Extracted from tissue	Coordinates	Date sampled	Estimated CFL (cm)	Estimated TW (kg)
M-TUN005	Powdered muscle	N 63.65 E 7.95	07.09.2018	n.a.	n.a.
M-TUN006	Powdered muscle	N 63.65 E 7.95	07.09.2018	n.a.	n.a.
M-TUN007	Powdered muscle	N 63.65 E 7.95	07.09.2018	n.a.	n.a.
M-TUN008	Powdered muscle	N 63.65 E 7.95	07.09.2018	n.a.	n.a.
M-TUN009	Powdered muscle	N 63.65 E 7.95	07.09.2018	n.a.	n.a.
M-TUN010	Powdered muscle	N 63.65 E 7.95	07.09.2018	n.a.	n.a.
M-TUN011	Powdered muscle	N 63.65 E 7.95	07.09.2018	n.a.	n.a.
M-TUN012	Powdered muscle	N 63.65 E 7.95	07.09.2018	n.a.	n.a.
M-TUN013	Powdered muscle	N 63.65 E 7.95	07.09.2018	n.a.	n.a.
M-TUN014	Powdered muscle	N 63.65 E 7.95	07.09.2018	n.a.	n.a.
M-TUN015	Fin skin	N 62.90 E 6.00	01.09.2020	238	215.46
M-TUN016	Fin skin	N 62.90 E 6.00	01.09.2020	233	202.86
M-TUN017	Fin skin	N 62.90 E 6.00	01.09.2020	225	182.7
M-TUN018	Fin skin	N 62.90 E 6.00	01.09.2020	273	313.74
M-TUN019	Fin skin	N 62.90 E 6.00	01.09.2020	271	309.96
M-TUN022	Fin skin	N 62.90 E 6.00	01.09.2020	224	181.44
M-TUN023	Fin skin	N 62.90 E 6.00	01.09.2020	242	225.54
M-TUN024	Fin skin	N 62.90 E 6.00	01.09.2020	219	170.1
M-TUN025	Fin skin	N 62.90 E 6.00	01.09.2020	229	194.04
M-TUN026	Fin skin	N 62.90 E 6.00	01.09.2020	240	220.5
M-TUN027	Fin skin	N 62.90 E 6.00	01.09.2020	235	206.64
M-TUN028	Fin skin	N 62.90 E 6.00	01.09.2020	252	250.74
M-TUN029	Fin skin	N 62.90 E 6.00	01.09.2020	228	190.26
M-TUN030	Fin skin	N 62.90 E 6.00	01.09.2020	259	270.9
M-TUN031	Fin skin	N 62.90 E 6.00	01.09.2020	227	187.74
M-TUN032	Fin skin	N 62.90 E 6.00	01.09.2020	226	186.48
M-TUN033	Fin skin	N 62.90 E 6.00	01.09.2020	256	264.6
M-TUN034	Fin skin	N 62.90 E 6.00	01.09.2020	248	241.92
M-TUN035	Fin skin	N 62.90 E 6.00	01.09.2020	267	296.1
M-TUN036	Fin skin	N 62.90 E 6.00	01.09.2020	255	260.82
M-TUN037	Fin skin	N 62.90 E 6.00	01.09.2020	238	214.2
M-TUN038	Fin skin	N 62.90 E 6.00	01.09.2020	219	170.1
M-TUN039	Fin skin	N 62.90 E 6.00	01.09.2020	234	205.38
M-TUN040	Fin skin	N 62.90 E 6.00	01.09.2020	224	181.44
M-TUN041	Fin skin	N 62.90 E 6.00	01.09.2020	225	182.7
M-TUN042	Fin skin	N 62.90 E 6.00	01.09.2020	233	202.86
M-TUN043	Fin skin	N 62.90 E 6.00	01.09.2020	227	189
M-TUN044	Fin skin	N 62.90 E 6.00	01.09.2020	234	204.12

Table S3: Metadata for the modern Atlantic bluefin specimens from the Eastern- (EMED), Central- (CMED), and Western- (WMED) Mediterranean Sea, as well as specimens from the Gulf of Mexico (GOM) and albacore samples from the Bay of Biscay. Approximate coordinates are marked with a star.

Sample-ID	Location	Coordinates	Year & Season sampled	Lifestage
MA-CYPR-LS-0-315	EMED	N 36.17 E 33.85	15/08/2013	YoY
MA-CYPR-LS-0-330	EMED	(N 36.17 E 33.85) *	Summer of 2013	YoY
MA-CYPR-LS-0-331	EMED	(N 36.17 E 33.85) *	Summer of 2013	YoY
MA-CYPR-LS-0-34	EMED	(N 36.17 E 33.85) *	Summer of 2013	YoY
MA-CYPR-LS-0-343	EMED	(N 36.17 E 33.85) *	Summer of 2013	YoY
MA-CYPR-LS-0-347	EMED	(N 36.17 E 33.85) *	Summer of 2013	YoY
MA-CYPR-LS-0-352	EMED	(N 36.17 E 33.85) *	Summer of 2013	YoY
MA-CYPR-LS-0-41	EMED	(N 36.17 E 33.85) *	Summer of 2013	YoY
MA-CYPR-LS-0-45	EMED	(N 36.17 E 33.85) *	Summer of 2013	YoY
MA-CYPR-LS-0-49	EMED	(N 36.17 E 33.85) *	Summer of 2013	YoY
MA-UNIB-SI-0-65	CMED	(N 36.93 E 13.18) *	Summer of 2013	YoY
MA-UNIB-SI-0-67	CMED	(N 36.93 E 13.18) *	Summer of 2013	YoY
MA-UNIB-SI-0-70	CMED	(N 36.93 E 13.18) *	Summer of 2013	YoY
MA-UNIB-SI-0-77	CMED	(N 36.93 E 13.18) *	Summer of 2013	YoY
MA-UNIB-SI-0-79	CMED	(N 36.93 E 13.18) *	Summer of 2013	YoY
MA-UNIB-SI-0-81	CMED	(N 36.93 E 13.18) *	Summer of 2013	YoY
MA-UNIB-SI-0-84	CMED	(N 36.93 E 13.18) *	Summer of 2013	YoY
MA-UNIB-SI-0-89	CMED	(N 36.93 E 13.18) *	Summer of 2013	YoY
MA-UNIB-SI-0-92	CMED	(N 36.93 E 13.18) *	Summer of 2013	YoY
MA-IEO-BA-0-104	WMED	N 39.28 W 0.04	22/09/2013	YoY
MA-IEO-BA-0-107	WMED	N 39.28 W 0.04	12/10/2013	YoY
MA-IEO-BA-0-109	WMED	N 39.28 W 0.04	13/10/2013	YoY
MA-IEO-BA-0-110	WMED	N 39.28 W 0.04	17/10/2013	YoY
MA-IEO-BA-0-113	WMED	N 39.28 W 0.04	25/10/2013	YoY
MA-IEO-BA-0-121	WMED	N 39.28 W 0.04	01/11/2013	YoY
MA-IEO-BA-0-63	WMED	N 39.28 W 0.04	15/09/2012	YoY
MA-IEO-BA-0-67	WMED	N 39.28 W 0.04	16/09/2012	YoY
MA-IEO-BA-0-68	WMED	(N 39.28 W 0.04) *	Summer of 2013	YoY
MA-IEO-BA-0-77	WMED	N 39.28 W 0.04	16/09/2012	YoY
MA-N17040108	GOM	N 26.1198 W 87.7773	10.05.2017	Larva
MA-N17040501	GOM	N 25.8438 W 88.1328	12.05.2017	Larva
MA-N18021808	GOM	N 28.3327 W 87.2497	15.05.2018	Larva
MA-N18021809	GOM	N 28.3327 W 87.2497	15.05.2018	Larva
MA-N18021810	GOM	N 28.3327 W 87.2497	15.05.2018	Larva
MA-W14050007	GOM	N 26.5346 W 93.582	07.05.2014	Larva
MA-W14050014	GOM	N 26.5346 W 93.582	07.05.2014	Larva
MA-W14050029	GOM	N 27.0388 W 93.0033	08.05.2014	Larva
MA-W14050096	GOM	N 27.9963 W 87.761	20.05.2014	Larva
MA-W14050097	GOM	N 27.9963 W 87.761	20.05.2014	Larva
MA-ALB_05	Bay of Biscay	(N 44.46 W 3.12) *	Summer of 2010	Juvinile (5-15 kg)
MA-ALB_09	Bay of Biscay	(N 44.46 W 3.12) *	Summer of 2010	Juvinile (5-15 kg))
MA-ALB_12	Bay of Biscay	(N 44.46 W 3.12) *	Summer of 2010	Juvinile (5-15 kg)
MA-ALB_21	Bay of Biscay	(N 44.46 W 3.12) *	Summer of 2010	Juvinile (5-15 kg)
MA-ALB_24	Bay of Biscay	(N 44.46 W 3.12) *	Summer of 2010	Juvinile (5-15 kg)
MA-ALB_27	Bay of Biscay	(N 44.46 W 3.12) *	Summer of 2010	Juvinile (5-15 kg)

*Approximate coordinates

Table S4: Laboratory protocols and process treatments for the ancient Atlantic bluefin specimens from Jortveit. One extract was diluted due to high concentration and is marked with a star.

Sample-ID	Tissue	Sand-blasted	Milling powder	Extraction protocol	Date of extraction	Qubit concentration	Library protocol
TUN001	Dentary	Yes	Fine	DD	11.12.2018	3.3	M&K DS
TUN002	Cleithrum	No	Fine	DD	11.12.2018	1.24	M&K DS
TUN003	Cleithrum	No	Fine	DD	11.12.2018	0.48	M&K DS
TUN004	Vertebrae	Yes	Fine	DD	11.12.2018	1.27	M&K DS
TUN005	Vertebrae	Yes	Fine	DD	11.12.2018	1.02	M&K DS
TUN006	Vertebrae	Yes	Fine	DD	11.12.2018	2.7	M&K DS
TUN023	Vertebrae	Yes	Fine	bleDD	11.05.2020	n.a.	M&K DS
TUN024	Vertebrae	Yes	Fine	bleDD	11.05.2020	n.a.	M&K DS
TUN025	Vertebrae	Yes	Fine	bleDD	11.05.2020	n.a.	M&K DS
TUN026	Vertebrae	Yes	Fine	bleDD	11.05.2020	n.a.	M&K DS
TUN027	Vertebrae	Yes	Fine	bleDD	11.05.2020	n.a.	M&K DS
TUN028	Vertebrae	Yes	Fine	bleDD	11.05.2020	n.a.	M&K DS
TUN029	Vertebrae	Yes	Fine	bleDD	11.05.2020	n.a.	M&K DS
TUN030	Vertebrae	Yes	Fine	bleDD	11.05.2020	n.a.	M&K DS
TUN031	Vertebrae	Yes	Fine	bleDD	11.05.2020	n.a.	M&K DS
TUN033	Vertebrae	Yes	Fine	bleDD	11.05.2020	n.a.	M&K DS
TUN034	Vertebrae	No	Coarse	bleDD	07.07.2021	1.28	SC SS
TUN035	Vertebrae	No	Coarse	bleDD	07.07.2021	13.3	SC SS
TUN036	Vertebrae	No	Coarse	bleDD	07.07.2021	5.6	SC SS
TUN037	Vertebrae	No	Coarse	bleDD	07.07.2021	1.6	SC SS
TUN038	Vertebrae	No	Coarse	bleDD	07.07.2021	2.8	SC SS
TUN039	Vertebrae	No	Coarse	bleDD	07.07.2021	5.56	SC SS
TUN040	Vertebrae	No	Coarse	bleDD	07.07.2021	19.6	SC SS
TUN041	Vertebrae	No	Coarse	bleDD	07.07.2021	3.54	SC SS
TUN042	Vertebrae	No	Coarse	bleDD	07.07.2021	11	SC SS
TUN043	Vertebrae	No	Coarse	bleDD	07.07.2021	6.94	SC SS
TUN044	Vertebrae	No	Coarse	bleDD	07.07.2021	2.8	SC SS
TUN045	Vertebrae	No	Coarse	bleDD	07.07.2021	10.9	SC SS
TUN046	Vertebrae	No	Coarse	bleDD	26.06.2021	89.6	SC SS
TUN047	Vertebrae	No	Coarse	bleDD	26.06.2021	1.87	SC SS
TUN048	Vertebrae	No	Coarse	bleDD	26.06.2021	19.9	SC SS
TUN050	Vertebrae	No	Coarse	bleDD	26.06.2021	26	SC SS
TUN051	Vertebrae	No	Coarse	bleDD	26.06.2021	1.9	SC SS
TUN052	Vertebrae	No	Fine	bleDD	26.06.2021	36	SC SS
TUN053	Vertebrae	Yes	Fine	bleDD	26.06.2021	78.8	SC SS
TUN054	Vertebrae	No	Fine	bleDD	26.06.2021	25.2*	SC SS
TUN055	Vertebrae	No	Fine	bleDD	26.06.2021	3.18	SC SS
TUN056	Vertebrae	No	Fine	bleDD	26.06.2021	3.06	SC SS
TUN057	Vertebrae	Yes	Fine	bleDD	26.06.2021	1.4	SC SS

*After 1:1 dilution. (Before dilution: >120)

Table S5: Laboratory protocols for the modern Atlantic bluefin specimens from Norway. Samples that were concentrated to increase DNA concentration are marked with a star.

Sample-ID	Tissue	Extraction protocol	Date of extraction	Qubit concentration
M-TUN005	powdered muscle	Qiagen B&T	23.07.2019	5.5*
M-TUN006	powdered muscle	Qiagen B&T	23.07.2019	20.6
M-TUN007	powdered muscle	Qiagen B&T	23.07.2019	20
M-TUN008	powdered muscle	Qiagen B&T	30.10.2019	4.45*
M-TUN009	powdered muscle	Qiagen B&T	30.10.2019	9.24*
M-TUN010	powdered muscle	Qiagen B&T	30.10.2019	5.2*
M-TUN011	powdered muscle	Qiagen B&T	30.10.2019	10.16
M-TUN012	powdered muscle	Qiagen B&T	30.10.2019	5.088*
M-TUN013	powdered muscle	Qiagen B&T	30.10.2019	11.7
M-TUN014	powdered muscle	Qiagen B&T	30.10.2019	6.02
M-TUN015	fin clip	Qiagen B&T	27.11.2020	53.4
M-TUN016	fin clip	Qiagen B&T	27.11.2020	43.75
M-TUN017	fin clip	Qiagen B&T	27.11.2020	31.4
M-TUN018	fin clip	Qiagen B&T	27.11.2020	83.7
M-TUN019	fin clip	Qiagen B&T	27.11.2020	27.25
M_TUN020	fin clip	Qiagen B&T	27.11.2020	41.75
M_TUN021	fin clip	Qiagen B&T	27.11.2020	13.4
M-TUN022	fin clip	Qiagen B&T	27.11.2020	44
M-TUN023	fin clip	Qiagen B&T	27.11.2020	91.9
M-TUN024	fin clip	Qiagen B&T	27.11.2020	28.5
M-TUN025	fin clip	Qiagen B&T	27.11.2020	81.3
M-TUN026	fin clip	Qiagen B&T	27.11.2020	58.75
M-TUN027	fin clip	Qiagen B&T	27.11.2020	19.05
M-TUN028	fin clip	Qiagen B&T	27.11.2020	23.6
M-TUN029	fin clip	Qiagen B&T	27.11.2020	73.4
M-TUN030	fin clip	Qiagen B&T	29.11.2020	70.5
M-TUN031	fin clip	Qiagen B&T	29.11.2020	38.7
M-TUN032	fin clip	Qiagen B&T	29.11.2020	41.2
M-TUN033	fin clip	Qiagen B&T	29.11.2020	48.3
M-TUN034	fin clip	Qiagen B&T	29.11.2020	31.95
M-TUN035	fin clip	Qiagen B&T	29.11.2020	21.8
M-TUN036	fin clip	Qiagen B&T	29.11.2020	43.2
M-TUN037	fin clip	Qiagen B&T	29.11.2020	36.05
M-TUN038	fin clip	Qiagen B&T	29.11.2020	36.25
M-TUN039	fin clip	Qiagen B&T	29.11.2020	43.75
M-TUN040	fin clip	Qiagen B&T	29.11.2020	32.55
M-TUN041	fin clip	Qiagen B&T	29.11.2020	66.5
M-TUN042	fin clip	Qiagen B&T	29.11.2020	20.4
M-TUN043	fin clip	Qiagen B&T	29.11.2020	32.55
M-TUN044	fin clip	Qiagen B&T	29.11.2020	71.85

* after SpeedVac concentration

Table S6: Pacific bluefin whole genome raw sequences downloaded from the DDBJ database (Kodama et al., 2012).

Sample-ID	DDBJ identifier	Filename	Last modified
PAC-DRR177383	DRA008331	DRR177383_1.fastq.bz2	12.04.2019
		DRR177383_2.fastq.bz2	
PAC-DRR177395	DRA008331	DRR177395_1.fastq.bz2	12.04.2019
		DRR177395_2.fastq.bz2	
PAC-DRR177400	DRA008331	DRR177400_1.fastq.bz2	12.04.2019
		DRR177400_2.fastq.bz2	
PAC-DRR177401	DRA008331	DRR177401_1.fastq.bz2	12.04.2019
		DRR177401_2.fastq.bz2	
PAC-DRR177402	DRA008331	DRR177402_1.fastq.bz2	12.04.2019
		DRR177402_2.fastq.bz2	
PAC-DRR177403	DRA008331	DRR177403_1.fastq.bz2	12.04.2019
		DRR177403_2.fastq.bz2	
PAC-DRR177404	DRA008331	DRR177404_1.fastq.bz2	12.04.2019
		DRR177404_2.fastq.bz2	
PAC-DRR177405	DRA008331	DRR177405_1.fastq.bz2	12.04.2019
		DRR177405_2.fastq.bz2	
PAC-DRR177406	DRA008331	DRR177406_1.fastq.bz2	12.04.2019
		DRR177406_2.fastq.bz2	

URL: https://ddbj.nig.ac.jp/public/ddbj_database/dra/fastq/DRA008/DRA008331/DRX167946/

Table S7: Filtering options used when generating the datasets used in this thesis. The bcftools explanations are adapted from GATK (2022b) and vcftools explanations are adapted from the VCFtools v.0.1.16 documentation (Auton & Marcketta, 2015).

Option	Threshold	Specification
bcftools: Fisher Strand (FS)	<60.0	Removes variants with FS score above 60 (threshold recommended by GATK) indicating high probability of stand bias. FS is the probability that an alternate allele occurs more frequent, or less frequent, on the forward or reverse strand compared to the reference allele. This is called strand bias and can cause biased evaluation of one DNA strand over another. The FS score is Phred-scaled, and a strand without bias will have FS = 0.
bcftools: Strand Odds Ratio (SOR)	<4.0	Removes variants with SOR score above 4, indicating high probability of stand bias. Sites that have more reads in one direction than the other tends to be penalized by the FS filter. While both filters penalize strand bias, SOR considers the ratio of reads that cover the reference allele and the alternate allele at each site.
bcftools: RMS Mapping Quality (MQ)	>30.0	Removes variants with low root mean square (RMS) mapping quality. Since the RMS mapping quality includes the standard deviation of the mapping qualities of reads across samples at each site, this filter allows for variation within the jointly filtered dataset. Although variation should be included, a high standard deviation may include sites that vary far from the mean. Good mapping quality typically gives a MQ score of 60 at the site. GATK recommends filtering MQ>40. Lowering the MQ filtering threshold allows for more variation in the dataset.
bcftools: Quality by depth (QD)	> 2.0	Removes variants with QD score below 2 (threshold recommended by GATK) $QD = \frac{Variant\ confidence}{Sequencing\ depth}$ The QD value is a normalization of the variant quality, to avoid inflated quality values at high coverage sites.
bcftools: SnpGap	10	Removes SNPs that are within 10 bp of an insertion or deletion (indel).
vcftools: minGQ	> 15.0	Excludes genotypes with GQ score below 15. $GQ = -10log_{10}(Error\ Rate)$ (Wall et al., 2014) . Genotypes with w high sequencing error rate will have a low GQ score.
vcftools: minDP	> 2.0	Excludes genotypes with read depth (DP) lower than 2, so that sites which are represented only once within all the reads are removed. Sites sequenced twice or more are included.
vcftools: remove-indels	n.a.	Removes variants that alters the length of the allele compared to the reference, i.e., insertion/deletion mutations.

Table S8: Outgroup samples downloaded from GenBank. Some of the sequences had to be curated to start in the D-loop to match the Atlantic bluefin samples.

Sample-ID	Genbank accession nr.	Date submitted	D-loop location	Restarted in D-loop
pelamis_GU256527_1	GU256527.1	03.12.2009	1..853	No
pelamis_NC_005316_1	NC_005316.1	28.01.2003	1..853	No
pelamis_KM605252_1	KM605252.1	22.09.2014	15663..16515	Yes
pelamis_JN086155_1	JN086155.1	03.06.2011	15663..16516	Yes
alalunga_ GU256526_1	GU256526.1	03.12.2009	1..866	No
alalunga_NC_005317_1	NC_005317.1	28.01.2003	1..866	No
alalunga_ JN086151_1	JN086151.1	03.06.2011	15663..16527	Yes
alalunga_ KP259549_1	KP259549.1	08.12.2014	1..865	No
orientalis_ GU256524_1	GU256524.1	02.12.2009	1..865	No
orientalis_ KF906721_1	KF906721.1	26.11.2013	15663..16529	Yes
orientalis_ NC_008455_1	NC_008455.1	15.07.2004	15663..16527	Yes
orientalis_ LC377898_1	LC377898.1	23.03.2018	15663..16527	Yes

Table S9: Summary statistics from Paleomix for the ancient Atlantic bluefin specimens from Jortveit. The clonality and endogenous contents are calculated from the alignment to the nuclear reference genome. Extraction blanks are colored grey.

Sample-ID	Reads (millions)	Clonality (%)	Endogenous DNA (fraction)	Mitochondrial coverage	Nuclear coverage	Mean fragment length (bp)
TUN001	22	15	0.01	1	0.01	124
TUN002	32	20	0.06	6	0.15	74
TUN003	42	21	0.13	13	0.45	64
TUN004	21	19	0.16	7	0.23	62
TUN005	31	13	0.50	38	1.15	62
TUN006	20	12	0.60	64	1.17	78
TUN023	5	19	0.25	5	0.10	77
TUN024	16	22	0.13	5	0.16	66
TUN025	17	21	0.47	16	0.59	63
TUN026	3	20	0.22	2	0.05	80
TUN027	13	23	0.44	13	0.45	66
TUN028	20	19	0.44	17	0.63	64
TUN029	26	15	0.49	26	1.01	67
TUN030	8	19	0.33	7	0.19	66
TUN031	10	21	0.18	3	0.12	70
TUN033	2	17	0.48	2	0.08	66
TUN034	6	7	0.33	10	0.24	100
TUN035	6	6	0.02	1	0.01	79
TUN036	88	5	0.18	107	1.80	109
TUN037	19	5	0.26	32	0.53	101
TUN038	9	6	0.34	17	0.31	86
TUN039	14	7	0.33	25	0.52	101
TUN040	12	6	0.03	3	0.05	109
TUN041	47	4	0.55	85	2.66	88
TUN042	14	8	0.22	20	0.28	81
TUN043	11	6	0.15	8	0.16	95
TUN044	16	6	0.32	31	0.49	85
TUN045	15	6	0.03	4	0.05	97
TUN046	13	7	0.08	9	0.10	106
TUN047	11	7	0.14	3	0.16	113
TUN048	15	6	0.11	12	0.18	120
TUN050	15	7	0.12	11	0.24	119
TUN051	12	6	0.12	10	0.16	111
TUN052	29	7	0.00	0	0.00	122
TUN053	14	9	0.15	12	0.22	116
TUN054	14	7	0.03	3	0.04	107
TUN055	93	4	0.54	151	4.17	75
TUN056	25	4	0.37	24	0.88	90
TUN057	9	6	0.11	2	0.11	121
GF044NCA	1	29	0.00	0	0.00	91
GF095NCE	5	15	0.00	0	0.00	87
EE011NCE1	0	8	0.00	0	0.00	92
EE013NCE1	0	0	0.00	0	0.00	95

Table S10: Summary statistics from Paleomix for the modern Atlantic bluefin specimens from Norway. The clonality and endogenous contents are calculated from the alignment to the nuclear reference genome.

Sample-ID	Reads (millions)	Clonality (%)	Endogenous DNA (fraction)	Mitochondrial coverage	Nuclear coverage	Mean fragment length (bp)
M-TUN005	75	16	0.69	2784	16.18	178
M-TUN006	59	13	0.73	1019	14.86	170
M-TUN007	56	13	0.73	1508	13.96	172
M-TUN008	79	9	0.75	1150	19.77	178
M-TUN009	69	9	0.76	823	17.68	172
M-TUN010	79	10	0.75	1633	20.48	169
M-TUN011	73	8	0.77	1163	19.16	170
M-TUN012	76	9	0.75	1811	19.02	175
M-TUN013	90	9	0.76	1960	23.35	171
M-TUN014	93	10	0.75	2345	24.05	171
M-TUN015	21	10	0.76	273	5.43	168
M-TUN016	19	11	0.75	307	4.83	168
M-TUN017	23	8	0.78	296	5.84	168
M-TUN018	19	9	0.76	247	4.68	170
M-TUN019	18	10	0.76	283	4.59	166
M-TUN022	22	9	0.76	370	5.38	170
M-TUN023	22	10	0.75	260	5.75	168
M-TUN024	33	11	0.75	512	8.45	169
M-TUN025	22	9	0.77	228	5.73	167
M-TUN026	19	10	0.75	251	4.90	168
M-TUN027	19	9	0.76	520	4.78	168
M-TUN028	17	8	0.77	286	4.28	166
M-TUN029	17	8	0.77	263	4.28	167
M-TUN030	23	9	0.77	301	5.91	168
M-TUN031	23	11	0.75	381	5.76	169
M-TUN032	21	10	0.76	389	5.43	169
M-TUN033	25	9	0.76	343	6.42	168
M-TUN034	25	10	0.76	349	6.53	166
M-TUN035	22	10	0.75	448	5.44	168
M-TUN036	23	8	0.77	419	5.89	169
M-TUN037	27	8	0.77	687	6.79	166
M-TUN038	22	7	0.78	543	5.49	168
M-TUN039	22	10	0.75	458	5.59	169
M-TUN040	18	10	0.76	417	4.73	166
M-TUN041	24	10	0.76	472	6.10	167
M-TUN042	23	9	0.76	356	5.70	168
M-TUN043	24	8	0.77	419	5.80	166
M-TUN044	24	10	0.75	425	5.92	169

Table S11: Summary statistics from Paleomix for the modern Atlantic bluefin specimens from the Gulf of Mexico (MA-N1, MA-W1*), and the Eastern- (MA-CYPR*), Central- (MA-UNIB*), and Western- (MA-IEO*) Mediterranean Sea. The clonality and endogenous contents are calculated from the alignment to the nuclear reference genome.*

Sample-ID	Reads (millions)	Clonality (%)	Endogenous DNA (fraction)	Mitochondrial coverage	Nuclear coverage	Mean fragment length (bp)
MA-CYPR-LS-0-315	24	2	0.68	716	2.28	112
MA-CYPR-LS-0-330	25	2	0.68	704	2.54	124
MA-CYPR-LS-0-331	22	2	0.69	336	2.22	118
MA-CYPR-LS-0-34	13	1	0.80	445	2.23	156
MA-CYPR-LS-0-343	48	2	0.48	2089	3.64	120
MA-CYPR-LS-0-347	37	2	0.49	1600	2.63	115
MA-CYPR-LS-0-352	31	3	0.67	708	2.72	105
MA-CYPR-LS-0-41	21	2	0.72	230	1.88	102
MA-CYPR-LS-0-45	19	2	0.71	363	1.65	100
MA-CYPR-LS-0-49	23	2	0.73	538	2.14	103
MA-UNIB-SI-0-65	36	2	0.35	1180	1.53	122
MA-UNIB-SI-0-67	32	2	0.30	666	1.50	126
MA-UNIB-SI-0-70	54	3	0.60	1385	2.53	69
MA-UNIB-SI-0-77	38	2	0.61	448	1.81	71
MA-UNIB-SI-0-79	32	2	0.71	745	2.99	106
MA-UNIB-SI-0-81	45	3	0.55	530	2.88	104
MA-UNIB-SI-0-84	36	2	0.35	176	2.10	128
MA-UNIB-SI-0-89	62	3	0.58	705	3.24	81
MA-UNIB-SI-0-92	51	4	0.58	533	1.85	60
MA-IEO-BA-0-104	24	2	0.68	1021	1.66	83
MA-IEO-BA-0-107	27	2	0.70	660	2.63	112
MA-IEO-BA-0-109	14	2	0.59	574	1.05	104
MA-IEO-BA-0-110	20	2	0.70	396	1.37	81
MA-IEO-BA-0-113	26	2	0.66	840	2.58	119
MA-IEO-BA-0-121	46	3	0.61	1462	2.61	80
MA-IEO-BA-0-63	63	4	0.58	1212	2.67	67
MA-IEO-BA-0-67	60	4	0.57	1183	2.21	62
MA-IEO-BA-0-68	41	2	0.69	410	3.22	95
MA-IEO-BA-0-77	74	3	0.65	460	3.91	70
MA-N17040108	80	2	0.66	696	4.27	69
MA-N17040501	51	2	0.38	972	2.42	111
MA-N18021808	30	2	0.49	565	1.71	106
MA-N18021809	52	2	0.56	881	3.28	100
MA-N18021810	44	2	0.47	966	3.63	128
MA-W14050007	26	2	0.69	319	1.67	78
MA-W14050014	46	2	0.69	49	2.85	75
MA-W14050029	26	2	0.65	34	1.37	67
MA-W14050096	67	3	0.55	910	4.78	102
MA-W14050097	53	2	0.60	430	2.45	66

Table S12: Summary statistics from Paleomix for the modern albacore specimens from the Bay of Biscay. The clonality and endogenous contents are calculated from the alignment to the nuclear reference genome.

Sample-ID	Reads (millions)	Clonality (%)	Endogenous DNA (fraction)	Mitochondrial coverage	Nuclear coverage	Mean fragment length (bp)
MA-ALB_05	37	3	0.59	277	2.68	99
MA-ALB_09	19	2	0.66	219	1.77	117
MA-ALB_12	28	2	0.65	103	2.76	124
MA-ALB_21	27	2	0.66	377	1.59	74
MA-ALB_24	12	2	0.70	243	1.01	95
MA-ALB_27	25	2	0.68	109	2.01	99

Table S13: Summary statistics from Paleomix for the modern albacore specimens from the Bay of Biscay. The clonality and endogenous contents are calculated from the alignment to the nuclear reference genome.

Sample-ID	Reads (millions)	Clonality (%)	Endogenous DNA (fraction)	Mitochondrial coverage	Nuclear coverage	Mean fragment length (bp)
PAC-DRR177383	121	14	0.72	2657	31.83	152
PAC-DRR177395	127	11	0.74	5107	34.79	151
PAC-DRR177400	109	8	0.76	2346	30.79	151
PAC-DRR177401	112	12	0.73	1361	30.25	151
PAC-DRR177402	107	8	0.76	4005	30.34	151
PAC-DRR177403	112	11	0.75	3345	31.03	151
PAC-DRR177404	99	9	0.76	3061	27.70	151
PAC-DRR177405	126	10	0.75	3465	34.85	151
PAC-DRR177406	114	10	0.74	4555	31.52	151

*Table S14: Population genomic statistics comparing jointly (joint) and separately (sep.) called and filtered datasets. The input-file for all the joint values was the **AllABFT** dataset.*

	S		π		TD		F	
Subset	**sep.**	**joint**	**sep.**	**joint**	**sep.**	**joint**	**sep.**	**joint**
JortveitAll	54	79	0.0003	0.0005	-2.562 (**)	-2.614 (**)	-3.731 (**)	-2.554 (*)
JortveitExIntrog	16	16	0.0001	0.0001	-2.177 (**)	-2.177 (**)	-2.687 (*)	-2.569 (*)
NorwayAll	608	606	0.0049	0.0048	-1.714 (n.s.)	-1.715 (n.s.)	-0.3191 (n.s.)	-0.183 (n.s.)
NorwayExIntrog	182	156	0.0012	0.0009	-2.109 (*)	-2.225 (**)	-2.522 (*)	-2.891 (*)
EMED	86	63	0.0013	0.0009	-1.464 (n.s.)	-1.619 (n.s.)	-1.636 (n.s.)	-1.347 (n.s.)
CMED	79	64	0.0012	0.0009	-1.703 (n.s.)	-1.861 (*)	-1.804 (n.s.)	-1.919 (n.s.)
WMEDAll	460	454	0.0059	0.0058	-2.059 (**)	-2.062 (**)	-2.374 (**)	-1.754 (n.s.)
WMEDExIntrog	68	54	0.0011	0.0008	-1.497 (n.s.)	-1.609 (n.s.)	-1.605 (n.s.)	-1.704 (n.s.)
GOM	67	50	0.0009	0.0007	-1.754 (*)	-1.858 (*)	-1.980 (n.s.)	-1.744 (n.s.)
modernABFT	664	664	0.0034	0.0034	-2.080 (*)	-2.080 (*)	-0.796 (n.s.)	-0.697 (n.s.)
modernExIntrog	268	236	0.0011	0.0008	-2.378 (*)	-2.481 (**)	-3.888 (**)	-3.905 (*)

Table S15: Φst P-values from Arlequin for the AllABFT and AllExIntrog datasets, corresponding to Figure 12A) and 12B) respectively.

AllABFT:

	Ancient All	Norway All	EMED	CMED	WMED All	GOM
Ancient All		0.98926 +- 0.0033	0.48145 +- 0.0150	0.29492 +- 0.0130	0.76953 +- 0.0083	0.38672 +- 0.0183
Norway All			0.51465 +- 0.0186	0.25195 +- 0.0136	0.80469 +- 0.0121	0.29199 +- 0.0148
EMED				0.16602 +- 0.0097	0.21387 +- 0.0158	0.43652 +- 0.0185
CMED					0.82031 +- 0.0119	0.35254 +- 0.0148
WMED All						0.16699 +- 0.0131
GOM						

AllExIntrog:

	Ancient ExIntrog	Norway ExIntrog	EMED	CMED	WMED ExIntrog	GOM
Ancient ExIntrog		0.87207 +- 0.0106	0.50195 +- 0.0147	0.15723 +- 0.0112	0.13379 +- 0.0111	0.34863 +- 0.0122
Norway Exintrog			0.64648 +- 0.0156	0.42676 +- 0.0159	0.52832 +- 0.0186	0.45703 +- 0.0155
EMED				0.60449 +- 0.0168	0.68262 +- 0.0143	0.27734 +- 0.0133
CMED					0.79688 +- 0.0116	0.37402 +- 0.0102
WMED ExIntrog						0.16406 +- 0.0110
GOM						

Table S16: Substitution models used for each dataset in different analyses. All models were selected according to the Bayesian Information Criterion (BIC) (Schwarz, 1978). The references for the selected models are listed below.

Analysis	Program used for model testing	Dataset	Selected model*
ML phylogeny	ModelFinder Plus	**All_alb** + all outgroups	TIM2
		AllExIntrog + Pacific bluefin outgroup	HKY
MrBayes phylogeny	jModelTest	**All_alb** + all outgroups	K81uf
		AllExIntrog + Pacific bluefin outgroup	TN93
BEAST phylogeny	bModelTest	**All_alb** + all outgroups	TN93
		AllExIntrog + Pacific bluefin outgroup	TN93
PHIst divergence analyses	jModelTest and bModelTest	**AllABFT**	TN93
		AllExIntrog	TN93
Coalescent Bayesian Skyline analyses	bModelTest	**AncientAll**	HKY
		AncientExIntrog	HKY
		modernABFT	TN93
		modernExIntrog	TN93
		AllABFT	TN93
		AllExIntrog	TN93

* Substitution model references:

- TN93: (Tamura & Nei, 1993)
- HKY: (Hasegawa et al., 1985)
- K81uf: (Kimura, 1981) with unequal base frequencies as per (Posada, 2003)
- TIM2: (Posada, 2003; Rodríguez et al., 1990)

Appendix B: Supplementary figures

Figure S1: Photographs of all ancient Atlantic bluefin specimens from Jortveit which were processed in this thesis.

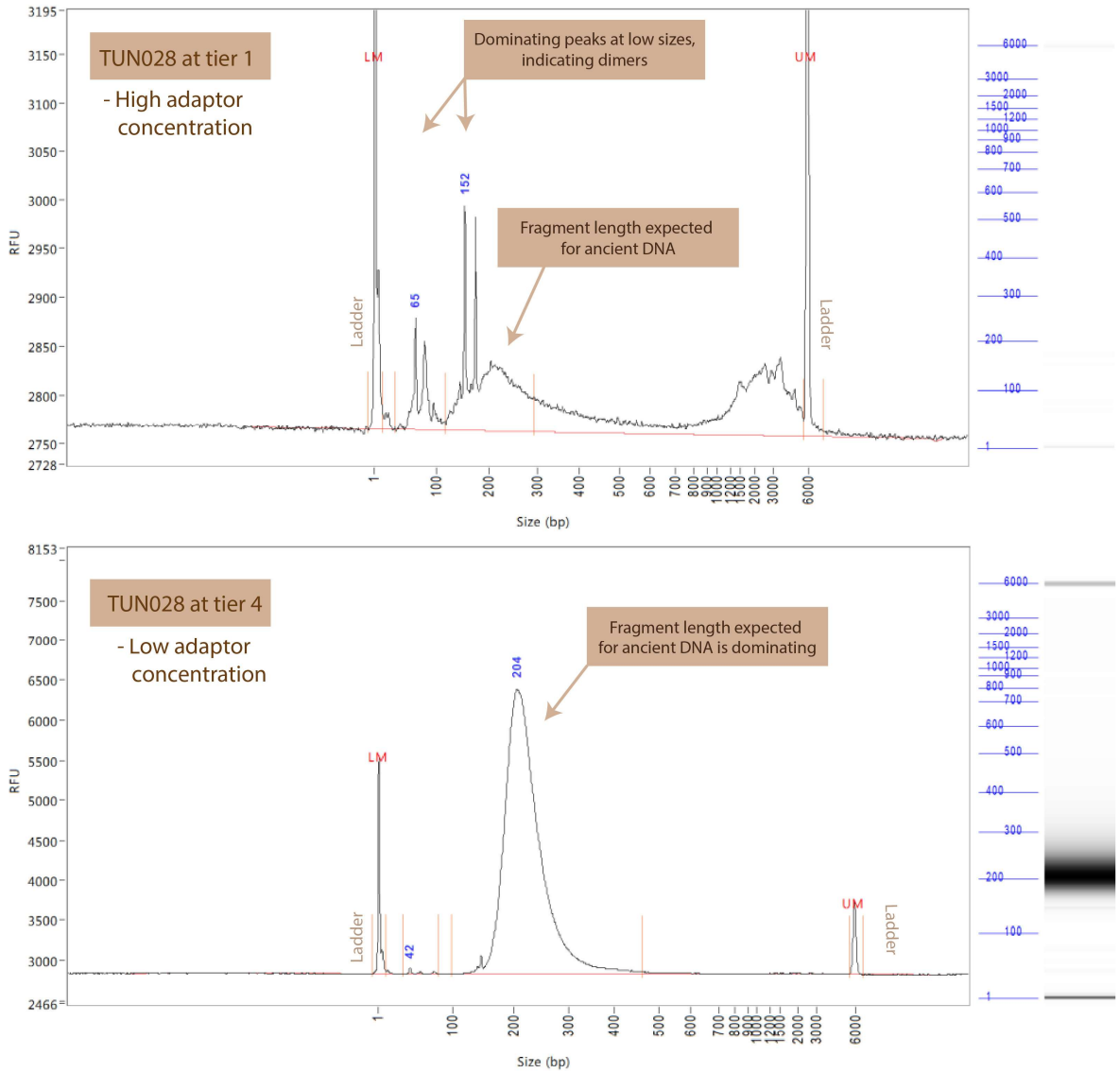

Figure S2: Fragment Analyzer plots from the trial runs of the SCR library protocol, using ancient sample TUN028. Using a high adaptor concentration resulted in short fragment dimers dominating the sample.

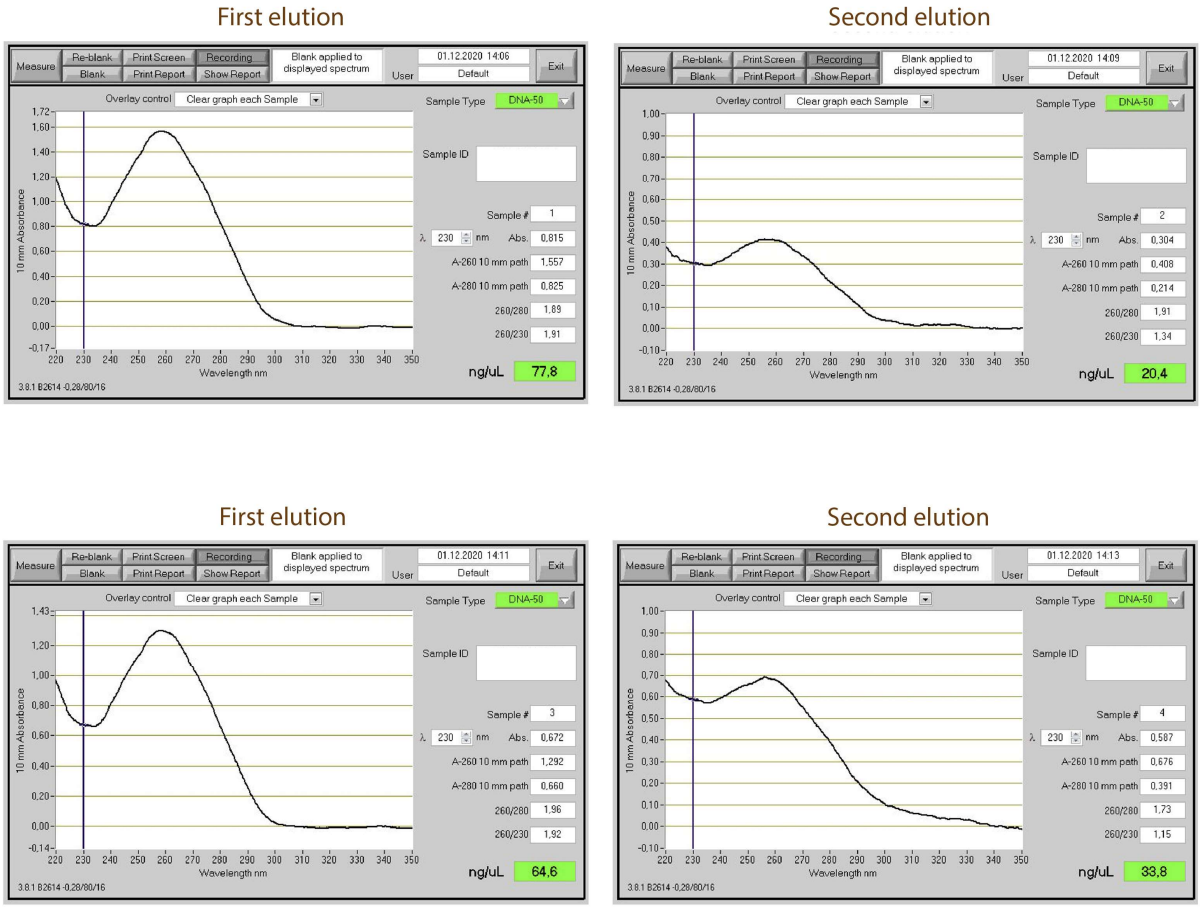

Figure S3: Examples of Nanodrop results of first and second elutions of two of the modern Atlantic bluefin specimens from Norway. First elutions showed a big peak at in absorbance at aound 260 nm wavelength, indicating clean DNA. Low absorbance at other wavelengths indicating low pollution in the sample. Second elutions had a flatter curve.

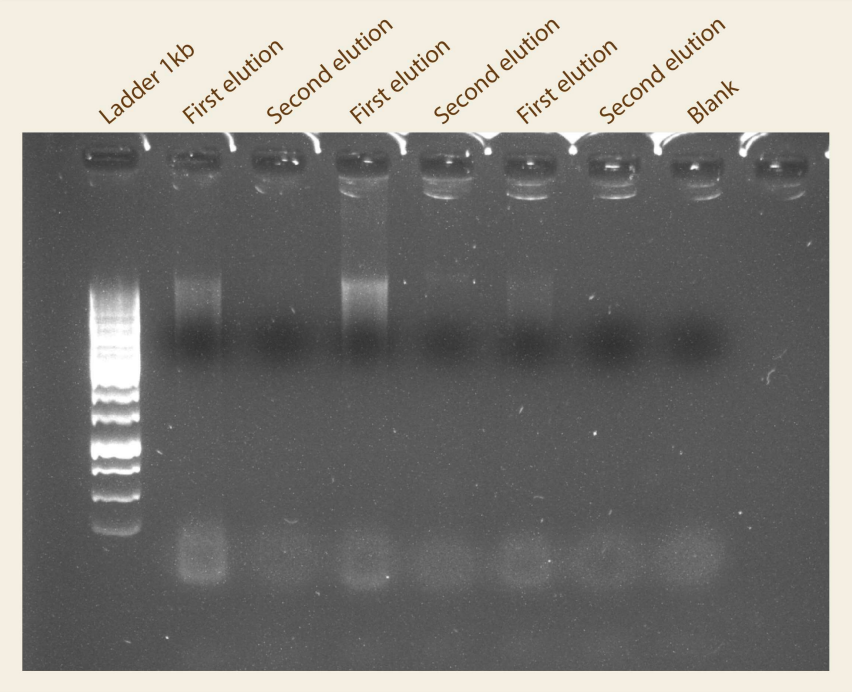

Figure S4: Example of an electrophoresis gel containing first and second elutions of three of the modern Atlantic bluefin specimens from Norway. Longer reads and more DNA indicate higher quality of the first elutions.

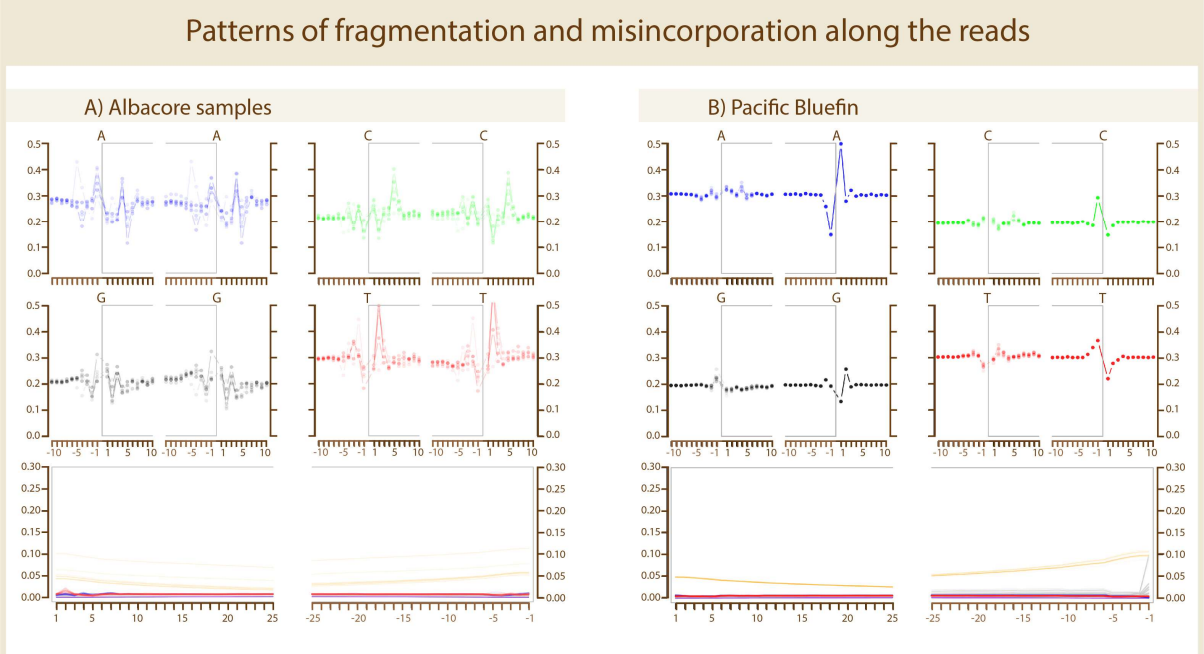

Figure S5: Fragmentation (upper panels) and misincorporation (lower panels) plots from mapDamage v.2.0.9, of the albacore (A) and pacific bluefin (B) samples. The fragmentation plots show the base frequency inside and surrounding the read, where the grey box indicates the location of where the reads have mapped to the reference. The misincorporation plots show the rate of substitutions along the positions of the read ends, relative to the reference (Red: C to T. Blue: G to A. Grey: All other substitutions. Green: Deletions. Purple: Insertions. Orange: Soft-clipped bases)

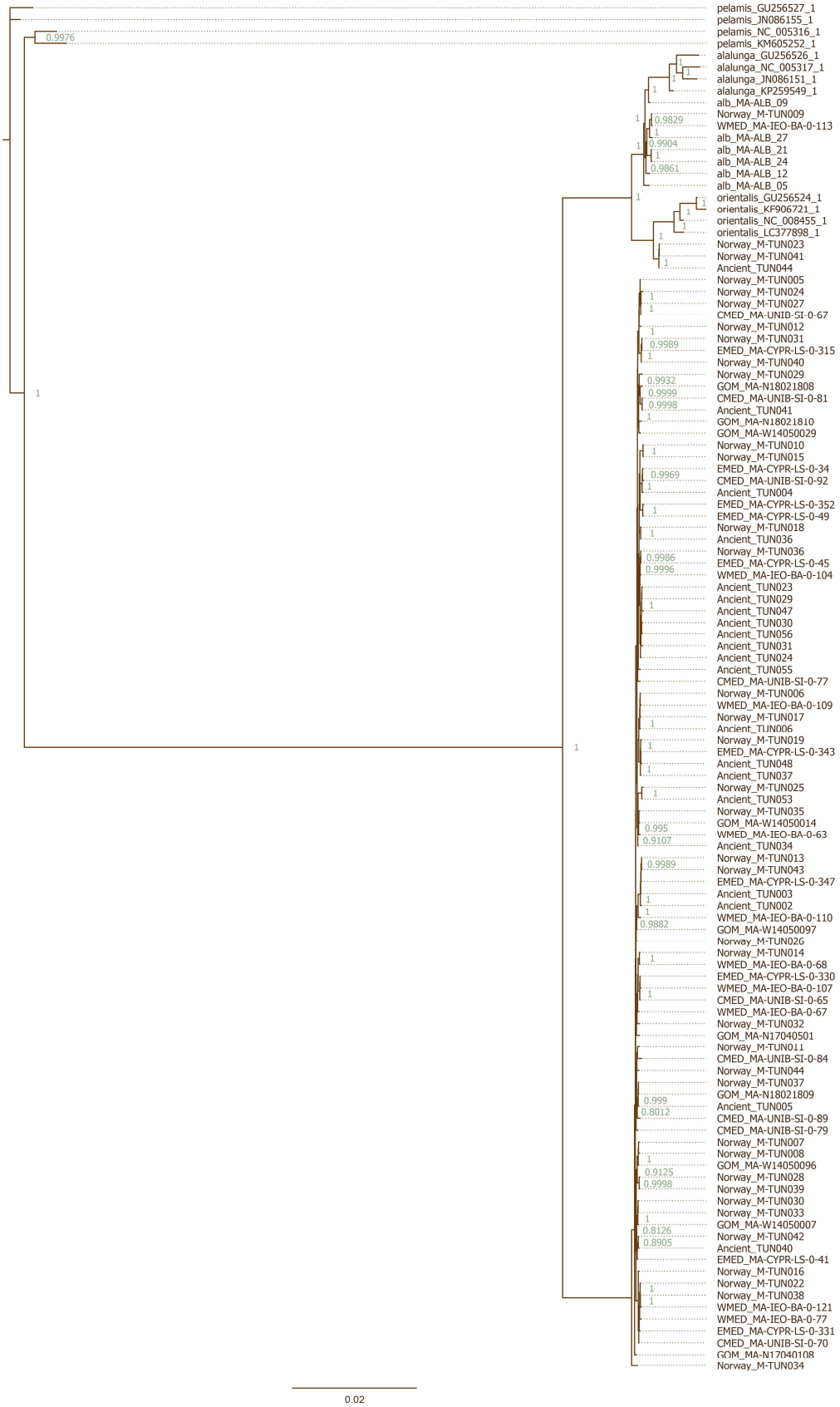

*Figure S6: MrBayes Bayesian interspecific phylogeny of all samples (dataset **All_alb**) and outgroups (Appendix A, Table S8). Posterior probability values over 0.8 are added in green.*

*Figure S7: BEAST 2 Bayesian interspecific phylogeny of all samples (dataset **All_alb**) and outgroups (Appendix A, Table S8). Posterior probability values over 0.8 are added in blue.*

*Figure S8: BEAST 2 Bayesian intraspecific phylogeny of non-introgressed Atlantic bluefin individuals (dataset **AllExIntrog**), using a Pacific bluefin individual as outgroup. Posterior probability values over 0.8 are added in blue.*

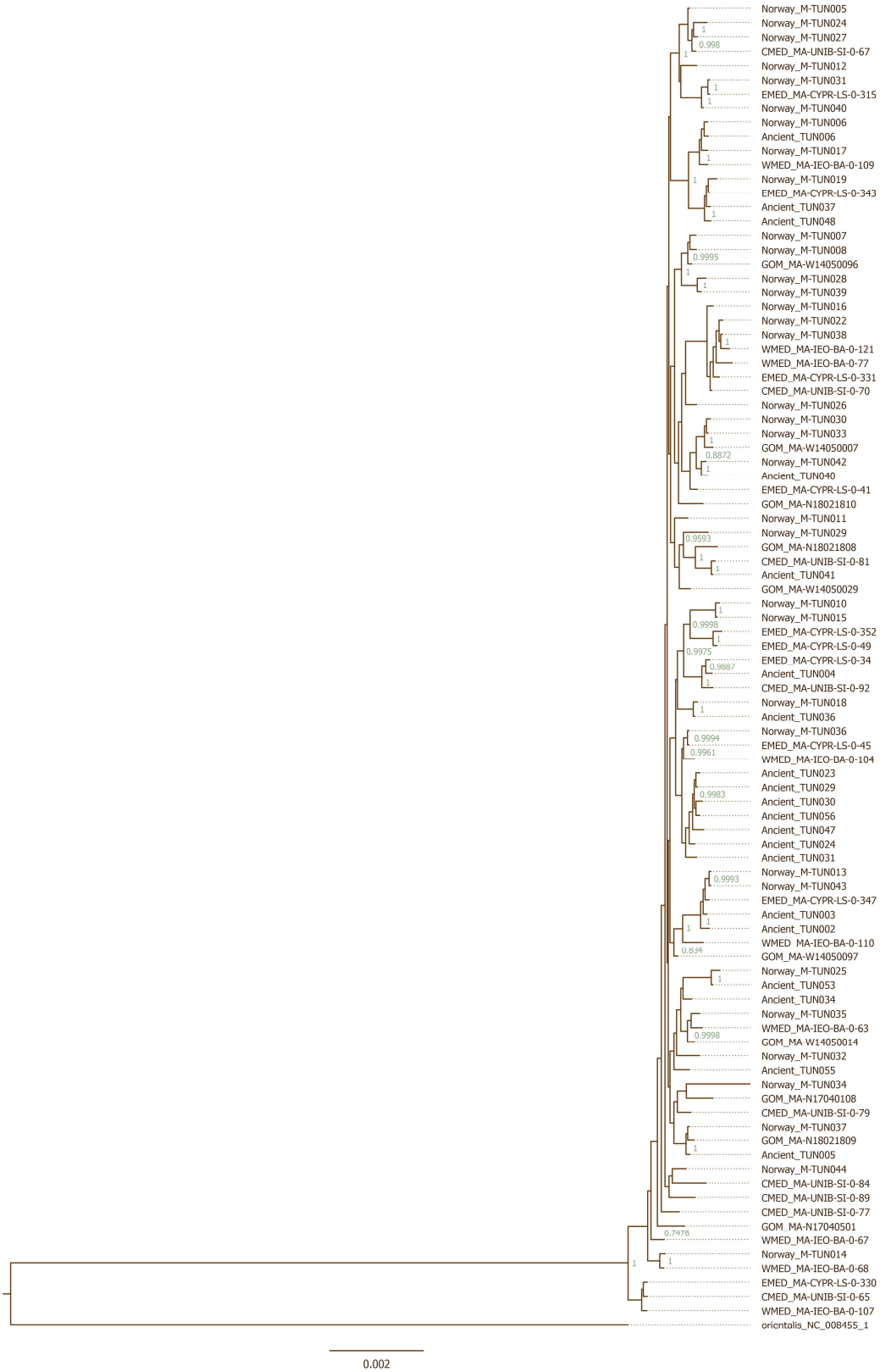

*Figure S9: MrBayes Bayesian intraspecific phylogeny of non-introgressed Atlantic bluefin individuals (dataset **AllExIntrog**), using a Pacific bluefin individual as outgroup. Posterior probability values over 0.8 are added in green.*

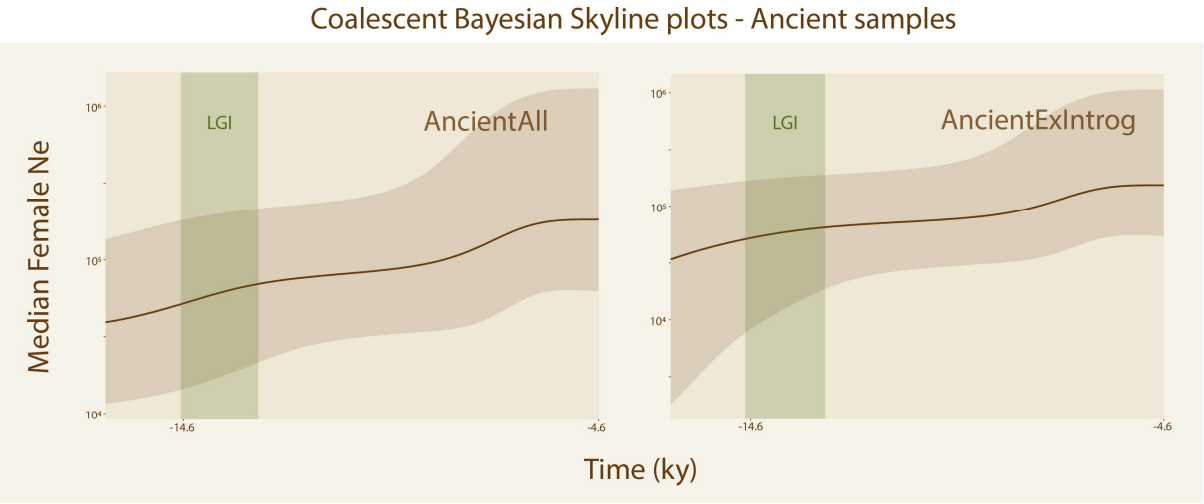

Figure S10: Female effective population size (Ne) modelled back in time, showing coalescent Bayesian Skyline (CBS) plots of only the ancient Atlantic bluefin samples. The Late Glacial Interstadial (LGI) is marked in the plot. The 95% confidence intervals are marked in dark brown.

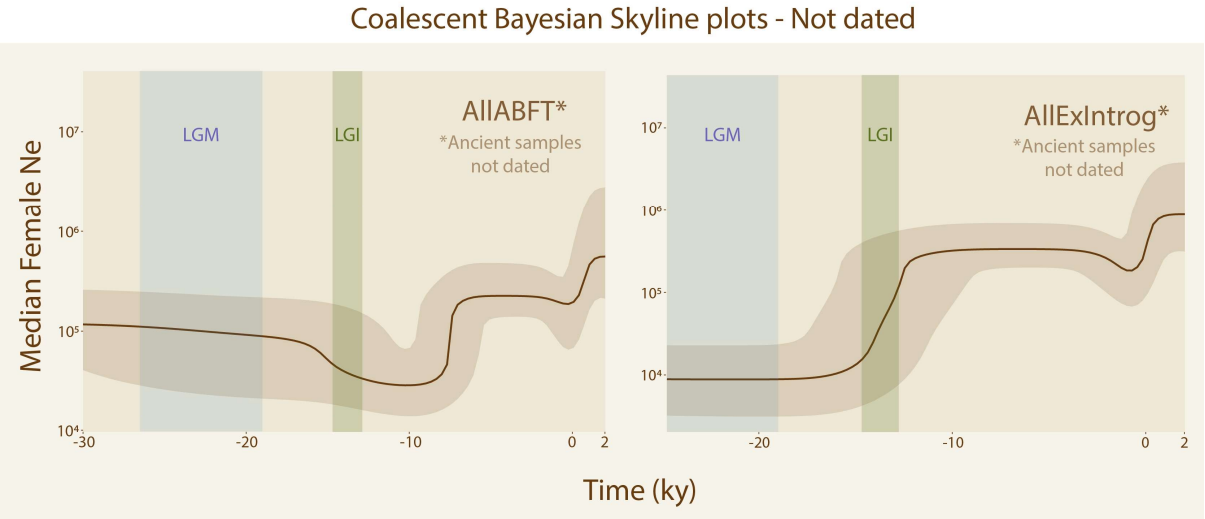

Figure S11: Female effective population size (Ne) modelled back in time, showing coalescent Bayesian Skyline (CBS) plots of modern and non-dated ancient samples. In these analyses, the anciet samples were treated as if they were modern by the model. Two major climatic periods are marked in the plot: The Last Glacial Maximum (LGM) and the Late Glacial Interstadial (LGI). The 95% confidence intervals are marked in dark brown.

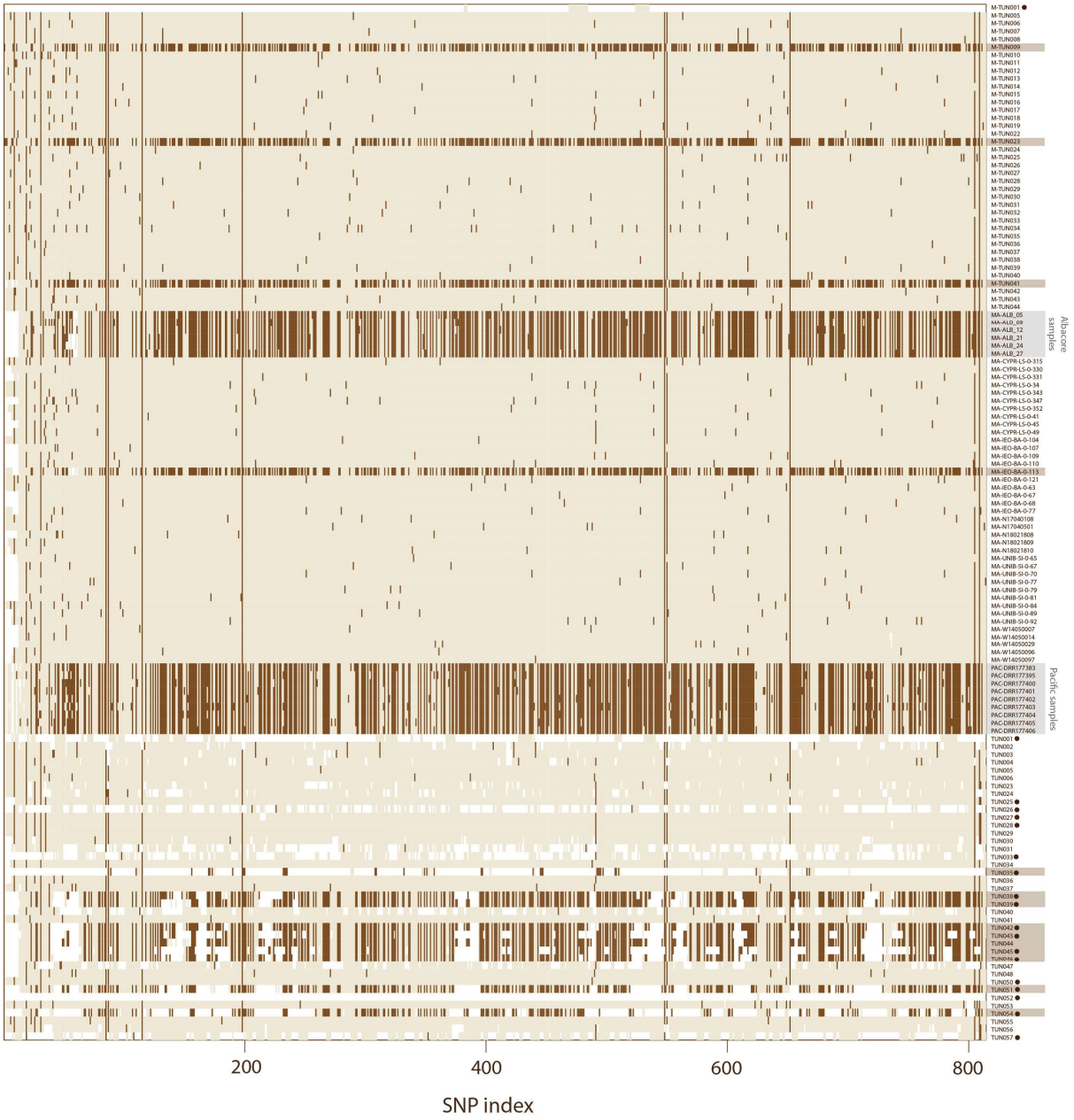

Figure S12: Result from exploratory analysis, including all samples prior to omission of identical- and high missingness samples. The plot shows the missing loci (white) and the presence of second alleles (dark brown). Samples that were excluded from subsequent population genomic analyses are marked with a dark brown circle by the sample name.

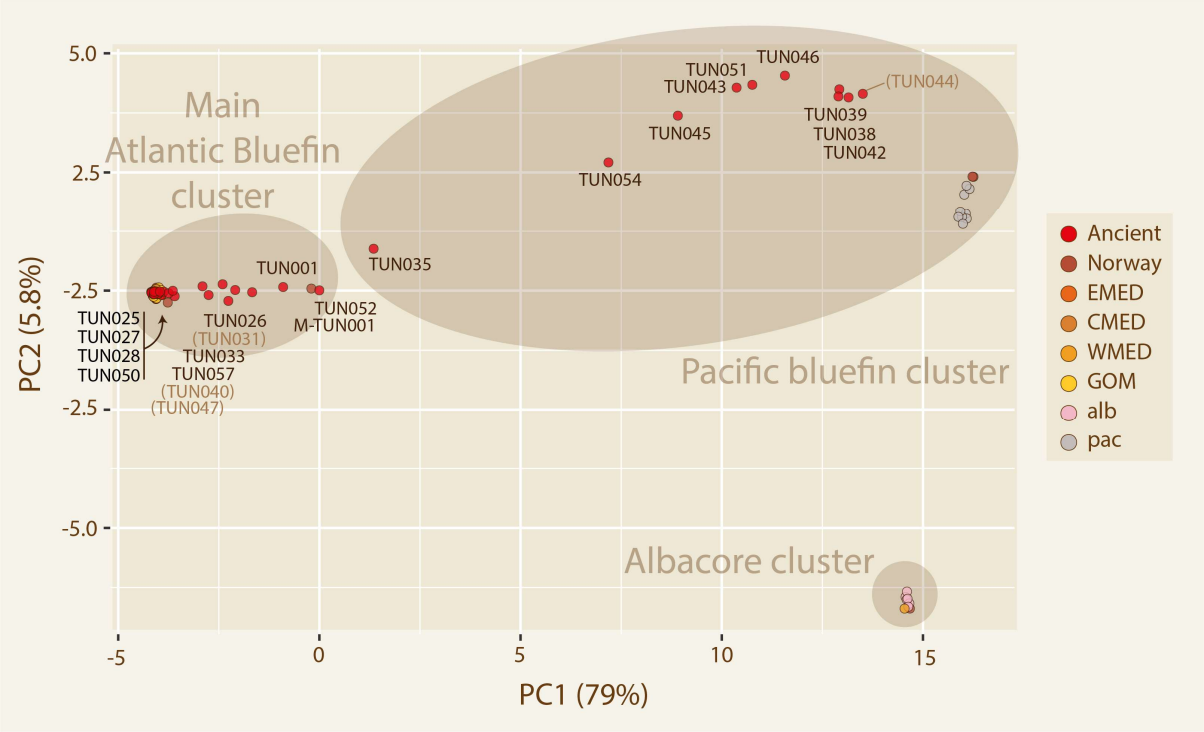

Figure S13: Result from exploratory analysis, including all samples prior to omission of identical- and high missingness samples. The plot shows an interspecific PCA. Samples that were excluded from subsequent population genomic analyses are marked with the sample name in dark brown. Sample names in parentheses indicate diverging samples that were kept in the population genomic analyses.

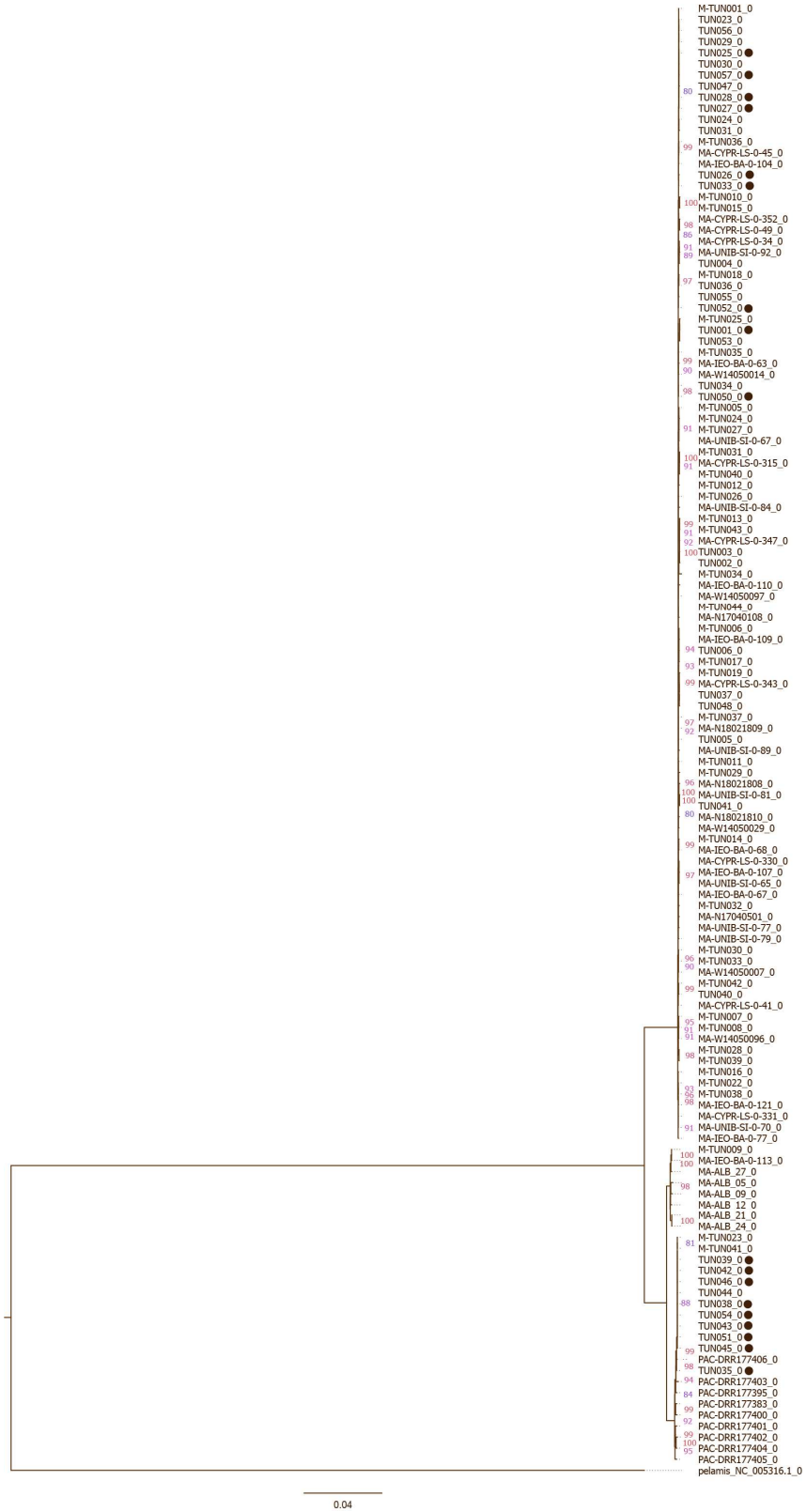

Figure S14: Result from exploratory analysis, including all samples prior to omission of identical- and high missingness samples. The figure shows an interspecific Maximum Likelihood (ML) phylogeny of all samples, using skipjack tuna (K. pelamis) as outgroup. Bootstrap values over 80 are shown in pink. Samples that were excluded from subsequent population genomic analyses are marked with a dark brown circle by the sample name.

Appendix C: Supplementary descriptions

Extraction protocol optimization for modern samples from Norway

The modern samples from Norway were using the DNeasy Blood & Tissue kit (Qiagen) and following the "Purification of Total DNA from Animal Tissues (Spin-Column Protocol)" from the manufacturer (DNeasy Blood & Tissue Handbook 07/2006, page 28-30) with modifications for optimal lysis and DNA yield. Sample tissue used in extraction was eight thin slices from each fin clip from the 2020-batch of modern samples, and 10 µL of freeze-dried muscle tissue from the 2018-batch of modern samples.

Modifications to the Spin-Column Protocol included using 30 µL of protein kinase instead of 20 µL, increasing the amount of ATL buffer from 180 µL to 300 µL, and adding 50 µL of 1M dithiothreitol (DTT) to the sample tube before lysis incubation. Increasing the amount of ATL buffer and protein kinase allowed for using more tissue from each sample, making sure the tissue was completely immersed in fluid during incubation. DTT is a widely used reagent in molecular biology, and is expected to facilitate protein digestion during in vitro reactions (Cantu et al., 2022; Fjelstrup et al., 2017; Kucera & Heidinger, 2018; Rohland et al., 2010). DTT is an electron donor which acts to stabilize enzymes by keeping the proteins in a reduced state (Fjelstrup et al., 2017). Compounds containing thiol are also known to protect DNA molecules from damage caused by oxygen and nitrogen radicals when used in the right concentration (Fjelstrup et al., 2017; Sölen et al., 1991). To create a 1M working solution, 3.09 g DTT powder was dissolved in 20 mL MilliQ water and stored at -20°C in 1 mL aliquots.

Lysis time varied from down to 1 hour for the fin clip samples, to overnight incubation of the muscle tissue samples. After lysis was complete, 7 µL RNase A 10mg/mL was added to the sample tubes before they were incubated for 2 minutes at room temperature. RNase A digestion is recommended by Qiagens Spin-Column Protocol (DNeasy Blood & Tissue Handbook 07/2006, page 28-30) to reduce RNA content when isolating genomic DNA, as RNA may copurify with DNA and interfere with subsequent quality control analyses and sequencing. To prevent filter clogging, samples were centrifuged for 2 min at 13000 rpm after lysis and RNase A digestion, and fluid was transferred to a new tube, leaving the sediment at the bottom.

The volume of Buffer AL and ethanol added to the samples was increased from 200 µL (DNeasy Blood & Tissue Handbook 07/2006, page 28-30) to 360 µL. Centrifugation speed was increased from 8000 rpm to 13000 rpm in step 4 and 5 of Qiagens Spin-Column Protocol (DNeasy Blood & Tissue Handbook 07/2006, page 28-30). Although increasing the

centrifugation speed during wash may cause some loss of DNA, this was preferred to ensure that buffer and contaminants were thoroughly removed. Elution was preformed using 105 µL and 200 µL Buffer EB (10 mM Tris-Cl) (Qiagen) for the fin-clip samples and powdered muscle samples respectively. To increase the release of DNA from the spin column membrane, the buffer EB was pre-heated to 50°C and allowed to incubate in the column for 10 minutes before centrifugation at 13000 rpm. The elution was preformed twice for each sample, resulting in two 105/200 µL tubes of finished extract. 5 µL of DNA isolate from each elution was aliquoted into a PCR strip and used for quantity and quality analysis of the DNA extract.

R-packages used in population genomic analyses

- vcfR (data loading) (Knaus & Grünwald, 2017)
- adegenet (ordination analysis) (Jombart, 2008)
- ape (phylogenetic analyses) (Paradis et al., 2004)
- pegas (population genomic statistics) (Paradis, 2010)
- ggplot in tidyverse (visualization) (Wickham et al., 2019)
- gridExtra (visualization) (Auguie and Antonov 2017)
- lemon (visualization) (Edwards 2017)

Identical modern samples

Several identical modern samples were identified by the python script. These samples were identical at both minDP2 and minDP3 filtering. Due to the sampling method ensuring different individuals, these samples were kept. It should be noted that the python script only counted the presence of base pair differences, conservatively ignoring gaps or missing positions as unique features. Therefore, these samples may be interpreted as unique by other, less conservative programs which may acknowledge gaps or missing sites as unique features.

- M-TUN013 = M-TUN043
- M-TUN023 = M-TUN041
- MA-UNIB-SI-0-70 = M-TUN038
- MA-CYPR-LS-0-315 = M-TUN031
- MA-CYPR-LS-0-45 = M-TUN036
- MA-N18021809 = M-TUN037